Quantum Mechanics and Raman Spectroscopy Refute Greenhouse Theory

Blair D. Macdonald © 2018

First Published: 2018-10-13

Update 2020-01-11

Abstract

Greenhouse theory (and radiation theory as a whole) presents a paradox and contradicts both quantum mechanics and thermodynamics. Its premise claims molecular nitrogen and oxygen (99 percent of the dry atmosphere) do not transfer (emit or absorb infrared) radiation at any temperature; however, all matter above absolute zero Kelvin radiates IR photons, and 'air' is a very poor thermal conductor of heat (0.0262 W/(m K)) – so how does it transfer heat? It was hypothesised these gases do radiate IR photons at their quantum mechanics predicted spectra at 2338cm^{-1} and 1556cm^{-1} respectively, and these predicted spectra are observed by (thermoelectric based) IR spectroscopy's complement instrument, the Raman Spectrometer. It was found the nitrogen and oxygen do possess quantum predicted emission spectra both within the IR range of the EMS, and these are only observed – and their respective temperatures and concentrations accurately measured – by Raman laser Spectrometers. It was concluded: using thermoelectric (IR) instruments alone without the complement Raman constitutes a systematic error and that greenhouse theory is misconceived. Raman spectrometers make IR spectroscopy redundant: they measure, more accurately the Keeling curve, and have application with meteorological Lidars and planetary atmospheric analysis. By the equipartition principle all spectra are equal through the Boltzmann Constant. The N_2-CO_2 Laser showed – contrary to current greenhouse theory – N_2 absorbs electrons and/or (IR) photons at its said– metastable 'long lasting' – spectra mode. It was argued atmospheric CO_2 is heated by the same mechanism as the N_2-CO_2 laser, as by physical law. N_2 and the entire atmosphere absorbs IR radiation directly from the Sun and other matter. With these findings, greenhouse theory as it stands is misconceived – all gases absorb and emit IR radiation at their said QM predicted spectra – and demands review.

Key Words: Greenhouse effect, Raman Spectroscopy, Quantum Mechanics, Non-Greenhouse Gases, N2-CO2 Laser, Spectroscopy

Preface

It should be made clear from the outset, nobody – whether proponents or sceptics to the ensuing climate debate – agrees with what I have uncovered here. I have had a fair amount of feedback since I first published it in late 2018 under the current title, but – again – from both sides nobody has told me where I am wrong and I have only received I get cocktail of fallacies to negotiate (no fallacy intended here). This includes many Professors and PhDs from both sides, including Professor Will Happer, Antony Watts of 'What's Up With That', and the GWPF. Indeed, these exchanges – one of which was 40 exchanges in total – have grown my understanding evermore. My investigation had its beginnings with trying to understand the BBC Professor Ian Stewart greenhouse gas investigation. For some reason I became interested in non-contact IR thermometers and IR cameras and then heard from a radio interview with Sceptic Christopher Monkton that there was an original greenhouse theory experiment conducted by John Tyndall in 1859 and that his instrument used the same thermopiles as still used in these said instrument. With further digging I soon found that there is a modern instrument that is complementary to the thermoelectric and it is Raman Spectroscopy. The more I dug, but more things fell into place. Today, with what I have uncovered, I believe I can reform all of thermal physics and update it.

My intention is to reduce this work down a publishable sized paper and push for publication. I am convinced the game play (of game theory) surrounding this issue is so strong no one will support me else risk their position and that it has to be me.

Table of Contents

1 Introduction 1

2 Methods 4

2.1 IR Spectra Prediction of N_2 and O_2 by Quantum Mechanics 5

2.2 Observing N_2 and O_2 with Raman Spectroscopy 5

2.2.1 Raman spectroscopy 5

2.2.2 Approach and Scope of the RER 6

2.2.3 Operation of the Raman Exhaust Report (RER) 6

2.2.4 Setup: 7

2.2.5 The Laser: 8

2.2.6 Temperature Measurement 8

2.3 No Confusion between Raman Spectroscopy and the Raman Effect 8

2.4 Raman Lidar for Remote Sensing of CO_2 Leakage at an Artificial Carbon Capture and Storage Site 9

2.5 Evidence of N_2's 2338 cm^{-1} IR Absorption: the N_2-CO_2 11

2.5.1 N_2-CO_2 Laser: A Practical Application of 'Radiated N_2 at 2338 cm-1 11

2.5.1.1 The CO_2-N_2 Laser 11

3 Results 12

3.1 N_2 and O_2 IR Spectra Predicted by Quantum Mechanics 12

3.2 Atmospheric IR and Raman IR Spectra Lines 13

3.3 Raman Gas Vibrational Modes Observation 15

3.3.1 N2 2338cm Raman Vibrational Mode Spectra 16

3.3.2 O_2 1556 cm^{-1} Vibration Mode and Concentration 17

3.3.3 H_2O 3652 cm^{-1} Vibrational Mode 18

3.3.4 CO_2 1338 cm^{-1} Vibrational Mode (and Temperature) 19

3.4 Gas Temperature Measurement by Raman Spectroscopy 21

3.4.1 N_2 Temperature 21

3.4.2 Raman CO_2 Temperature 23

3.5 Gas Concentrations by Raman Spectroscopy 25

3.5.1 H_2O Concentrations 25

3.5.2 CO_2 Concentration 25

3.5.3 N_2/O_2 Ratio 26

3.5.4 NO 27
3.6 RER Conclusion 27
3.7 Raman lidar sensing of CO_2 leakage - Results 28
3.8 N_2-CO_2 Laser Results 29
3.9 Natural N_2-CO_2 Lasers 31
3.9.1 'Blackbody CO_2 Laser' Showing N_2 Heated by Sunlight 32
3.9.2 Experimental Setup 33
4 Discussions 35
4.1 The Laws and Physics Central to Radiation Theory 36
4.1.1 Planck's Law 36
4.1.2 Boltzmann Constant 36
4.1.3 The Stefan-Boltzmann Law 36
4.1.4 Kirchhoff's Law of thermal radiation 37
4.1.5 Spectroscopy: 37
4.1.6 Quantum Mechanics Schrödinger Equation 37
4.1.7 Equipartition Principle 37
4.2 Quantum Mechanics IR Spectra Predictions 38
4.3 Temperature Measurement by Raman Spectroscopy 38
4.3.1 Raman Thermometry 38
4.3.2 Measurement at Ambient Temperatures 39
4.3.3 Raman Flame Temperature Measurement 40
4.3.4 Temperature Detector Equivalence 42
4.3.5 Raman Temperature Measurements and the Boltzmann Constant 45
4.3.6 Raman Measurements and the Stefan Boltzmann Law 45
4.3.7 N_2 and O_2 and Planck's Law 46
4.3.8 Liquid H_2O Temperature Measurement 46
4.3.9 H_2O and Emissivity 47
4.3.10 Equivalence – Dual Modes H_2O 47
4.4 Raman Mapping and Thermal Imaging with Raman Spectroscopy 48
4.5 The Significance of Equipartition and Degrees of Freedom and Normal Modes 48
4.5.1 CO_2's 1338 cm^{-1} and the Principle of Equipartition 49
4.6 Towards an Equation of the 'Raman' Atmosphere - 49
4.6.1 A Raman spectroscopy derived equation of the atmosphere. 51
4.7 Raman lidar sensing of CO_2 leakage - Discussions [17] 51

4.8 Other Applications of Raman Spectroscopy 52
4.8.1 Measuring Atmospheric Gas Concentrations (Keeling Curve) with Raman 52
4.8.2 Measurement of Agricultural Emissions 53
4.8.3 Raman Solar System Space Probe Applications 53
4.8.3.1 Venus 54
4.8.4 (Raman) Aircraft Instrumentation 55
4.8.5 Laser-based air data system for aircraft control using Raman 56
4.8.6 Raman LIDAR and the Atmosphere 58
4.8.6.1 Lidar can reveal the temperature of the atmosphere: 59
4.8.7 Other Uses for Raman Spectroscopy 62
4.9 'Radiating' N_2: N_2-CO_2 LASER – Discussions 63
4.9.1 Stimulated and Spontaneous Emission 63
4.9.2 Does Discharge of Electrons Constitute Radiation? 63
4.9.3 Frank-Hertz Experiment 64
4.9.4 Collisions Implausible: Convection Paradox 64
4.9.5 Implications for IR Spectroscopy 65
4.9.6 N_2 and Kirchhoff's Law 65
4.9.7 Metastable N_2 and the Greenhouse Atmosphere 65
4.9.8 Metastable N_2 from 'Collisions' and not Radiation Inconsistency 66
4.9.9 Radiationless Transfer of Energy 67
4.9.10 IR Photon Absorbing Atmospheric N_2: An Atmospheric Law of Physics 67
4.10 Raman and IR Spectroscopy Complementary Instruments and Spectra 68
4.10.1 Other Molecules with Dual Raman thermoelectric. 68
4.10.1.1 Ethanol 69
4.10.2 CO_2's 1338 cm^{-1} Raman Active mode showing on IR spectra. 71
4.10.3 N_2O's Shared IR and Raman Modes 72
4.11 H_2O: Dual Raman and IR Active 72
4.11.1 H_2O's 3652 cm^{-1} a Contravention of the Rule of Mutual Exclusion 73
4.11.2 Solar IR Insolation Radiation Heats Water 74
4.12 Ozone O_3 IR and – inferred by – Raman 75
4.13 Augmenting the IR Spectroscopy and Raman Atmosphere 76
4.13.1 The Augmented Raman active TE Greenhouse Atmosphere Spectrum 77
4.14 *Ad hoc* Inclusion of N_2, O_2, and CO_2 's Non-IR Raman Active Modes on Blackbody Emission Spectra [80] 78
4.14.1 Addressing Raman Spectra between Solar and Earth 'Blackbody Curves 79

4.15 The Implications of Raman Spectroscopy on Current GH Theory 80
4.15.1 Fog Dispersal and Evidence of Direct Solar IR Radiation 81
4.15.2 Towards a Complete Theory of the Atmosphere 82
4.16 Strengths and Limitations 83
4.16.1 N_2 Absorbing in the 'Hot' Thermosphere and the Aurora 83
4.16.2 IR Absorption and Thunder Creation: Lightning Heating the Air 83
4.16.3 Non-Radiant and Non-Conductive N_2 and O_2 Heat Capacity Paradox 84
4.16.4 Standard (bottle) Greenhouse Experiments, and SHC Measurement 85
4.16.5 Real Measurement of Gas Heat Capacity: Equivalent to GH Demonstrations 86
4.16.5.1 Measurement of GHGs Specific Heat proves non-GHGs absorb IR 87
4.16.6 Vibrational Behaviour and Specific Heat Capacity 87
4.16.7 IR Absorption and the Incandescent Light Bulb 88
4.16.7.1 Non-TE/IR Non-Raman Argon 88
4.17 What is Next? 88
4.17.1 Why is it N_2 and O_2 do not show up in – what I have termed thermoelectric – IR Spectroscopy? 88
4.17.2 A Proposed N_2 and O_2 Absorption Experiment 89
5 Conclusions 89
6 Acknowledgements 92
7 References 93
8 Appendix 105
8.1 Other Uses for Raman 105
8.1.1 CO2's 1388cm-1 Excitation: The Dicke effect 105
8.1.2 Medical – anesthetic RASCAL – Capnography Application 105
8.1.3 Geology CO_2 1388 cm^{-1} 106
8.1.4 Automobile Emission Testing. 106
8.1.5 Atmospheric measurement using Raman Spectroscopy 107
8.2 Understanding Raman Backscatter and the Low Wavenumbers 108
8.2.1 Raman Laser to Wavenumber Correction Calculation 109
8.3 Raman spectra for Non-GHGs and GHGs 110
8.3.1 O_2 and N_2 110
8.3.2 O_2 Spectra 111
8.3.3 N2 2338 cm^{-1} 112

8.3.4 O_2 1556 112
8.3.5 CH_4 113
8.3.6 H_2 115
8.3.7 H_20 Raman 115
8.3.8 H_2O TE IR 116
8.3.9 Ge Germanium 116

1 Introduction

The current 'standard' model of greenhouse (GH) theory – first developed in the mid 19th Century, a time before 20th century quantum mechanics – claims the entire thermal-radiation behaviour of the atmosphere is explained by 1-2% of its constituent gases, together known as the special greenhouse gases (GHGs). The GHGs are assumed to be the only gases to absorb infrared (IR) radiation; the non-GHGs nitrogen (N_2) and oxygen (O_2) – 99% of the dry atmosphere – do not absorb or emit any IR radiation[1][2][3], at any temperature. The following text is the explanation given as to why N_2 and O_2 are not GHG's:

"*N_2 and O_2 have no dipole, so they are not greenhouse gases. N_2 is symmetrical AND made of identical atoms. Even with rotation or vibration, there is no unequal sharing of electrons between one N atom and the other. So N_2 has no dipole, and an EM photon passes by without being absorbed. Similarly, for O_2.*" [4]

It is assumed that any heat-energy that is transferred to these (said IR transparent) non-GHGs comes only from 'collisions' with the special GHGs. The GHGs and the surface of the Earth are said to absorb short wave radiation and this heat is transferred by the process of thermal conduction to the non- GHGs, emitting long-wave radiation [5][6]. The problem with this assumption is that air is known to be a very poor conductor of thermal energy with a – near zero – value of 0.026 w/(mK); methane (CH_4) has a thermal conduction value of 0.003 and Carbon dioxide (CO_2) 0.0146. These values alone should eliminate them – and all the other gases as they have similar – as being capable of doing what it is claimed to do; they just do not thermally conduct. For this reason, it must fall upon radiation to be the leading form of heat/energy transfer of gases. The problem is that the assumptions of atmospheric GH theory – based on black body radiation theory – state they do not radiate either. All this is in direct contradiction with modern quantum mechanics where Planck's law of radiation states all matter above absolute zero Kelvin absorbs and emits infrared radiation. This law should apply to N_2 and O_2 also. While the science surrounding

climate theory is said to be 'settled' – as it is claimed; it appears at the fundamentals the physics and chemistry not. Either quantum mechanics is wrong, or GH theory is wrong?

In more detail, all atoms and thus molecules possess quantum predicted absorption-emission spectra lines (or modes) by which they radiate and absorb throughout the electromagnetic spectrum (the EMS). In the IR range of the EMS – important to GH theory – these predicted spectra-bands are observed by one of two types of IR spectrometers: either IR spectrometers, or Raman spectrometers – and some modes, H_2O in particularly, are by both IR and Raman measured. It is important to note that spectra of a molecule are assumed to equally – by the equipartition principle – share their energy and radiate, irrespective of whether they are 'IR' of not. To emphasis this understanding, in a Molecular Spectroscopy introduction film from 1962: from University of California [9] the three vibrational modes of the CO_2 molecule are described and demonstrated. In it is demonstrated the harmonic vibration of the molecules using a basic ball and spring scale model with a harmonic vibration generator, Figure 1 (A and B). The three vibrational modes of CO_2 without any separation or discrimination of them are all identified (C): at 7.05 x 10^{13} (corresponding to the 1338 cm^{-1} mode), 4.16 x 10^{13} (corresponding to the Raman Active 2349 cm^{-1} mode) and 2 x 10^{13} (corresponding to the 667cm^{-1}).

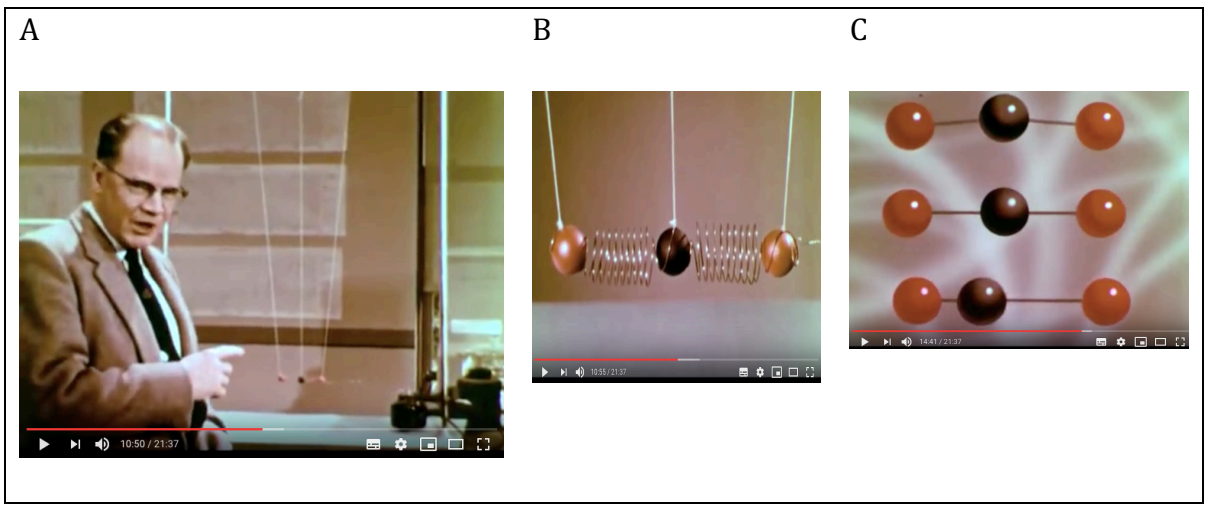

Figure 1. Demonstration of Harmonic Vibration of all of CO_2's Modes. Frame A, a model the CO_2 molecule is vibrated by frequency producer at different frequencies; frame B, close up of the spring and ball model attached to the devise on the right; and Frame C, the film showing – in an age before Raman Spectroscopy – all CO_2's modes and their positions.

The significance of this film highlights the gap in the knowledge with respect to atmospheric and radiation theory in general; these spectra now have an instrument that can measure them, it is the modern laser-based Raman spectrometer. The Raman Spectrometer is itself a product of quantum mechanics and is indeed a key instrument in the defence of it as it observes these predicted so-called non-IR spectra. The Raman IR spectrometer is a complimentary instrument to the IR spectrometer and observes – just as it was explained too in all demonstrations of it – the IR modes IR instruments cannot. At the time this film was made there is no understanding of what are now termed and understood by chemists as the Raman active modes, not to mention measuring them; the film is only on the said IR (thermoelectric) modes and how they are measured. But all the spectra modes are equivalent – again by the equipartition principle – and they resonate at their respective vibrational frequency positions. The Raman spectrometer can measure CO_2's the third mode, and it is clearly stated in the film the diatomic – N_2 and O_2 – share the same properties of resonance and so they too should and can be observed by this new Raman instrument.

In a demonstration on the theory and application of Raman IR Spectroscopy, Professor Mike Bradley says the follows with respect to the differences between 'IR' and Raman spectroscopy – they give the 'same information'.

"(With Raman spectroscopy) we are looking at a vibrational excitation that …is the same think we are looking at when we are doing IR spectroscopy. They have different selection rules and different kinds of vibrations we are looking at; never the less it is the same information." 5:17 [10]

It was hypothesised in this investigation that there has been a non-random systematic error by the exclusion of Raman instruments to measure the IR atmosphere. The molecules N_2 and O_2 do obey to the laws of radiation physics, they have spectra, and they too are GHGs. The non-GHGs are only special from GHGs in that they are measured by a different instrument. It is the instruments that are special and not the gases as such. To prove this, N_2 and O_2 should possess spectra lines in the IR range of the EMS; these lines should be predicted

by quantum mechanics, and these bands should be able to be observed by other spectrometers. Further to this, these facts should be able to be applied in a demonstration or real-life application to show absorption and emission of IR photons. By measurement and by practical application these so-termed - by default – non-GHGs are too GHGs. There are no special GHGs; only special instruments. If the non-GHGs are found equivalent to the special GHGs, and it is found that it is the instruments that are special and not the gases; from first principles 0^{th} and 1^{st} Laws of Thermodynamics all gases should transfer their energy towards equilibrium, where previous to this N_2 and O_2 were exempt.

Without evoking any of the arguments posited in the current ensuing 'great' political-climate debate surrounding GH theory, this paper aims to address the problem by looking at the 'first principles' physics (4.1). The paper points to the problem being GH theory as it stands is based on 19^{th} Century IR spectroscopy and neglects modern quantum mechanics and the laser-based instruments – derived themselves from quantum knowledge.

This investigation will be in the form of a review of the 'science' surrounding the non-GHGs and quantum mechanics, followed by practical applications and experiments with Raman IR spectroscopy and the said gases. It will review Raman spectroscopy's application in atmospheric studies.

While reading this work, one should keep in mind the question; what if there were only Raman spectrometers? Or, what if Raman spectroscopy was developed before its complement – thermoelectric based IR spectroscopy? If these were both so; what then would we make of these claimed special GH gases, and indeed (thermoelectric derived blackbody) radiation theory as a whole?

2 Methods

No experiment as such was undertaken, but rather a first principles review of literature, theory, application, and instruments with respect to the hypothesis. The following order of methods in this section is maintained in the results and discussions section.

1. The quantum mechanics IR spectra were researched;
2. Two experiments using Raman spectroscopy to observe these IR spectra was reviewed: The Raman Exhaust Report (RER); and the '...Raman Lidar for Remote Sensing of CO2 Leakage at an Artificial Carbon Capture and Storage Site';
3. An IR absorption application of predicted N2 spectra was reviewed: the N_2-CO_2 laser.

2.1 IR Spectra Prediction of N_2 and O_2 by Quantum Mechanics

A review of the literature was undertaken with respect to the predictions made by quantum mechanics of IR spectra of the said gases. I was looking for evidence N2 and O2 have QM predicted spectra within the IR range of the EMS.

2.2 Observing N_2 and O_2 with Raman Spectroscopy

A review the literature surrounding the observation of the IR emission spectra modes of atmospheric molecules was made.

2.2.1 Raman spectroscopy

"That branch of spectroscopy concerned with Raman spectra and used to provide a means of studying pure rotational, pure vibrational and rotation-vibration energy changes in the ground level of molecules. Raman spectroscopy is dependent on the collision of incident light quanta with the molecule, inducing the molecule to undergo the change." [11]

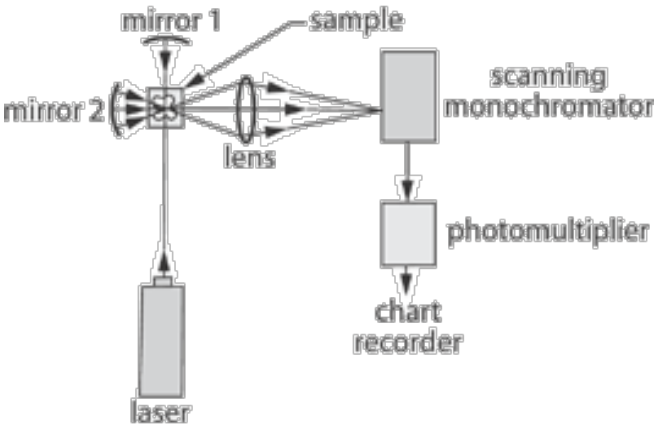

Figure 2 Raman Spectroscopy Configuration.

No direct primary experiment was undertaken in this investigation, but rather – among others – a report of a previously conducted Raman spectrometer application was referred to. This report called the: FIELD TESTS OF A LASER RAMAN MEASUREMENT SYSTEM FOR AIRCRAFT ENGINE EXHAUST EMISSIONS - 1974 [12]. For the purposes of this investigation 'The Raman Exhaust Report' was termed the RER. The operation of this Raman device (the RER) should correspond to our understanding of quantum mechanics and thermodynamics in that it will measure the predicted vibrational modes of each and every molecule it can, and; also measure the corresponding temperature/energy. Finally, the RER application should invoke questions at the fundamentals of physics: if N_2 and O_2 do radiate, how is it so – if it is assumed by GH theory not to? How have they become so hot so quickly from collision (conduction) alone when they are assumed they do not absorb any IR heat-energy.

This 1974 RER paper is supported by a similar 2002 publication: Combustion Temperature Measurement by Spontaneous Raman Scattering in a Jet-A Fueled Gas Turbine Combustor Sector [13].

Also supported by: Rotational Raman-Based Temperature Measurements in a High-Velocity Turbulent Jet [14]

2.2.2 Approach and Scope of the RER

While this paper will evaluate Raman spectrometers for their equivalence to TE/IR spectrometers – with respect to testing the atmosphere gases – it will also explain where and how physics has misconceived the standard 'special' GHGs. To prove the hypothesis, the Raman vibrational modes of the atmospheric gases will be evaluated for their respective IR radiative propensity. An already performed experiment – where 'hot' air is measured using both IR/TE transducers and Raman spectrometers for its thermal properties – is referred to, along with applications of IR, and quantum theory.

2.2.3 Operation of the Raman Exhaust Report (RER)

The RER directed a high-power Nitrogen laser Raman spectrometer into the outlet flow of an operating (T-53) jet engine to measure the gas temperature, and concentration. To calibrate and compare measurements made by the Raman

laser; ‘conventional’ - IR spectrometers (table 1 p.25) and thermocouples were used.

The following are extracts from the report pertaining to the Raman method and could be repeated in any other gaseous context.

“Laser induced Raman and fluorescent measurements were made in the exhaust of a T53-Ll3A gas turbine engine with a new field portable instrument devised specifically for gas turbine exhaust emission measurements. The gas turbine exhaust was analysed by conventional instruments for CO, CO_2, NO, NO_2, total hydrocarbons, smoke and temperature, and these data were used as a "calibration" standard for the evaluation of the laser Raman instrument, (p. v). “

2.2.4 Setup:

The laser beam was pointed at and through the jet outlet as shown in the reports figure 28 (p. B46)

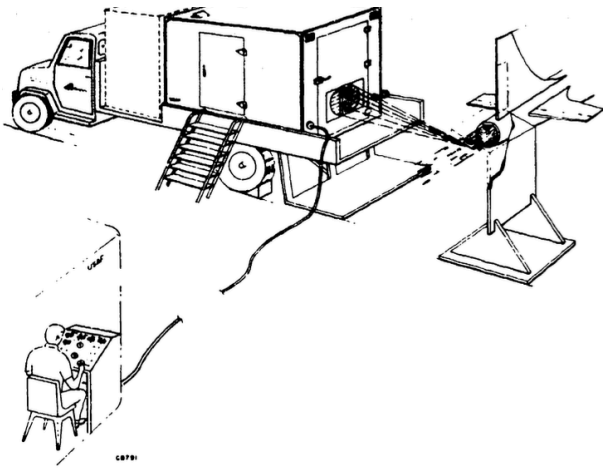

Figure 28 Schematic of Laser Raman Aircraft Engine Exhaust Emissions Measurement System

Figure 3. RER Setup. Pg. 46 [15]

“The gas analysis equipment used as a comparative standard for the laser Raman consisted of detectors similar to those specified by the SAE. They consisted of infrared detectors for CO, CO_2, and NO, a flame ionization detector for total hydrocarbons, and a polarographic detector for NO and NO_2 as shown in the schematic of Figure 14. Thus, NO was measured by two different detectors. A list of the instruments used and their ranges is given in Table I.” (P.20)

2.2.5 The Laser:

"The laser transmitter was an Avco Model C5000 pulsed nitrogen laser operating at a wavelength of 3371 Å (337.1 cm^{-1})." (p.4)

2.2.6 Temperature Measurement

"Raman spectroscopy can be used to determine the temperature of a material when other more direct means are either impractical or not possible. The material's temperature can affect the peak position of Raman bands. When a Raman band shifts significantly with temperature, the monitoring of the peak position can be the most straightforward manner of determining temperature provided the Raman spectrometer has sufficient spectral resolution. Another method is to determine the temperature from the ratio of the Stokes and anti-Stokes signal strengths of a given Raman band. The latter method requires the ability to detect light at wavelengths longer and shorter than that of the laser and an accurate measurement of the wavelength-dependent instrument response function." [16]

Temperature measurements were made from the Raman laser unit and from conventional thermoelectric devices.

"Room temperature experiments were conducted in room air to measure for nitrogen..."

"The temperature of the T53 exhaust was measured by means of the N2 Raman density method whereby the temperature is assumed to be inversely proportional to the density of nitrogen, with a constant static pressure. "

"Raman spectra at elevated temperatures were obtained from the exhaust of a propane/air burner. Figure 18 shows the measured spectrum of the nitrogen Raman band at 3658Å at a temperature of 1000 K and measured with a thermocouple in the burner exhaust." Pg. 32 [15]

2.3 No Confusion between Raman Spectroscopy and the Raman Effect

For clarification purposes: by using the word 'Raman' is not to assume a Raman effect is a mechanism leading to thermal heating of the atmosphere. Pre-publishing reviewers made persistent claims to this effect. To counter this, this

paper claims Raman Spectrometers identify or infer the predicted molecular vibrational modes of the 'non-GHGs' in the IR range of the EMS, and also the different parameters measured – such as temperature. Raman spectrometers exploit the Raman effect with their lasers. The vibrational modes of the atmosphere are described and predicted by QM and are observed by Raman Spectroscopy.

Appendix 8.2 addresses this discrepancy between the Raman 'Spectroscopy' and the Raman 'Effect'.

Raman spectroscopy shows these modes are real (Figure 8), and we shall soon learn they correspond to IR radiation.

More reference and background to Raman Spectroscopy can be found at Appendix from 8.2.

2.4 Raman Lidar for Remote Sensing of CO_2 Leakage at an Artificial Carbon Capture and Storage Site

Raman lidar was used to detect CO_2 leakage: Development of Raman lidar for remote sensing of CO2 leakage at an artificial carbon capture and storage site [17],

The apparatus, methods and the techniques are standard 'Raman spectroscopy' as described in this paper and shown below on in Figure 4. CO_2 concentration mixing ratios were measured.

"*Since N2 is present at a constant rate in dry air, the N2 Raman signal, PN2, is used as a measure of dry air [13]. The CO2 mixing ratio can be derived from the normalization signal, which is the quotient of the CO2 Raman signal divided by the N2 Raman signal*." Page 3.

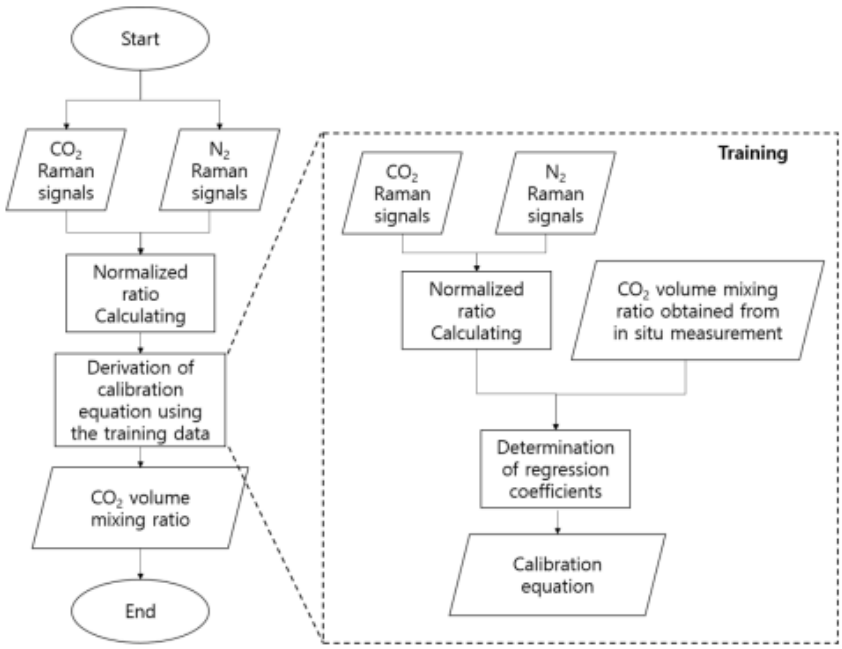

Figure 1. Flow chart for calculating the CO_2 volume mixing ratio using the Raman lidar system.

Figure 4 Show Raman spectroscopy process towards Concentration Ratios N_2 and CO2

In an experiment the Raman Lidar was setup (Figure 5) to measure CO_2 concentrations from a mock gas leak. Results were compared to an 'IR' thermoelectric CO_2 measuring instrument (CO_2 in situ).

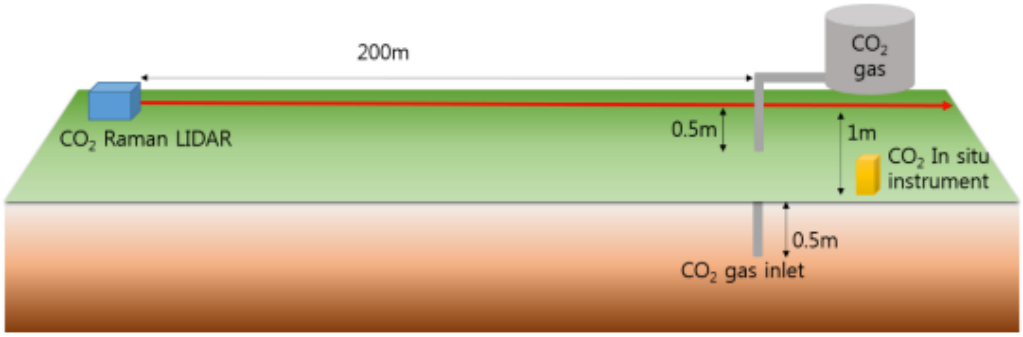

Figure 7. Schematic representation of the Eumseong Environmental Impact Evaluation Test Facility for the seepage of geologically stored CO_2.

Figure 5. Raman Lidar CO_2 'leakage' Experiment.

An experiment was also setup to measure the CO_2 output from car on a motorway over a distance of 750 metres (Figure 20).

2.5 Evidence of N_2's 2338 cm^{-1} IR Absorption: the N_2-CO_2

For the Raman theory – of a radiating 'non-GHG' atmosphere – to have any validity, there should be instances that show coherence with the theory. The following are instances where the non-GHG modes are radiated, and in total compliance with quantum mechanics offer such examples: the CO_2 laser and absorbing thermosphere N_2 molecules – where there is only radiation as a transfer of heat-energy.

2.5.1 N_2-CO_2 Laser: A Practical Application of 'Radiated N_2 at 2338 cm-1

The CO_2 Laser offers a pragmatic real-life application – or kind of experiment – invoking and testing both of the key atmospheric gases in question, N_2 and CO_2, revealing their real relationship between them when they are radiated – though it is not currently interpreted as so. After an understanding of the CO_2 Laser process it could be assumed – contrary to standard belief – N_2 in the atmosphere is the gas that affects – and actually forces – the CO_2.

All theory surrounding the CO_2 Laser points to the role of N_2 has in 'pumping' the CO_2 as an essential part of the process; so much so – it is explained in all textbooks – the laser will not operate without this 'absorbing/emitting' property of N_2 when radiated. The relationship is so close these lasers are technically termed **N_2-CO_2 Lasers**. A closer look at the physics behind the laser reveals N_2's true nature, and it absorption property at its **2338**cm^{-1}mode; a property absolutely ignored in atmospheric 'GH' theory. It is as if the scientist describing the CO_2 laser are oblivious of the ramifications this knowledge would mean to GH theory; that they are using the very same mechanics – both physics and chemistry – that the Raman measurements point to in the atmosphere; only here the gas is excited at the said modes.

2.5.1.1 The CO_2-N_2 Laser

Lasers all have the following key components:

1. An active medium – for the CO_2-N_2 laser it is the CO_2 and N_2 that are of interest;
2. Energy input/ pumping source/ high voltage discharge
3. Optical Feedback, this is not of interest in the investigation

4. Population inversion, this in essential – more electrons must be in an excited state that lower state; this is very important.

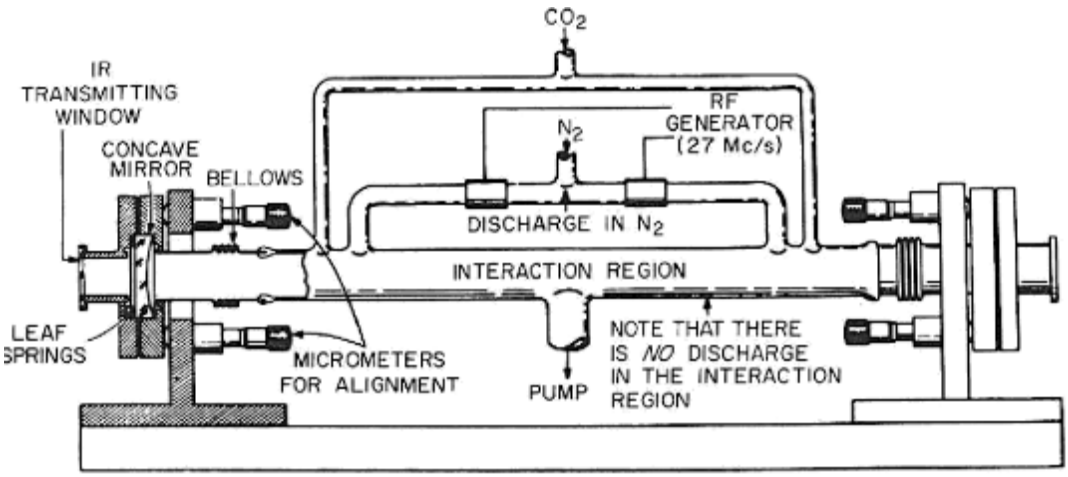

Fig. 1.1. System developed by Patel (1964b) demonstrating laser emission due to transfer of vibrational energy from N_2 to CO_2.

Figure 6.The CO^2 Laser [18]

"Infrared laser emission from CO_2 was first reported by Patel (1964) and others in pulsed discharges through pure CO_2. In this system N_2 is excited in a ef discharge to form vibrationally excited N_2 molecules which stream into and interaction region to mix with unexcited CO_2. The CO_2 is the in vibrationally excited through the reaction which occurs efficiently. " Pg. 1 [18]

3 Results

The results will follow in the order they are presented in the methods section.

3.1 N_2 and O_2 IR Spectra Predicted by Quantum Mechanics

N_2 and O_2's modes are predicted at the frequencies **2360 cm^{-1}** and **1580cm^{-1}** respectively – well within the infrared band of the electromagnetic spectrum, [19]. These modes are identified in the context of temperature, many papers reveal these predicted vibration functions[20], [21],[22]. Table 1 (below) is one example: and shows the predicted wavenumber where ω_e (column 3) of N_2 and O_2's predicted modes at 2360 cm^{-1} and 1580 cm^{-1}. In the RER these predicted modes of are revealed by Raman Spectroscopy in Figure 9 and Figure 10.

Table 1. Table of predicted N_2 and O_2 vibration modes derived from the Schrodinger equation [19]. The third column from the left shows the vibration mode wavenumbers. Note H_2 is predicted (and also Raman observed).

Molecular Data and Statistical Weights of the *J* Levels for some Linear Molecules[a]

Molecule	Molecular data: B_e (cm^{-1})	ω_e (cm^{-1})	$\omega_e x_e$ (cm^{-1})	α_e (cm^{-1})	r_e (Å)	Nuclear spin	Statistical weight (g_n): *J* (even)	*J* (odd)
$^1H_2$	60.80	4395	117	2.99	0.742	1/2	1	3
$^2H_2$	30.43	3118	64.1	1.05	0.742	1	6	3
$^{14}N_2$	2.010	2360	14.46	0.0187	1.094	1	6	3
$^{16}O_2$	1.446	1580	12.07	0.0158	1.207	0	0	1
$^{19}F_2$	0.86	892	...	...	1.435	1/2	1	3
$^{35}Cl_2$	0.2438	565	4.0	0.0017	1.988	3/2	6	10
$^{12}C^{16}O$	1.931	2170	13.46	0.0175	1.128	...	1	1
$^1H^{35}Cl$	10.59	2990	52.05	0.302	1.275	...	1	1
$^{12}C^{16}O_2$[b]	0.3906 (B_0 = 0.3895)				1.162 (r_0 = 1.163) 1.202 (CC)	0	1	0
$^{12}C_2{}^1H_2$[b]	1.1838 (B_0 = 1.1769)				(r_0 = 1.207) 1.059 (CH) (r_0 = 1.059)	1/2	1	3

[a] Reference (*1*).
[b] Reference (*6*).

570 / *Journal of Chemical Education*

3.2 Atmospheric IR and Raman IR Spectra Lines

Table 2 below shows all the emission spectra modes for the atmospheric gases, derived solely from the radiation physics principles listed above (4.1). The modes are both IR and the Raman. The outstanding issue from this table, and the central issue to this paper, is that the listed Raman Modes or Spectra (also shown on the spectrogram Figure 52) are not considered to behave as so-called 'IR-active' modes; in that they do not radiate or emit any IR radiation – further contravening with the above principles of physics. These are the Raman modes as they are known. They are: CO_2's **1338 cm^{-1}**, H_2O's **3652 cm^{-1}** and CH_4's two **2914 cm^{-1}** and **1303 cm^{-1}**. These Raman modes, among others, are shown clearly in Figure 7 in normal atmosphere by Raman spectroscopy.

Table 2. Atmospheric Gases with their Respective IR Range Vibrational Modes. Modes highlighted in red are of particular interest; they, through the law of equipartition show all modes are the equivalent – and it as the detectors of them that are different.

Molecule	Vibration Mode or Band: Wavenumber (frequency)	IR (Thermoelectric) and IR Raman Spectroscopy Properties	Mode Type
H_20	**3652 cm^{-1} (2.74μm)**	**IR and Raman**	**Symmetric**
	1595 cm^{-1} (6.25μm)	**IR and Raman**	**Asymmetric**

	3756 cm^{-1} (2.66μm)	IR and Raman	Asymmetric
CO_2	1388 cm^{-1} (7.2μm) 2349 cm^{-1} (4.257μm) 667 cm^{-1} (14.992μm)	IR and Raman IR IR	Symmetric Asymmetric Asymmetric
CH_4	3020 cm^{-1} (3.312μm) 2914 cm-1 (3.431μm) 1508 cm^{-1} (6.5μm) 1303 cm-1 (7.7μm)	IR Non IR; Raman IR Non IR; Raman	Asymmetric Symmetric Asymmetric Symmetric
N_2	2338 cm-1 (4.2μm)	Non IR; Raman Active	Symmetric
O_2	1556 cm-1 (6.25μm)	Non IR; Raman Active	Symmetric
O_3	1103 cm-1 (9.1μm) 1042 cm-1 (9.6μm) 701 cm-1 (14.3μm)	IR (Raman Active?) IR IR	- - -
N_2O	2224 cm^{-1} (4.5μm) 1285 cm-1 (7.8μm) 589 cm-1 (17μm)	IR IR IR	- - -

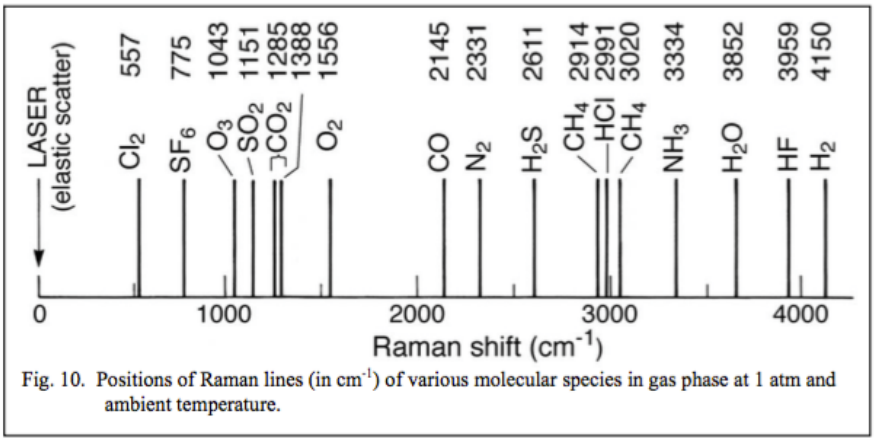

Fig. 10. Positions of Raman lines (in cm^{-1}) of various molecular species in gas phase at 1 atm and ambient temperature.

Figure 7. The Raman Atmosphere. Spectrograph of the Earth's Atmospheres gases and their Raman modes. [23] Notice these frequencies (of the molecules) are not (from the table above) IR in nature, and are not symmetric in nature.

3.3 Raman Gas Vibrational Modes Observation

Raman Spectrometers – the complement instrument of 'IR' spectrometers – were found to observe the QM predicted IR spectra modes of the non-GHGs.

The Raman active vibrational modes of atmospheric gases N_2, O_2 and CO_2 were observed at the (Table 2) predicted wave numbers and shown as a report in Figure 8 below:

"...infrared and Raman spectra: the interaction of the molecule with electromagnetic radiation. The interaction of the electric vector of the electromagnetic radiation with the molecule will give rise to infrared absorption and inelastic scattering (Raman) spectra..."pg. 12 [24]

"Raman data were obtained which could be used to accurately measure the mole fractions of the major species in the flow, i.e, N_2, 0_2, and $C0_2$ over the entire range of engine operation conditions from idle to full power. These Raman measurements were compared with the expected values of the specie concentrations as calculated from the measured fuel:/air ratio of the various operating conditions." (P.2) [25]

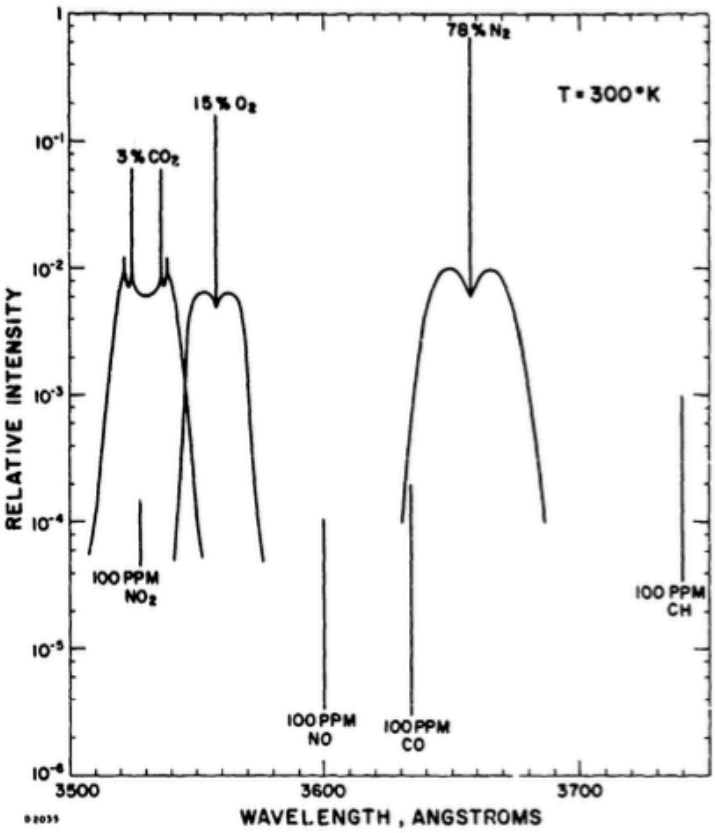

Figure 3 Typical Raman Spectrum from Room Temperature Combustion Gases Using a 3371 Å Laser Source

Figure 8. RER Raman Atmosphere Spectra. Pg. 7 [15]

Notice not only the wave numbers for the different gases are shown but also their respective concentrations.

The following figures show Raman Spectra in detail:

"*Initial tests were conducted in air at the AVCO Everett Laboratories to verify the predicted performance of the laser Raman field unit. Figures 18, 19, and 20 show spectra obtained in the spectral regions that correspond to vibrational transitions in N2, NO and H20 at 2330 cm-1, 1876 cm-1 and 3652 cm-1 that will produce Raman lines at 3658, 3600, and 3844 Å, respectively. "* Pg. 43

3.3.1 N2 2338cm Raman Vibrational Mode Spectra

The Raman spectra of N_2 molecule's 2338 cm^{-1} mode is shown below in Figure 9.

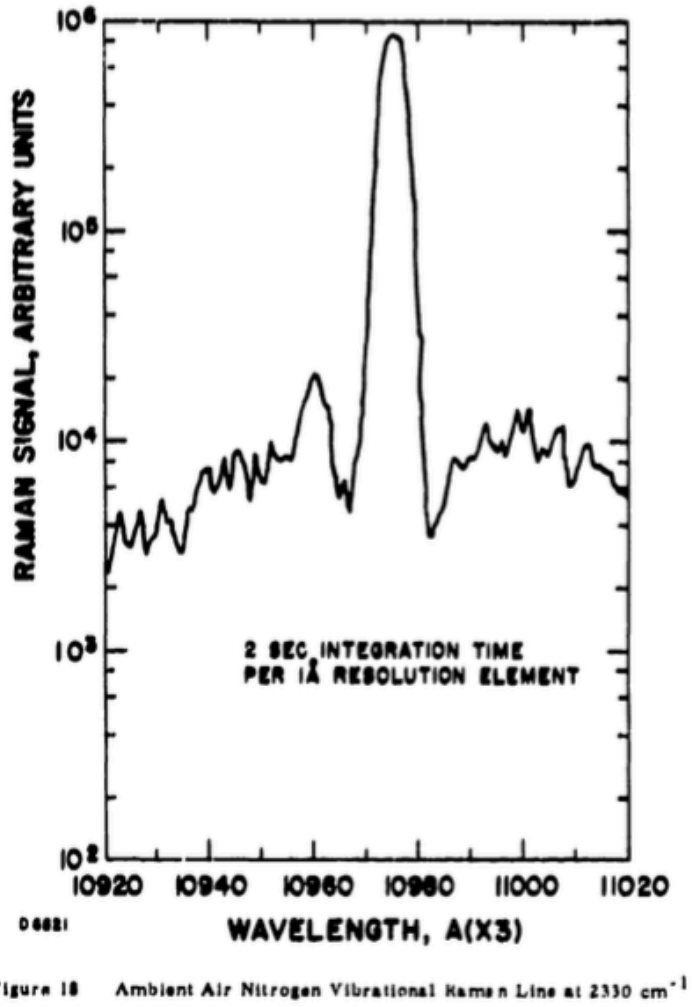

Figure 9. 'Figure 18' N_2 2330 cm^{-1} Raman Spectra. Pg. 32 [25]

3.3.2 O_2 1556 cm^{-1} Vibration Mode and Concentration

O_2 was not the molecule of attention; however, the Raman spectra were observed to calculate concentration levels.

"Raman measurements were made of the 0_2 concentrations in the T-53 engine exhaust. These measurements show excellent agreement when compared with the expected values of the concentration on the basis of the measured fuel/air ratio from the operating engine. Typical data of the O_2 vibrational Raman line in the hot exhaust gases are shown in Figure 31. The system was calibrated in the field for effective cross section and system transfer function by using the $0_2/N_2$ ratio obtained from ambient air and by assuming that air is 21% 0_2 and 78% N_2 on a mole basis. "(P.43)

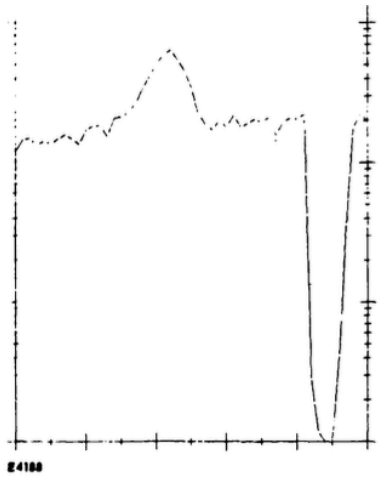

Figure 31 Typical Spectral Data of O_2 in Hot Exhaust Gases

Figure 10. O_2 1556 cm^{-1} Raman Spectra. Pg. 41 [25]

3.3.3 H_2O 3652 cm^{-1} Vibrational Mode

H_2O's Raman mode was observed; its spectra is shown in Figure 11 below.

"Water vapor detection is shown in Figure 20 (below), where a signal/noise ratio of about 100 at a relative concentration of about 1% of the atmospheric nitrogen signal is observed." (P. 31)

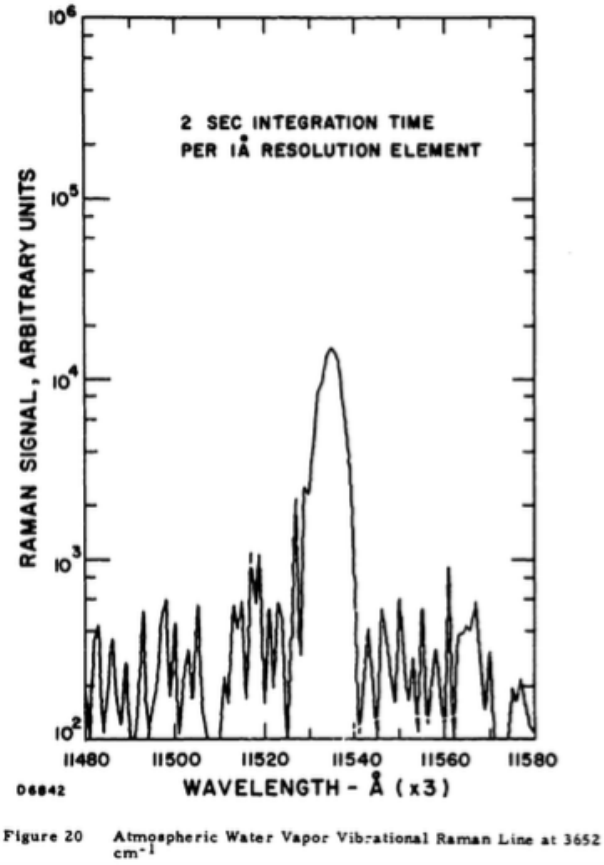

Figure 11. H_20 3652 cm^{-1} Raman Spectra. Pg. 34 [25]

3.3.4 CO_2 1338 cm^{-1} Vibrational Mode (and Temperature)

Carbon dioxide's predicted 1338 cm^{-1} mode was observed and its spectra are shown in Figure 12 below.

"A further example of a room temperature Raman spectrum is shown in Figure 17, which is the spectrum of the CO_2 doublet at 1285 cm^{-1} and 1388 cm^{-1} wave numbers."

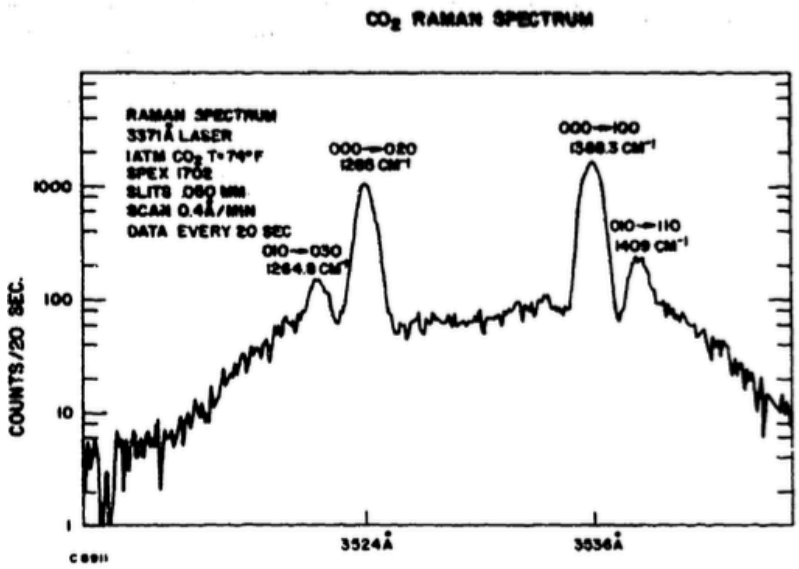

Figure 17 Experimental Raman Spectrum of Carbon Dioxide at Room Temperature

Figure 12. CO_2 1338 Raman Spectra [15]

"Of special interest is the appearance of secondary peaks at 1265 cm^{-1} and 1409 cm^{-1} wave numbers which correspond to transitions from the lowest excited vibrational level of CO_2, the 010 level. This level is appreciably populated even at room temperature. Measurement of the ratio of the secondary to the primary peak is a sensitive means of temperature measurement throughout the temperature range of interest for turbine exhausts as will be shown later in this report." [15] (P.32)

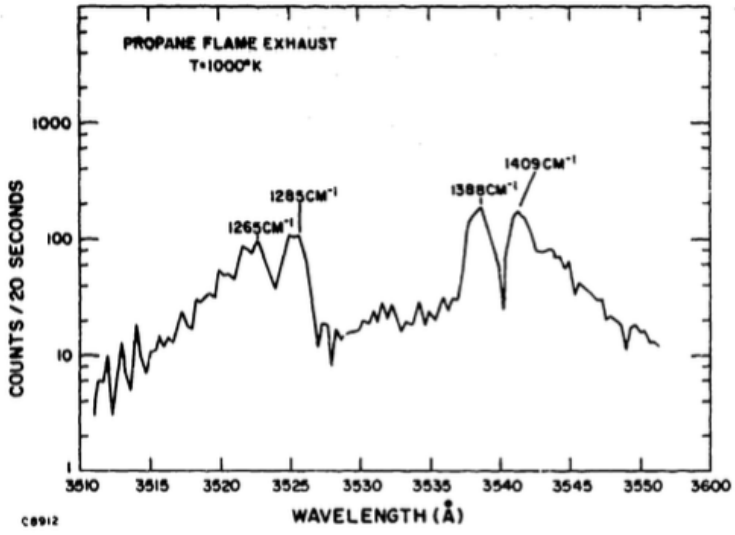

Figure 20 Experimental Raman Spectrum of Carbon Dioxide at ~1000°K in a Propane/Air Burner Exhaust

Figure 13. CO2 Spectra. Pg. 33 [15]

3.4 Gas Temperature Measurement by Raman Spectroscopy

Temperature measurements were made from Raman Active modes of the atmospheric gases, as follows:

"The temperature profiles obtained in this way (Raman) are plotted in Figure 37 and appear quite reasonable. Thermocouple measurements in the exhaust stream gave an average of 7250 K for the 7% power point and 8900 K for the 100% power point, which is good agreement with the Raman data. ***Since it is not subject to thermocouple heat loss corrections, the laser Raman data is inherently a more reliable and accurate' thermometer than a thermocouple****. Further work is required however to definitely establish the precision of the laser Raman method as a hot gas temperature measurement technique. (p. 54)"*

3.4.1 N_2 Temperature

"Accurate temperature profiles were obtained in the T-53 ***exhaust using laser Raman scattering from nitrogen*** *via the density method. The spectral analysis of "hot bands" was found to be a less accurate method in the T-53 exhaust because of the high level of laser induced fluorescence. Although the feasibility has now been demonstrated, further work is required to quantify the precision of the laser Raman method for temperature measurements in aircraft engine exhaust streams." (Pg. 59)[25]*

"The sensitivity of the method is shown in Figure 27, which is a plot of the ratio of the Raman scattering at 3634 Å to the Raman scattering at 3658 Å for pure nitrogen as a function of temperature. Over the expected range of turbine exhaust operation, i. e. 9000K to 12000 K. the uncertainty in the ratio is 9% per 100°K or about 1%per 11K temperature uncertainty- an attainable value using the (010)/(000) CO2 Raman ratio method as.. discussed. Since the Raman intensity in the AJ = -2 side band of N_2 (with circular polarization) corresponds to about an apparent level of 1000 PPM of CO a 1% measurement of the side band intensity

would enable detection and measurement of 10 PPM CO. This is difficult, requiring an S/N of 100 at low signal levels, but can in principle be done." (P.41)[15]

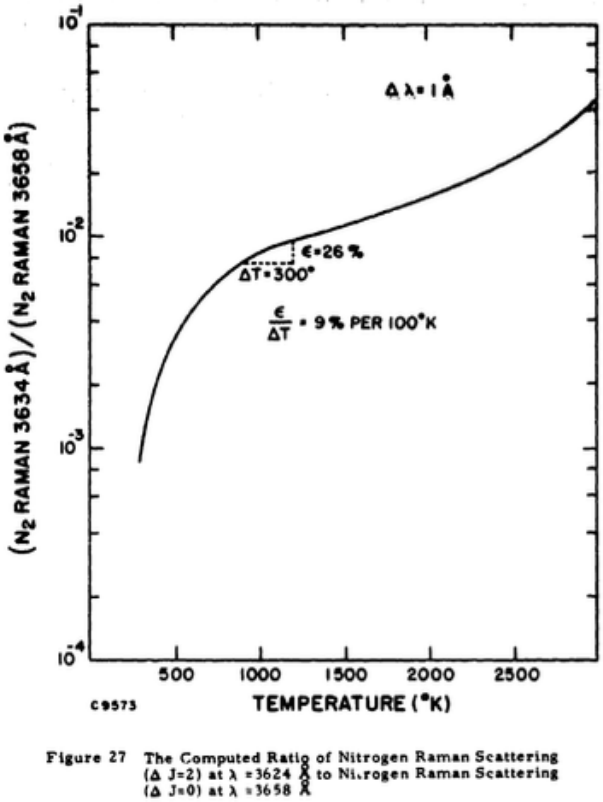

Figure 27 The Computed Ratio of Nitrogen Raman Scattering (Δ J=2) at λ =3624 Å to Nitrogen Raman Scattering (Δ J=0) at λ =3658 Å

Figure 14. N_2 Prediction to Observation. Temperature measurement of a Non GHG by Raman spectrometer at N_2's 2330 **cm^{-1}** predicted mode. Pg.43 [15]

"5. TEMPERATURE SENSITIVITY

The effects of increasing temperature become important to the laser Raman turbine exhaust analysis system in many ways. Foremost is the effect on the ratio of the peak Raman signal intensity of a particular species to the actual concentration of that species. The tacit assumption in previous work has usually been that the Raman signal is proportional to species concentration. However, over the temperature range of interest this proportionality constant is somewhat temperature dependent. "

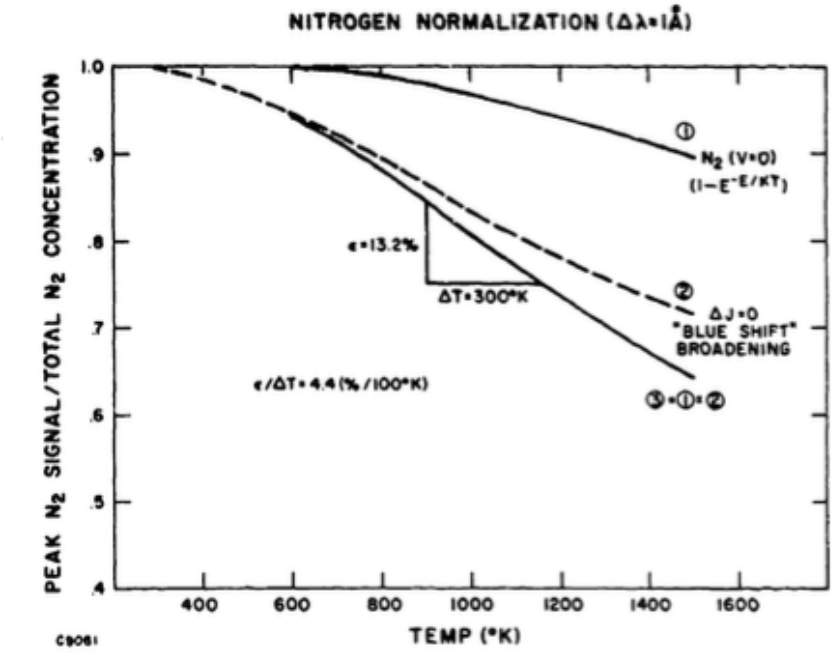

Figure 21 Computed Nitrogen Normalization Error as a Function of Temperature for a Detector with a Resolution of 1 Å

Figure 15. N_2 Temp. Pg.34 [15]

3.4.2 Raman CO_2 Temperature

"Figure 22 shows the estimated ratio of the peak (000) CO_2 signal to the total CO_2 concentration as a function of temperature.

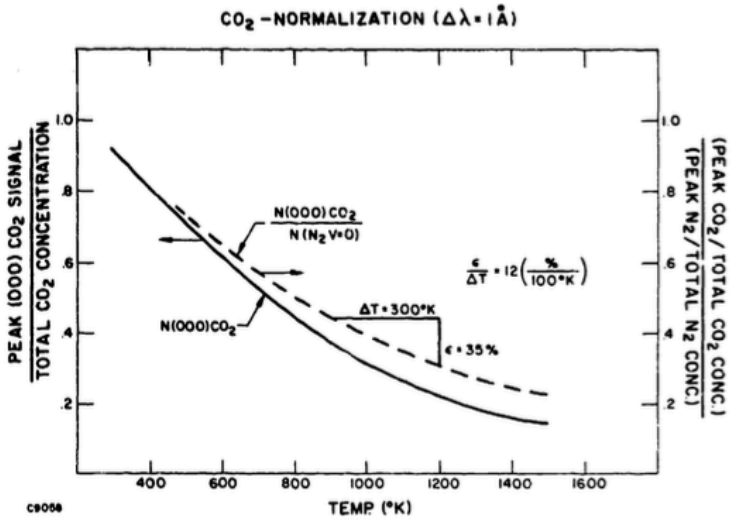

Figure 22 Computed Carbon Dioxide Normalization Error as a Function of Temperature for a Detector with a Resolution of 1 Å

Figure 16. CO_2 Temperature Measurement by Raman Spectrometer. Pg 35[15]

From the above, it is apparent that an independent method of temperature measurement is a desirable adjunct to a laser Raman turbine exhaust measurement system. The use of the CO_2 Raman spectrum seems to be a reasonable means to satisfy this requirement. ***In particular the measurement of the ratio of the (000) CO_2 peak to the (010) CO_2 peak seems especially well suited for a temperature determination.***

Also shown in Figure 23 are two experimental points representing a room temperature determination which agreed exactly with the theoretical curve and a higher temperature data point obtained from the propane/air burner exhaust CO2 spectra.

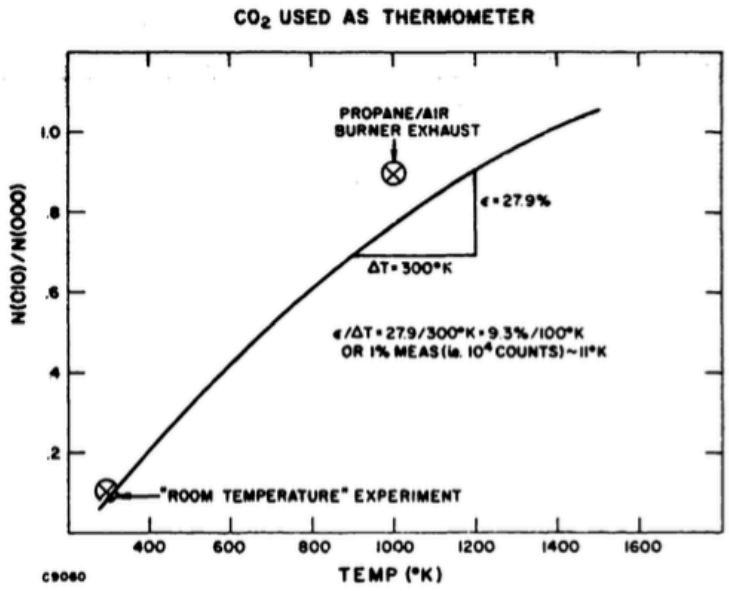

Figure 23 The Computed Temperature Dependence of the Ratio of the Raman Scattering from the 010 Level of CO_2 to the Raman Scattering from the 000 Level of CO_2. Two Experimental Points are shown.

Figure 17. CO_2 as Thermometer – by Raman Spectroscopy. Pg. 37 [15]

The disagreement of the high temperature data point with respect to theory is probably caused by a combination of noise and the positioning error of the thermocouple used to measure the temperature vs. the position of the laser focal point in the propane burner exhaust. More careful experiments to verify this theoretical curve and/or to calibrate the functional relationship of N(010)/N(000) vs temperature should be conducted. " [15](P.32)

3.5 Gas Concentrations by Raman Spectroscopy

Gas concentrations for the following atmospheric gas were measured:

3.5.1 H_2O Concentrations

"The water vapor Raman data that was obtained from the exhaust of the T-53 engine is shown in the following tabulation: "

Power Setting	*Raman Measurment*	*Calculated From F/A*
(1)	*(2)*	*(3)*
7%	*0.0274*	*0.0372*
30%	*0.0216*	*0.0416*
100%	*0.0226*	*0.0567*

The Raman Measurement values in (2) are the ratios of the peak value of the water Raman signals in the 3652 cm^{-1} band to the peak value of the nitrogen Raman signals at 2330 cm^{-1}. The system was calibrated - using the ambient air values. The calculated values used the same F/A data as was used in the above O_2 and CO_2 comparisons and included a slight correction for the ambient air water vapor."(P.51)

3.5.2 CO_2 Concentration

"The response of the laser Raman instrument to $C0_2$ was calibrated at the beginning of the test program with a T53 engine by using the previous conventionally measured C02 concentration from this engine at the 60% power setting. ... These data are displayed in Figure 33, which shows the volume percent CO_2 as a function of the percent shaft horsepower of the engine." Pg. 59 [25]

"Similar Raman measurements were made of the CO_2 concentration in the T53 turbine engine exhaust and are shown in Figure 33 (below). ***The Raman data were normalized to the (IR) gas analysis data at the 60% power point****. Absolute CO2 calibrations using the atmosphere were not conducted in the field*

because of the uncertainty in the C02 concentration of the air in the Bridgeport, Connecticut industrial area." (P.48)

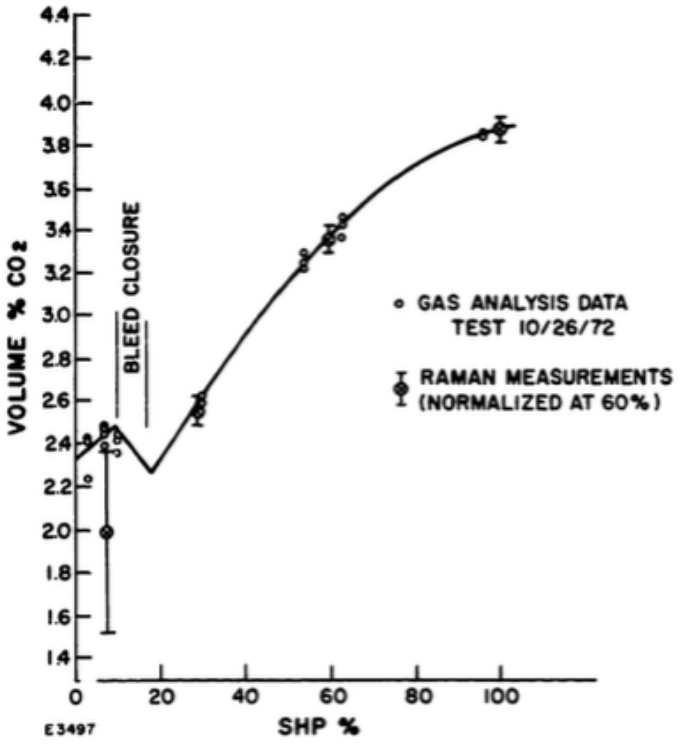

Figure 33 Volume % CO_2 as Measured from Raman Scattering vs Shaft Horse Power (SHP), %

Figure 18. CO2 Raman vs IR. Raman measurements taken at 1338 cm-1 match the IR 2349 cm-1 mode. Pg.50 [25]

3.5.3 N_2/O_2 Ratio

"The ratio of the corrected O_2 to N_2 Raman signals can then be used to obtain the O_2/N_2 mole ratio. The system was calibrated in the field for effective cross section and system transfer function by using the O_2/N_2 ratio obtained from ambient air and by assuming that air is 21% O_2 and 78% N_2 on a mole basis. The results of the oxygen measurements are shown in Figure 32 where the 0_2 /N_2 mole ratio is calculated from the fuel/air ratio of the operating T-53 engine, using an approximate value of hydrogen/carbon mole ratio of 2.0. Perfect agreement would cause the data to fall in the line connecting zero with the point labelled "air".

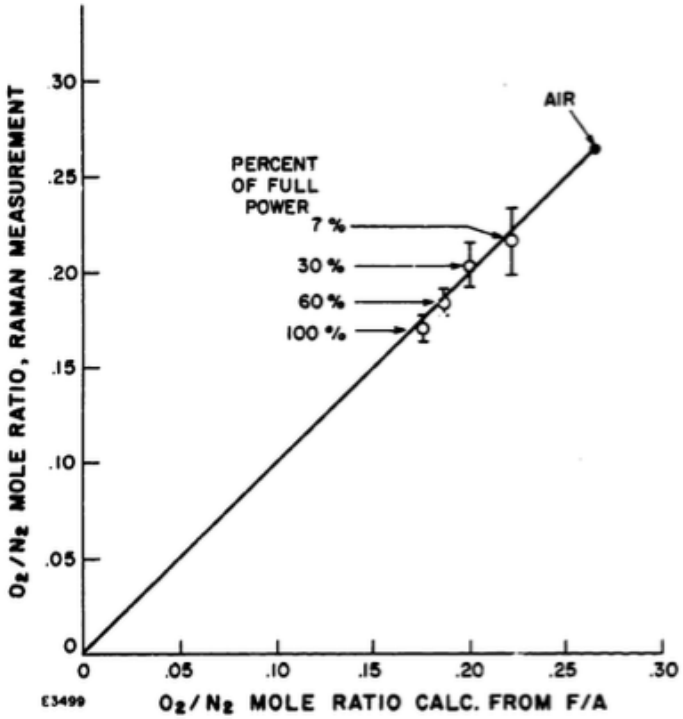

Figure 32 O_2/N_2 Mole Ratio for T-53 Engine Raman Measurement vs Calculated Value

Figure 19. N_2 O_2 Concentration Raman Measurements. Pg. 49 [25]

3.5.4 NO

"An attempt was made to detect nitric oxide (NO) in the T53 exhaust using the 1876 cm^{-1} vibrational Raman transition. The T53 engine typically produces 100 ppm of NO when operating at full power. Because the fluorescence level in the T53 at full power was about 100 times greater than the expected signal from NO, the required integration times for detection were longer than the test time available." (p. 51)

3.6 RER Conclusion

The following is the conclusion to the Raman exhaust report:

1. *Excellent agreement of (Raman) 02 and CO2 measurements with conventional exhaust gas measurements and correlations with engine fuel-air ratio.*

2. *Excellent agreement with smoke number measurements, with a calibration at one point only.*

3. *Good agreement of temperature profile measurements with thermocouple data.*

4. *Total hydrocarbons were detected and compared to flame ionization measurements to within a factor of +2 over a range of three decades of concentration.*

5. *Water vapor has been detected in exhausts under all conditions. Calibration requires fundamental water cross-section data as a function of temperature, which is not now available. "*

3.7 Raman lidar sensing of CO_2 leakage - Results

The Raman Lidar detected CO_2 concentrations at its Non-GHG Spectra Mode and Non-GHG N_2 as shown in Figure 20.

"Figure 6b shows the Raman signals of CO_2 and N_2 as a function of distance from the lidar system and the motorway. The increased CO2 Raman signals found at 400 and 750 m from the lidar system represent the locations of a local motorway (A) and the Gapcheondosi Expressway (B), respectively. The enhanced Raman signals of CO_2 at locations A and B in Figure 6b imply that the lidar system is capable of detecting spatially resolved Raman signals of CO_2 emitted from motor vehicles. The Raman lidar obtained clear and stable Raman scattering signals of N2 and CO2 at a distance of 900 m from the lidar system." Page 7.

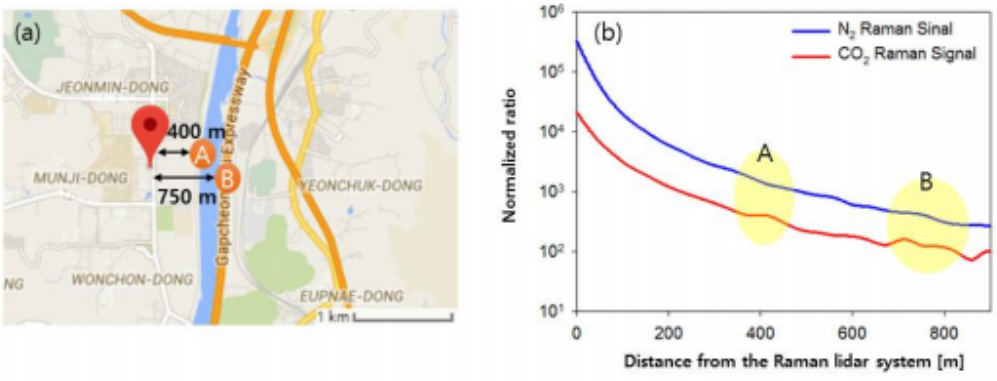

Figure 6. **(a)** Study area in Daejeon, Korea; **(b)** N_2 and CO_2 Raman signals measured by the Raman lidar system.

Figure 20. Raman Lidar Detecting CO_2 (at its Non-GHG Spectra Mode) and Non-GHG N_2.

In Figure 21 the Raman CO_2 measurement raises steadily, not showing the erratic ratios of the ground level detector, presumably a thermoelectric divice.

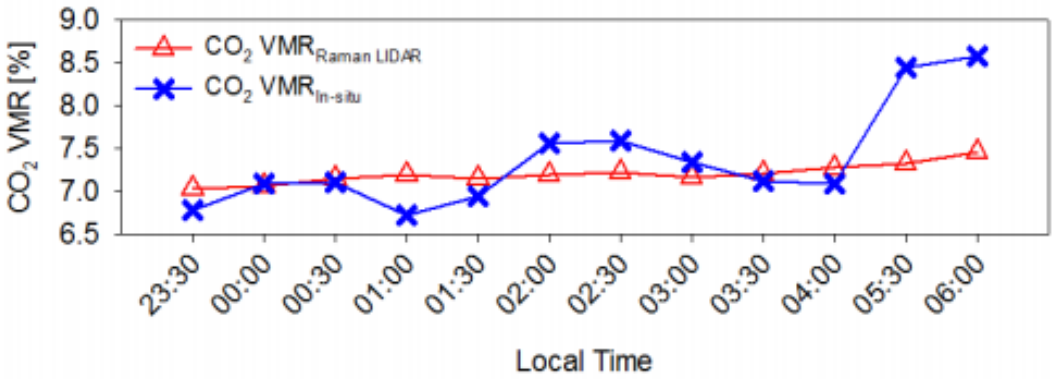

Figure 8. Time series of CO_2 $VMR_{In\text{-}situ}$ and CO_2 $VMR_{Raman\ LIDAR}$ on November 23, 2017.

Figure 21 Raman vs. IR Thermoelectric technology.

3.8 N_2-CO_2 Laser Results

The following is an exert on how a CO_2 laser operates from the book LASER PHYSICS by PETER W. MILONNI JOSEPH H. EBERLY page 51 [26]. It is a typical description of how the CO_2 laser directly implicates N_2's **2338** cm^{-1} mode. I have posted the direct text to show this is standard knowledge. It is important to look out for are the wavenumbers of the gases: particularly, N_2's **2330** cm^{-1} and CO_2's **1388** cm^{-1} and their role in the laser process.

"The electric-discharge carbon dioxide laser has a population inversion mechanism similar in some respects to the He –Ne laser: the upper CO_2 laser level is pumped by excitation transfer from the nitrogen molecule, with ***N_2 itself excited by electron impact****. The relevant energy levels of the CO_2 and N_2 molecules are vibrational-rotational levels of their electronic ground states. We discussed the vibrational-rotational characteristics of the CO_2 molecule in Section 2.5, and indicated in Fig. 2.10 the relative energy scales of the three normal modes of vibration, the so-called symmetric stretch, bending, and asymmetric stretch modes (Fig. 2.9). Like all diatomic molecules, N_2 has a single "ladder" of vibrational levels corresponding to a single mode of vibration (Fig. 2.7) (**2338**cm^{-1}). In Fig. 11.9 we show the CO_2 and N_2 vibrational energy level diagrams side by side. Figure 11.9 shows that the first*

excited vibrational level (v ¼1) of the N_2 molecule lies close to the level (001) of CO_2. Because of this near resonance, there is a rapid excitation transfer between N_2 (v ¼ 1) and CO2(001), the upper laser level. ***N_2 (v ¼ 1) is itself a long-lived (metastable) level, so it effectively stores energy for eventual transfer to***

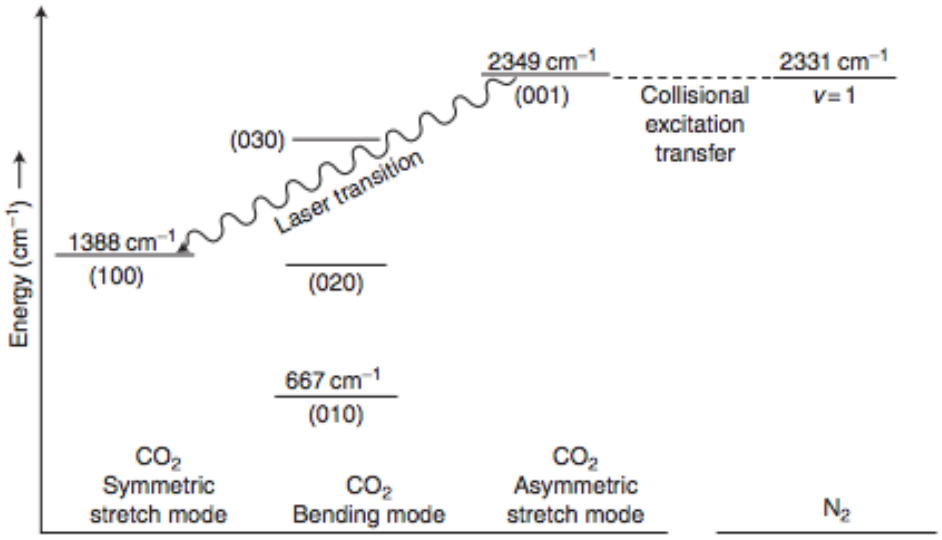

Figure 11.9 Vibrational energy levels of CO_2 and N_2. The energies are given in cm^{-1}, a unit corresponding to a frequency $(c)(1\ cm^{-1}) \approx 3.0 \times 10^{10}$ Hz, or an energy $h\nu \approx 1.2 \times 10^{-4}$ eV.

Figure 22 Vibrational Energy Levels of CO2 and N2. The claim of this paper is the quantum mechanism for the CO2 laser should be universal and stand for the atmosphere also.

CO_2 (001); it is also efficiently pumped by electron-impact excitation. As in the case of the He–Ne laser, therefore, advantage is taken of a fortuitous near resonance between an excited state of the lasing species and an excited, long-lived collision partner. Laser action in CO_2 lasers occurs on the vibrational transition (001) → (100) of CO2. This transition has a wave number around (2349–1388) cm^{-1} ¼ 961 cm^{-1} (Fig. 11.9), or a wavelength around (961 cm^{-1}) 21 ¼ 10.4 mm in the infrared. The laser wavelength depends also on the rotational quantum numbers of the upper and lower laser levels. For the case in which the upper and lower levels are characterized by J ¼ 19 and 20, respectively, the wavelength is about 10.6 mm, the most common CO_2 laser wavelength. The (100) and (020) vibrational levels of CO_2 are essentially resonant. This "accidental degeneracy" results in a strong quantum mechanical coupling in which states in effect lose their separate identities.

Furthermore the (010) and (020) levels undergo a very rapid vibration-to-vibration (VV) energy transfer:

$CO_2(020) + CO_2(000) \rightarrow CO_2(010) + CO_2(010)$: *(11:7:1)*

For practical purposes, then, the stimulated emission on the (001) → (100) vibrational band takes CO_2 molecules from (001) to (010). The (010) level thus acts in effect like a lower laser level that must be rapidly "knocked out" in order to avoid a bottleneck in the population inversion.

Fortunately, it is relatively easy to de-excite the (010) level by vibration-to-translation (VT) processes:

$CO_2(010) + A \rightarrow CO_2(000) + A$, *(11:7:2)*

where A represents some collision partner. The VT de-excitation of (010) effectively depopulates the lower laser level and also puts CO_2 molecules in the ground level, where they can be pumped to the upper laser level by the VV excitation transfer

$N_2(v ¼ 1) + CO_2(000) \rightarrow N_2(v ¼ 0) + CO_2(001$ *(11:7:3)*

In high-power CO_2 lasers the lifetime of the $CO_2(010)$ level may be on the order of 1 ms due to collisions of CO_2 with He, N_2, and CO_2 itself. Of course, the VT process (11.7.2) is exothermic and results in a heating of the laser medium; some of the other VT and VV processes in the CO_2 laser have the same effect. This heating of the laser medium is a very serious problem in high-power lasers. In the next section we will see how it may be overcome. Electron impacts excite CO_2 as well as N_2 vibrations. "

3.9 Natural N_2-CO_2 Lasers

NASA and others have discovered natural lasers on the likes of Mars and Venus [27] and below [28] is demonstrated how they – in the similar way as the laboratory ones – operate. Again, this repeats the role of radiation has on atmospheric gases.

*"000 to 101 followed by a resonant collisional energy transfer of a V3 quantum to another CO2 molecule (**2349**cm^{-1}), which is similar to the laboratory CO2 laser (Fig 8.6)."*

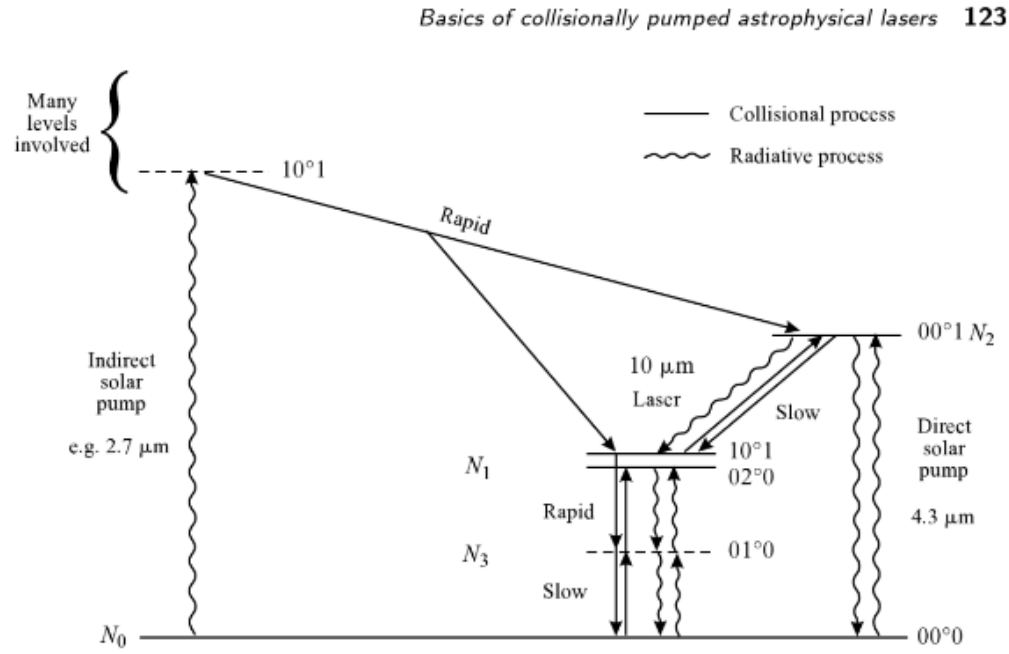

Fig. 8.6 Molecular physics of a natural CO_2 laser. Radiative and collisional processes affecting the pumping of this laser in the mesospheres of Mars and Venus are identified.

Figure 23 Natural CO_2 Lasers. Showing CO_2 lasers are natural and that N_2 is implicated at its respective vibration mode.

3.9.1 'Blackbody CO_2 Laser' Showing N_2 Heated by Sunlight

It is very difficult to directly show N_2 is directly radiated by the Sun's energy, absorbing IR photons; however, the following experiment shows indirect confirmation of the hypothesis: N_2 is 'heated' (and heats) – i.e. absorbs (and emits) – by sunlight.

The extract below is taken directly from the 'NASA Technical Paper': A Blackbody-Pumped CO_2-N_2 Transfer Laser, by Young and Higdon [29].

"One laser concept that may achieve such efficiencies is the blackbody-pumped CO_2 transfer laser. Such a system is called a fluid-mixing or transfer gas-dynamic laser and is shown in conceptual form in figure 1.

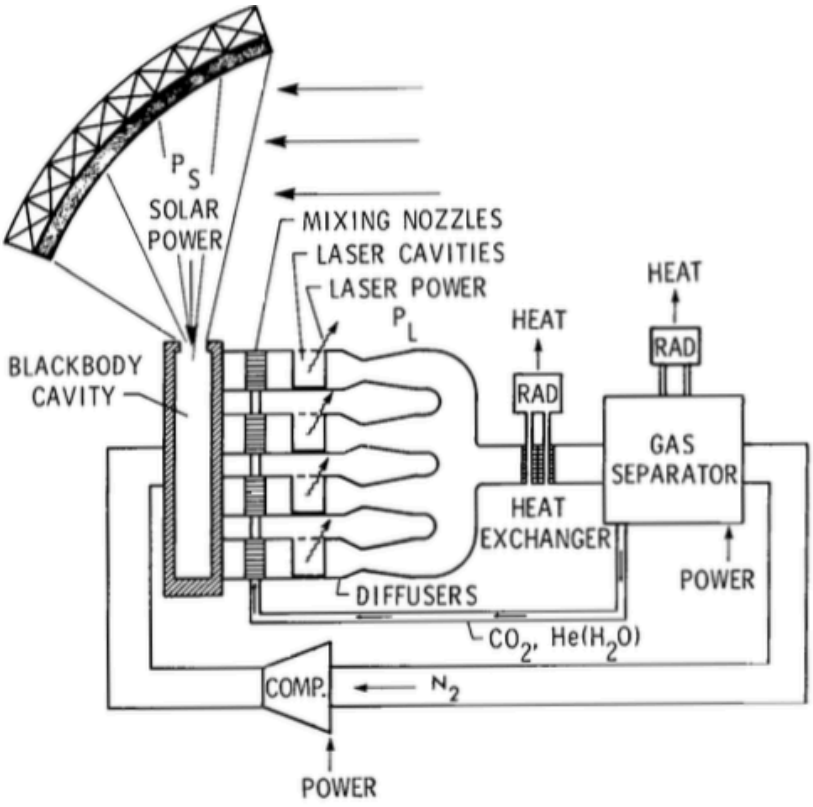

Figure 1. A conceptual design of a space-based blackbody N_2-CO_2 transfer laser.

Figure 24. Demonstrating N_2 Excitation from the Sun.

In this system, a black body cavity is heated by collected sunlight ('solar power') to a temperature of approximately 2000 K. ***Nitrogen gas passing through the cavity is heated to the blackbody temperature.*** *The vibrationally excited N_2 then passes through a nozzle into a low-pressure laser cavity. Here CO_2 and He are mixed with the vibrationally excited N_2. A coincidence between N_2 (v=1)* ***(2338*** *cm^{-1}) and the 001 asymmetric longitudinal mode (**2349 cm^{-1}**) of CO_2 allows rapid transfer of the N_2 (v = 1) vibrational energy into the CO_2 001 upper laser level. Lasing commences between the 001 and the 100 levels at 10.6 microns. "*

3.9.2 Experimental Setup

"Standard purity N_2 flowed through a quartz tube within an electrically heated, which in the present experiment simulates a solar-heated blackbody cavity. The oven temperature and pressure were monitored. The gas velocity was slow enough (226 cm/sec) to allow the N_2 temperature to come into equilibrium with the oven

temperature... CO_2 and He were then mixed with the vibrationally excited N_2 to cause a transfer of energy from the N_2 ($v = 1$) to the CO_2 upper laser level. "

4 Discussions

I found N_2 and O_2 do have spectra in the IR range of the electromagnetic spectrum. These spectra are predicted by the quantum mechanics Schrodinger equation, and these spectra, along with their respective temperatures, are only observed and measured by Raman Laser Spectroscopy – IR spectroscopy's known complement instrument. With respect to this finding alone, there has been a clear **systematic error** identified with respect to measurements of the IR qualities and quantities. It was further found, by the application and operation of the N_2-CO_2 laser N_2 absorbs radiation – whether by (radiation) of electrical discharge or by photons, at the predicted and observed spectra. These findings contradict and collapse GH theory, as we understand it.

If we think of the different IR spectra as colours – not an unreasonable assumption considering they share the same quantum properties as the 'visual' colours – using only 'IR' instruments we are literary colour blind – hence the systematic error. With Raman Spectroscopy we are no longer 'IR' colour blind to the non-IR colours, the picture is full.

The standard reason given for this discrepancy between the GHGs and non-GHGs is clear: spectra-modes without an electric dipole moment are assumed not to absorb, and as N_2 and O_2 only have one spectra mode in the IR, so this rules them out. I argue this interpretation is wrong. I have found the Raman active modes are IR. H_2O for instance was found to be both IR and Raman active, and argon's mode, on the other hand, was found to be neither 'IR' or Raman active – but none the less shares a comparable specific heat capacity, so something is missing there too.

The following discussion first addresses the direct question of this paper and then expands to address issues arising from the findings – what really are the special GHGs? While this section will focus directly on the above RER experiment results, it will– using principles and applications known to physics – also broaden to address the implications of this work on thermoelectric and Raman spectroscopy application and theory, and our general understanding of climate and other related areas. It will also bring in applications of Raman and

thermoelectric devices, and applications of atomic radiation theory, all in support of this paper's hypothesis.

4.1 The Laws and Physics Central to Radiation Theory

Before discussing the experiment, it may be important to show and remind ourselves of the physics at stake when it is assumed matter does not radiate IR. The following is a list the physics behind radiation theory. It was tested whether these apply to the atmospheric molecules – whether or not they are GHGs.

4.1.1 Planck's Law

"Planck's law describes the spectral density of electromagnetic radiation emitted by a black body in thermal equilibrium at a given temperature T."

4.1.2 Boltzmann Constant

The Boltzmann constant is a fundamental constant of the universe, which links the kinetic energy movement of molecules in a gas with temperature. By the Boltzmann constant, the observation of these and all vibrational modes at the said predicted frequencies, and their respective temperature measurement thereof, implies these modes are moving and thus are radiating IR.

4.1.3 The Stefan-Boltzmann Law

The Stefan-Boltzmann law is a central pillar to radiation theory, and states the following:

"All objects actually emit radiation if their temperature is greater than absolute zero. Absolute zero is equal to zero Kelvin, which is equal to -273°C or -460°F. An object that absorbs and emits all possible radiation at 100 percent efficiency is called a blackbody.

*The Stefan-Boltzmann law, a fundamental law of physics, explains the relationship between an object's temperature and the amount of radiation that it emits. This law (expressed mathematically as E = σT4) states that all objects with temperatures above absolute zero (0K or -273°C or -459°F) emit radiation at a rate proportional to the fourth power of their absolute temperature. E represents the maximum rate of radiation (often referred to as energy flux) emitted by each square meter of the object's surface. The Greek letter "**σ**" (sigma) represents the*

Stefan-Boltzmann constant (5.67 x 10^{-8}W/m^2K^4); and T is the object's surface temperature in Kelvin. The W refers to watt, which is the unit used to express power (expressed in joules per second)." [30]

4.1.4 Kirchhoff's Law of thermal radiation

For an arbitrary body emitting and absorbing thermal radiation in thermodynamic equilibrium, the emissivity is equal to the absorptivity. Good emitter; good absorber.

4.1.5 Spectroscopy:

*"The study of the interaction between electromagnetic radiation (**h**ν) and matter is called spectroscopy; where radiation is emission or transmission of energy in the form of waves or particles through space or through a material medium. Interaction takes place by absorption and by emission, and is explained by quantum mechanics. **Emission spectroscopy** is a spectroscopic technique which examines the wavelengths of photons emitted by atoms or molecules during their transition from an excited state to a lower energy state. Each element emits a characteristic set of **discrete wavelengths** according to its electronic structure, and by observing these wavelengths the elemental composition of the sample can be determined. Emission spectroscopy developed in the late 19th century and efforts in theoretical explanation of atomic emission spectra eventually led to quantum mechanics." General reference.*

4.1.6 Quantum Mechanics Schrödinger Equation

From quantum mechanics – the fundamental physics theory in which describes nature on the smallest scales of energy levels of atoms and subatomic particles – this equation, the Schrödinger equation, is used to calculate the predicted vibrational modes or absorption-emission spectra of atoms and molecules.

4.1.7 Equipartition Principle

By all accounts, the equipartition simply states that the energy absorbed or emitted is shared equally over all modes or spectra of a molecule. This assumption is an essential assumption to understand to unlocking the systematic error presented here.

4.2 Quantum Mechanics IR Spectra Predictions

All modes, particularly for this investigation N_2 and O_2, are predicted by the quantum mechanics and the Schrödinger equation – the centrepiece of modern atomic physics. This prediction is consistent with standard quantum mechanics and emission spectra understanding. This equation predicts the atomic vibrational mode frequencies for all matter, including the atmospheric gases

In the IR of the EMS the modes are divided into 'IR active' and Raman Active'.

GH theory totally ignores these Raman modes of the diatomic molecules, and the 'Raman active' modes within the so-called GH gases. N_2 and O_2 are not the only molecules affected by this assumption. The **1338 cm^{-1}** mode of CO_2 itself is also out; so too are all of water's (H_2O) modes, particularly its 3652 cm^{-1}, and also two of CH_4's modes, 2914 cm^{-1} and 1303 cm^{-1} – all for the same assumed reason: no electric dipoles at those modes. This is not a coincidence; that they have been divided and one group dismissed – it is a mistake.

4.3 Temperature Measurement by Raman Spectroscopy

It has been demonstrated throughout this paper thermoelectric detectors cannot measure the temperature of N_2 or O_2; but, here Raman spectrometers demonstrate clearly, they can not only detect the modes or spectra of the molecule, they can also measure the temperature of the molecule from the intensity or kinetic energy of the spectra signal. This fact alone should make Raman spectroscopy the default GHG-detecting instrument.

The following is from a range of papers and current knowledge associated with the temperature measuring properties of Raman spectrometers.

4.3.1 Raman Thermometry

The following is from expert by David Tuschel on Raman Thermometry [16]; it defines – among other – how it works.

"Raman spectroscopy can be used to determine the temperature of a material when other more direct means are either impractical or not possible. The material's temperature can affect the peak position of Raman bands. When a Raman band shifts significantly with temperature, the monitoring of the peak

position can be the most straightforward manner of determining temperature provided the Raman spectrometer has sufficient spectral resolution. Another method is to determine the temperature from the ratio of the Stokes and anti-Stokes signal strengths of a given Raman band. The latter method requires the ability to detect light at wavelengths longer and shorter than that of the laser and an accurate measurement of the wavelength-dependent instrument response function…"

In and other paper, the ability of Raman spectrometers to measurement the temperature of CO_2 is made clear. Keep in mind the 'Raman' spectra for CO_2 - like N_2's and O_2's is non-GHG and thus assumed not to absorb or emit (IR) heat.

Vibrational Raman scattering temperature measurements[31]

Abstract

"Experimental data and analyses are presented for the determination of gas temperature by measurements of vibrational Raman scattering intensity ratios of Stokes Q-branch fundamental bands. The method is demonstrated for two thermal equilibrium experiments: (1) CO2 (a gas well-suited for use in multi-component mixtures near ambient temperatures) in a test cell, and (2) N2 (a gas well-suited for use at elevated temperatures) in a flame. This method of temperature measurement is of particular value for non-thermal equilibrium conditions, for which vibrational excitation temperatures can be assigned to each pair of vibrational level corresponding to observable Raman bands."

4.3.2 Measurement at Ambient Temperatures

It appears Raman spectroscopy does not have the accuracy to measure ambient temperatures so well – as summarised in the following NASA paper:
DETERMINATION OF GAS TEMPERATURES FROM LASER -RAMAN SCATTERING [32]

SUMMARY

A theoretical model of the Raman rotational spectrum of a gas mixture was formulated and applied to an air mixture of oxygen and nitrogen. Theoretical

spectra were calculated as a function of temperature and compared directly to spectra obtained experimentally. The comparison, made at temperatures within the range 243 to 313 K, showed the model to be accurate. An error analysis was then performed yielding theoretical and experimental temperature measurement accuracies. The theoretical error predicted for the temperature range used was ±20 K (~7 percent), which compared well with experimental data. The best experimental error was ±13 K (~5 percent). It was concluded that, within the limits of this experiment and the preceding accuracies, the temperature of a gas mixture can be measured by using Raman scattering."

However, in a paper titled: Atmospheric temperature measurements made by rotational Raman scattering [33] Raman is found to be able to measure the atmosphere's temperature: *"Rotational Raman scattering of light from the second harmonic of a Nd:YAG laser is used to measure atmospheric temperature at altitudes of 3 to 20 km."*

This is also supported by: Rotational Raman-Based Temperature Measurements in a High-Velocity Turbulent Jet [14]

4.3.3 Raman Flame Temperature Measurement

Raman spectrometers exquisitely measure the temperatures of flames – and the surrounding air. The following image shows how it works. From this we should ask: does a flame radiate? Does it have an emissivity? And if so, does this legitimise Raman spectroscopy as a measure of radiation?

Of course, the flame radiates IR radiation; and it does so from the quantum predicted spectra that are observed and measured here by Raman spectrometers.

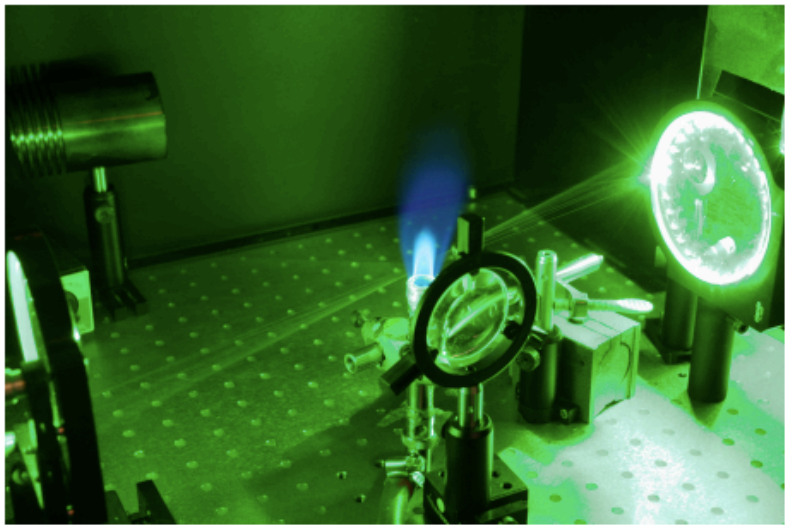

Figure 5: *Photography of the cavity taken during flame measurements, showing the two mirrors, the laser beam focused in the flame, and the first of the two lenses focusing the Raman-scattered signal into the spectrometer.*

Figure 25. Raman Flame Temperature Measurement. [34]

The following is taken from experts in the field of Raman flame measurement. It gives strong support to Raman theory and atmospheric measurements [35].

Raman spectroscopy is a technique that has one benefit and one major drawback. The benefit is that you can theoretically measure all different species in a region at once. The drawback is that the signal strength is very low, usually limiting measurements to the major species. In flames this usually means N2, fuel, O2, CO2 and H2O.

The Raman signal depends on a number of parameters. The most important are the so-called Raman cross section and the wavelength of the incoming light. The Raman cross section reflects the probability for Raman scattering and is species specific. The wavelength of the incoming light is important since it strongly affects the strength of the Raman signal. Just like for Rayleigh scattering, the signal strength depends on the wavelength raised to the fourth power. This means that if you change laser wavelength from 532 to 266 nm you gain roughly a factor of 16 in signal intensity. Remembering the extremely low signal intensity of Raman scattering, this is very useful. The Raman signal is further temperature and pressure dependent through the number density N that, given the ideal gas law, follows N = pV/RT.

In Fig. 1 is shown an image if the Raman signal from a Bunsen burner. The upper image shows the spatially resolved spectrum acquired just over the burner edge. The y-axis denotes the distance from the center of the burner. The x-axis shows the Ramanshift in cm-1 from the laser wavelength, 266 nm. The lower image shows the Raman signal along three different positions in the flame. The difference in relative species concentrations is evident.

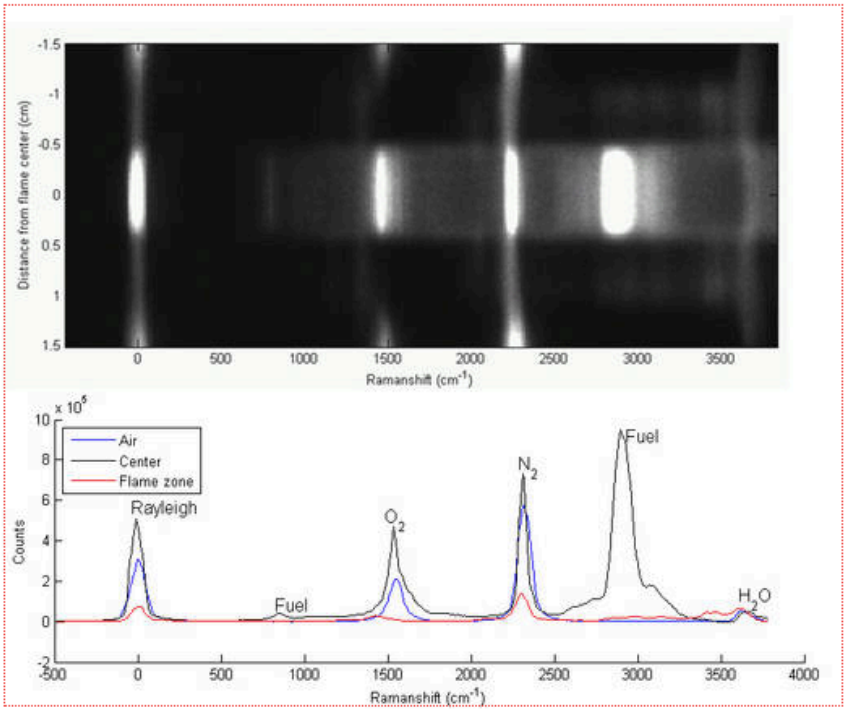

Figure 1. *Image of the Raman spectra from a Bunsen burner just over the burner edge. In the upper image the x-axis indicates the Raman shift and the y-axis indicates the distance from the centre of the burner along the laser beam. The lower image shows the Raman signal along three different positions in the flame.*

Figure 26. Raman Flame Temperature Measurement.

There are three different regions in this image. At the top and bottom is air with only O2 (1556 cm-1), N2 (2331 cm-1) and H2O (3651 cm-1) visible, between 0.5 and 1 cm is the flame zones with lower signal due to the higher temperature and a lot more species. In the middle, around 0 cm there is mixed fuel with the air as indicated by the large CH peak around 2930 cm-1.

4.3.4 Temperature Detector Equivalence

From Raman RER experiment it is demonstrated the two detectors used within the IR range of the EMS, Raman and thermoelectric, are equivalent in terms of the vibrational and temperature behaviour of the molecule. H_2O's 3659 cm^{-1} mode is equivalent, (as above section 4.3) thus the detectors of IR and Raman are equivalent. What is more, the temperature was measured from CO_2's Raman active 1338 cm^{-1} mode alone (3.4.2); and this value compared well and calibrated 'favourably' by Raman's complimentary instrument the thermoelectric IR detector – Figure 48 above. From this, it can be implied all modes and thus molecules, are equivalent; they are only separated or discriminated by the detector 'observing' them. The RER shows temperature measurement of all atmospheric gases can be made reliably and accurately from the Raman vibrational modes alone; the Raman detector on its own could measure and quantify the 'special GHGs' (thermoelectric gases). As evidence to

this Raman instruments is used as an instrument of choice on solar system space probes– more on this in a following section.

From the above equivalences, we can say a GH atmosphere without this Raman vibrational mode knowledge is incomplete: these Raman temperature observations are not – as it stands today – used or discussed in GH theory and they should.

In a separate paper: Using Raman Spectroscopy to Improve…[36] it is well explained the direct relationship between thermocouple and Raman spectrometers temperature measurements – shown below in Figure 27.

The following study pertains to issues of N_2 radiation behaviour uncovered with the N_2/CO_2 laser – section 63.

"…the presence of nitrogen gas inside the optical cell is primarily meant to quench the rate of radiative spin-destruction, achieved by collisions with electronically excited alkali metal atoms. The energy transferred as a result of these collisions is pooled in the rotational and vibrational modes of the N2 molecules; these modes quickly relax to the translational degrees of freedom, thereby increasing the local gas temperature inside of the cell.

Since SEOP must take place inside a closed system due to the high reactivity of alkali metals in air, physical insertion of a thermocouple is impractical for the reasons listed above, and merely measuring the cell surface temperature does not provide a true account of the internal temperature, nor the corresponding energy transport processes occurring within the cell. Virtually all of the laser energy absorbed by Rb is transferred to the rotational and vibrational degrees of freedom in the N2 buffer gas, which then rapidly equilibrates with the translational temperature (corresponding to the local temperature of the gas mixture). Remote sensing of the N2 rotational (and vibrational) temperatures inside the pump cell during SEOP can be achieved using in situ Raman spectroscopy." (2.2)

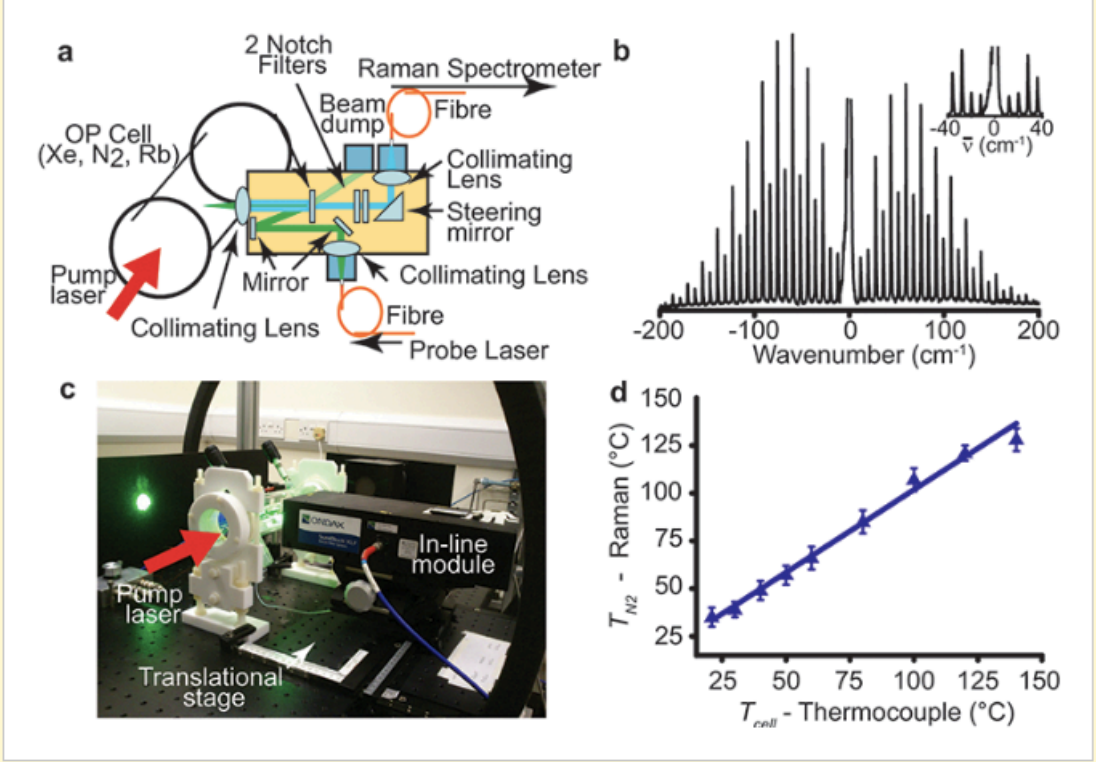

Figure 6.

(a) Schematic representation of in-line Raman module. (b) Example N2 rotational Raman spectrum (baseline-corrected) at room temperature, without SEOP (3 atm N2). The inset shows a close-up of the ultra-low frequency region that is spectrally resolvable using the in-line apparatus. (c) Photograph of in-line Raman module. The inline module is mounted onto a translational stage to allow three-dimensional mapping of TN2 within the cell. (d) Plot of oven temperature (T cell) measured via thermocouple (located in the oven inlet airstream) versus TN2 measured via Raman spectroscopy; experimental data (triangles) are shown in comparison with simulation assuming 1:1 correlation (line); error bars are least-squares fit errors of Bhc/kT plots [19].

Figure 27. Thermoelectric (thermocouple) and Raman Spectroscopy Correlation Line [36].

Also explained – justifying Raman's superior application – was the history and application of Raman temperature measurements.

"(Professor William) Happer et al. also noticed that the N2 rotational temperature was elevated compared to the surface temperature of the glass walls of the pump cell (measured via thermocouple). (Figure 28) The extent of the temperature elevation changed with absorbed pump laser power and gas loading." [37]

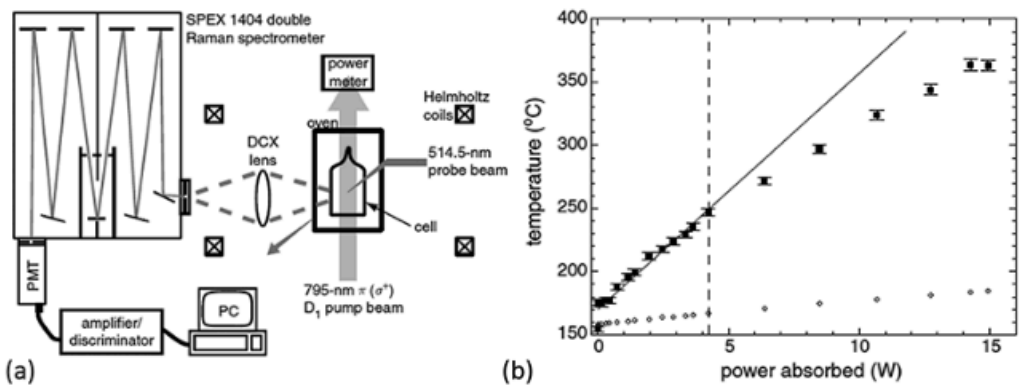

Figure 3.

(a) Schematic representation of Happer's experimental setup showing SEOP pump cell, 795 nm Rb excitation source, and orthogonal Raman probe/detect configuration. 514.5 nm Raman probe beam furnished by a 15 W water cooled argon-ion laser, with resulting Raman scattering imaged directly into spectrometer. (b) N2 rotational temperature (solid squares) as a function of absorbed laser power for a cell loading of 2 amg He and 0.33 amg N2 in a 40 cm3 OP cell, with an external cell surface temperature of 170°C (open diamonds). Solid line fits to data points up to 4.3 W of absorbed energy, after which the experimental data deviate significantly from a purely conductive energy dissipation model [2].

Figure 28. Happer's Experiment. [37]

4.3.5 Raman Temperature Measurements and the Boltzmann Constant

By the Boltzmann constant, the observation of these and all vibrational modes at the said predicted frequencies, and their respective temperature measurement thereof, implies these modes are resonating and thus are radiating IR photons. By observation, from this experiment, these modes are radiating – IR heat – consistent with thermodynamics and quantum mechanics; if they were not there would be a contradiction.

4.3.6 Raman Measurements and the Stefan Boltzmann Law

As both N_2 and O_2 – independently – show a temperature value, as measured by Raman laser detectors, they must be said to be radiating in accordance to the Stefan-Boltzmann law. The Stefan-Boltzmann law is a central pillar to radiation theory, and states the following: expressed mathematically as

$$E = \sigma T4.$$

This Raman signal is in total contrast to current GH theory – where it is not allowed. This misconception can only be due to the Raman detectors measuring the N_2 and O_2, and the TE/IR detectors not measuring it. This finding has direct significance to blackbody radiation theory and suggests it is incomplete, requiring updating with respect to the Raman observations made here, and everywhere in the fields of modern chemistry and physics.

More on the significance to this is covered in section 4.14.

4.3.7 N_2 and O_2 and Planck's Law

The above claim also pertains to Planck's Law. Planck's law – with the addition of the Raman-IR modes, suggesting they are 'blackbody' emitters – will require amending. This is further covered in section 4.14.1.

4.3.8 Liquid H_2O Temperature Measurement

In the paper titled: Optical remote sensing of water temperature using Raman spectroscopy [38] the application of Raman spectroscopy was fully evaluated.

Abstract

"A detailed investigation into the use of Raman spectroscopy for determining water temperature is presented. The temperature dependence of unpolarized Raman spectra is evaluated numerically, and methods based on linear regression are used to determine the accuracy with which temperature can be obtained from Raman spectra. These methods were also used to inform the design and predict the performance of a two-channel Raman spectrometer, which can predict the temperature of mains supply water to an accuracy of ± 0.5 °C."

Figure 3.19 shows regression plots of the temperature predicted from Raman spectra versus physically measured reference temperature values with 200 cm^{-1} channel widths.

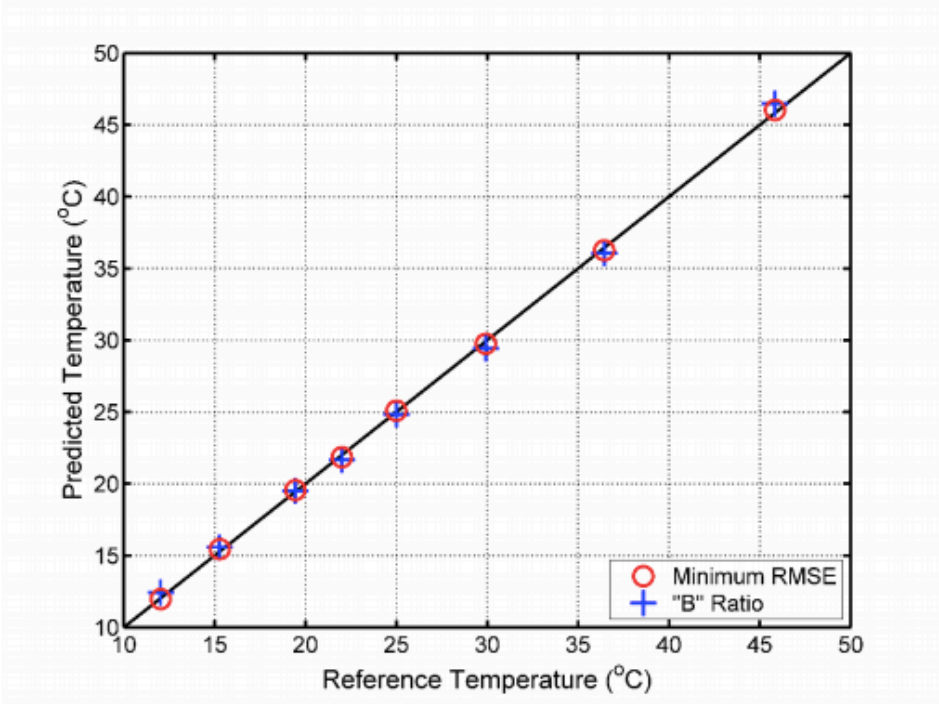

Figure 3.19 – Reference vs. predicted temperature for the unpolarised two–colour ratio with 200 cm^{-1} channel widths (Minimum RMSE: ±0.1 °C, B Ratio RMSE: ±0.4 °C).

Figure 29. Raman H2O Temperature Measurement Accuracy. [38]

4.3.9 H_2O and Emissivity

The significance of this paper offers support to Raman spectroscopy's (RS) utility in updating radiation theory. That RS can measure the temperature of H_2O by its emission spectra, the same spectra as observed by IR spectroscopy, and that this is an accurate measure, tells us something about 'emissivity'. Emissivity is currently solely determined by thermoelectric detectors. H_2O has an emissivity value of near 0.98.

4.3.10 Equivalence – Dual Modes H_2O

Some modes appear to be both thermoelectric and Raman active for some molecules, H_2O the best example. This indicates that although most substances do not share this (for CO_2 for example), substances must be understood to be radiating from their predicted modes, whether they are IR-thermoelectric or Raman active. If there is a mode; there is, quantum mechanics, radiation – emission and absorption, all in accordance with the physics.

4.4 Raman Mapping and Thermal Imaging with Raman Spectroscopy

A whole field of instrumentation has developed around Raman spectroscopy termed Raman Mapping[39] and thermal images are now derived from these maps. Figure 30 below shows an 'IR' thermoelectric image alongside a Raman image. Such images show the strength and potential of Raman spectroscopy to measure the temperature of substances.

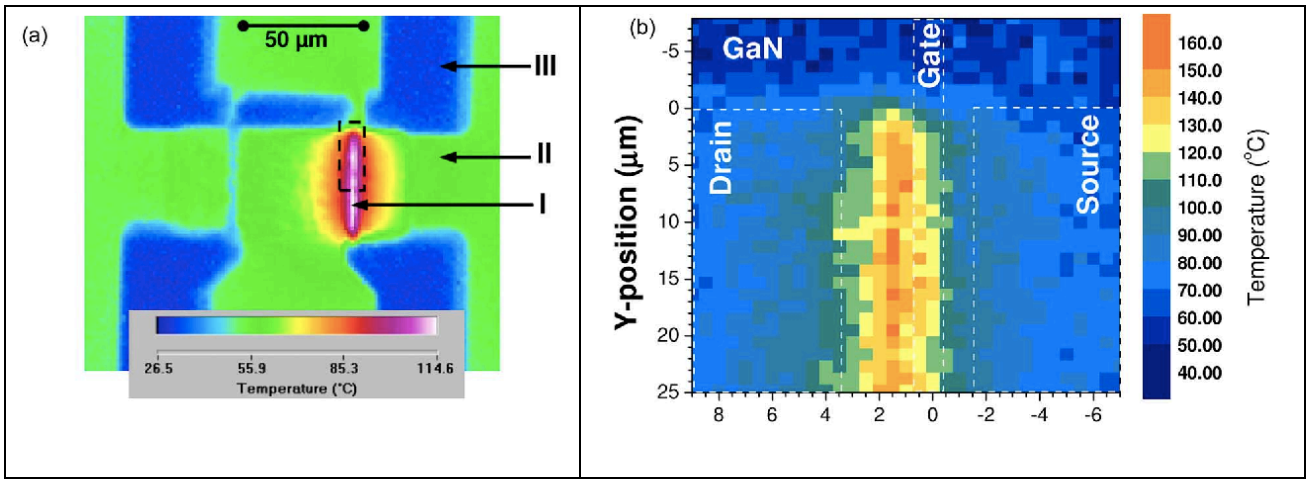

Figure 30. "Fig. 3. (a) IR temperature map of AlGaN/GaN HFET at Vsd = 40 V and I = 25 mA. Numbers denote (I) hot spot, (II) area covered by metal contacts, and (III) area free from metal contacts. (b) Raman temperature map of GaN and (c) SiC temperatures measured over the area depicted by a dashed rectangle in (a) " [40]

4.5 The Significance of Equipartition and Degrees of Freedom and Normal Modes

Normal modes (IR spectra bands) are derived from how many degrees of freedom a molecule has; and it says they are equal in their output. So, it is significant; they are equal in terms of heat-energy radiation.

"In classical statistical mechanics, the equipartition theorem relates the temperature of a system to its average energies. The original idea of equipartition was that, in thermal equilibrium, energy is shared equally among all of its various forms; for example, the average kinetic energy per ***degree of freedom*** *in translational motion of a molecule should equal that in rotational motion.[41]"*

The following address this equipartition by showing many IR spectra are identified by both Raman the thermoelectric (IR) spectroscopy.

4.5.1 CO_2's 1338 cm^{-1} and the Principle of Equipartition

Notwithstanding this mode is present on 'IR' spectrograph Figure 45 and Figure 47, CO_2's third QM predicted vibration mode or vibrational spectra – the mode not included in GH theory – is observed at 1338 cm^{-1} by the RER (Figure 12) in the IR of the EMS: only with Raman spectrometers. This mode is not observed with IR thermoelectric detectors as it does not have an electric dipole moment and thus does not generate an electromotive force – more on this in a following section. By the Principle of Equipartition[41], this Raman vibrational mode should be emission equivalent to the TE/IR (GHG) modes and assumed so. If it were not for Raman spectroscopy this mode would only be predicted and not observed. That there is a mode implies there is vibration, and through the Boltzmann constant this vibration implies a temperature equivalent IR emission and absorption proportional to the vibrational energy of the mode – as all spectra lines do.

4.6 Towards an Equation of the 'Raman' Atmosphere -

Building on all the evidence demonstrated thus far with respect to Raman spectroscopy the following presentation by Wolfgang Meier titled Temperature measurements in turbulent flames using Raman spectroscopy [42] describes also the mathematics Raman spectroscopy and comes to an equation. He has represented Raman spectroscopy in the mathematics (he is not the first to do this); connecting it to general radiation theory, and particularly the Boltzmann constant – a term connected atomic vibrational behaviour to temperature. It is with this equation that I believe Raman spectroscopy is legitimate and stands as a total contradiction to modern GH theory – as it encompasses the so-called non-GHGs.

"Signal intensity

$$I_{RS} = I_L \cdot N_i \cdot d\sigma/d\Omega \cdot \Omega \cdot \varepsilon \cdot q \cdot L$$

I_{RS} : detected Raman intensity

I_L : laser intensity

N_i : molecular density of species i

$d\sigma/d\Omega$: differential scattering cross section

Ω : solid angle of detection optics

ε : optical efficiency

q : quantum efficiency of detector

L : length of measuring volume

• Molecular density can be determined from the Raman signal.

• The constants are typically determined by calibration measurements.

Raman-shift and scattering cross sections of major species in flames

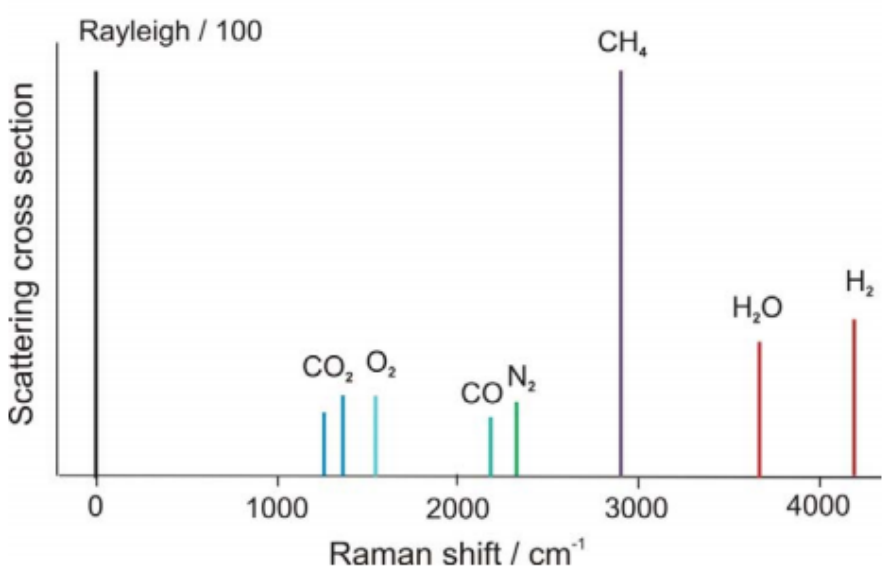

Figure 31. Raman Flame Measurement Towards Equation[42]

In principle, all these species can be detected simultaneously (in flames)

If all (major) species are detected simultaneously the total number density N_{total} can be determined:

$$N_{total} = \Sigma N_i$$

With knowledge of the pressure p the temperature can be determined via the ideal gas law:

$$T = p / (k \cdot N_{total}) \quad (1)$$

k: Boltzmann constant

Temperature and major species concentrations can be determined simultaneously

→ wonderful measuring technique! But, …

Low signal levels, high laser power needed, only applicable in “clean” flames.”

4.6.1 A Raman spectroscopy derived equation of the atmosphere.

It is from this application-based equation – equation (1) – I deduce a general equation with respect to temperature of the atmosphere. It unifies temperature, pressure, gaseous molecules with the Boltzmann constant; and it is Raman spectroscopy that observes and defends it.

$$T = p / (k \cdot N_{total}) \qquad (1)$$

4.7 Raman lidar sensing of CO_2 leakage - Discussions [17]

The introduction lines of the paper cannot be overlooked without comment:

“The average temperature of Earth has increased by 0.8 ◦C since the beginning of the twentieth century, garnering worldwide interest [1]. This global warming is reported to be caused by an increase in the concentrations of greenhouse gases (e.g., CO2, CH4, N2O, O3, and CFCs) produced by human activities such as fossil fuel combustion, industrial processes, and deforestation. “

The authors are concerned about the GHGs but seem unaware or oblivious they are using Raman Laser detectors that expose and exploit the non-IR spectra – the non- GHG deriving spectra modes.

In this experiment the Raman lidar is used to detect CO_2 leakage: this is the most unlikely of possibilities, unthinkable before the development of laser Raman technology. This experiment totally rebuts the claim the non-GHGs do not absorb or emit IR or have emission spectra. It is clearly shown by practical application the said gases have spectra and radiate at their quantum predicted positions. The experiment also reveals properties of CO_2, namely its molecular weight: the gases do not appear to defuse in the atmosphere but rather due to it density sink into the earth.

4.8 Other Applications of Raman Spectroscopy

The following are applications of Raman spectroscopy revealing N_2 and O_2 (and CO_2 's Raman 1338 cm^{-1}) Radiating IR. More examples are listed in Appendix 8.1.

4.8.1 Measuring Atmospheric Gas Concentrations (Keeling Curve) with Raman

The fact that Raman devices can measure gas concentrations – as demonstrated in the RER, section 3.5 in this paper – has implications on the measurement of GH gas concentrations in general.

"...Raman scattering can be used to determine the nature of the molecular sample and is known as Raman spectroscopy. ***Additionally, the intensity of the measured Raman lines is proportional to the molecular composition****. This means that Raman spectroscopy cannot only be done qualitatively, but also for* ***quantitative analysis****. It is routinely used in a range of applications for the compositional analysis of solid and liquid samples. The advancement of photonics technology has seen an increase in the popularity of Raman spectroscopy of gases in recent years. It has the additional advantage that it is a non-contact, inline multi-species gas analysis technique."[43]*

Indeed, it has been found even the Keeling curve of GH gases – namely CO_2 – need not be measured by TE/IR thermoelectrics alone. The GH gases can be measured by Raman Lasers, just as they are on Solar system space probes; this is demonstrated in the following papers. In a paper titled "Determination of atmospheric carbon dioxide concentration using Raman spectroscopy"[44] the topic of measurement with Raman spectroscopy is directly addressed. Its abstract is as follows and is very convincing:

The paper demonstrates the possibility of measuring the carbon dioxide (CO2) concentration in atmospheric air using Raman spectroscopy. Three methods have been studied for deriving the CO2 concentration from the Raman spectra (the peak intensity ratio, the integrated intensity ratio, the contour fit method). The best results were obtained when the contour fit method is applied for Raman spectra processing. In this case the deviations from reference mixtures of known concentration were below 3 ppm. Methods for improving the sensitivity of the Raman gas analysis method are proposed and the possibility for using this

technique for the simultaneous determination of the concentrations of significant amount of greenhouse gases in air with single device is discussed.

The paper uses the same knowledge and application as followed with this paper and concurs Raman Spectroscopy is a substitute instrument, based on the identification of quantum IR spectra, to its mostly IR thermoelectric counterparts.

Also see appendix 8.1.5 for more on atmospheric measurement of gas molecules by Raman Lidar.

4.8.2 Measurement of Agricultural Emissions

It occurred to me there should be an application for Raman Spectroscopy to measure emissions from farmed animals – one of the leading outputs of emissions – by a setup similar to the 'CO2 Leakage experiment' and its results Figure 20. Though Raman is not commonly used in this application for practical reasons, in a paper titled Agricultural and Environmental Management with Raman Spectroscopy [45] it is claimed it most certainly could be. The same article – interestingly – identifies Raman and IR (thermoelectric) detectors are together complements and should be used together for best results.

"A drawback of using Raman spectroscopy alone is that not all target particles (or gas spectra) of interest are Raman active. Thus, a complementary imaging modality would be required to positively identify these species. As such, several papers have reported results using a combination of imaging methods, most notably Fourier transform infrared (FT-IR) spectroscopy (28,30), combined with Raman spectroscopy "

Recall, if this is so, the use of two contradicts GH theory as they both exploit quantum theory.

4.8.3 Raman Solar System Space Probe Applications

On modern-day solar system space probes Raman detectors are becoming the detector of choice: it makes sense, the detect oxygen and CH_4 – accentual part

indicators of the existence of life – and CO_2, and N_2. In the review '**Remote Raman Spectroscopy of Minerals at Elevated Temperature** 2012' [46]

Raman was extensively evaluated for its obvious complementary merits.

*"...thus, using strictly visible light sources and receivers Raman spectroscopy **can yield complementary information** about the vibrational transitions observed in infrared emission or reflection spectra."*

This statement was followed by a standard misunderstanding (as interpreted for this research) between Raman and TE/IR: the following is not consistent with the findings of this paper.

"Raman spectroscopy is not directly equivalent to infrared (IR) spectroscopy, as the strengths of individual features can be quite different between IR and Raman spectroscopy due to different selection rules. The activity of Raman vibrational modes is a function of the change in polarizability during the vibrational mode, whereas the activity of infrared modes is associated with the change in permanent dipole moment during a normal mode of molecular vibration. Raman spectra of samples contain a wealth of information that can be used to identify minerals and chemical compounds based on the vibrational frequencies, relative intensities, and number of bands in the spectra."

4.8.3.1 Venus

Below (Figure 32) is a Raman spectrogram of Venus's atmosphere. Notice CO_2 is measured at its 1338 cm^{-1} mode. If the detection of CO_2 through this mode is good enough for Venus, why not for planet Earth? If TE/IR were used on Venus, no N_2 or O_2 would be measured – at any temperature.

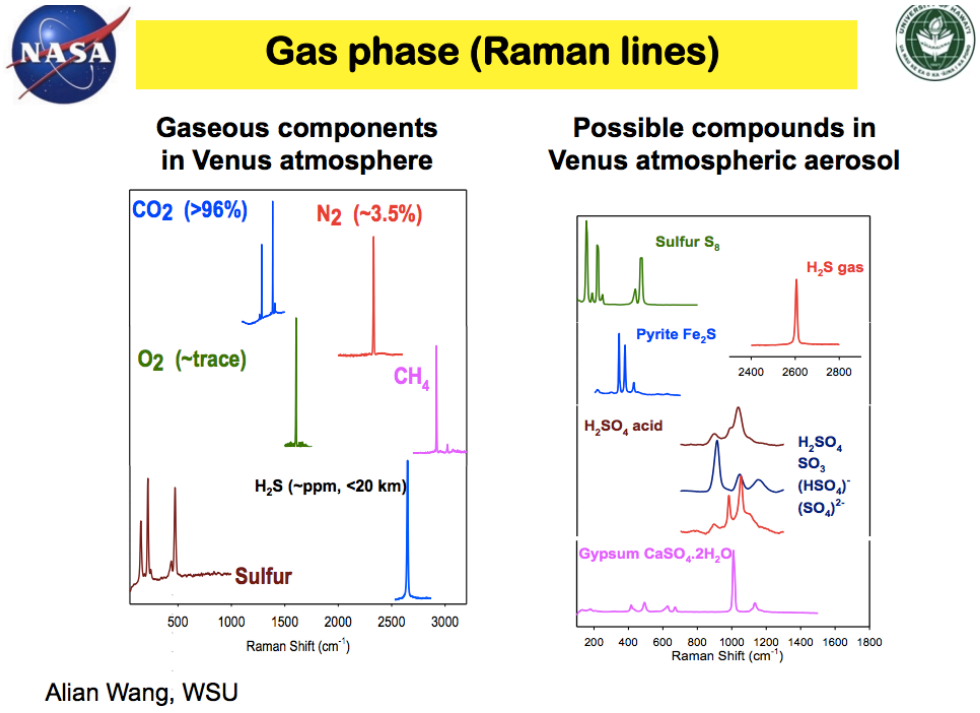

Figure 32. Venus Atmosphere 'Raman Lines' Showing molecules with their respective modes in Venus's atmosphere. [47]

Supporting papers to the above are as follows:

Space-borne profiling of atmospheric thermodynamic variables with Raman lidar [48]

Abstract: The performance of a space-borne water vapour and temperature Raman lidar has been simulated, with a specific attention to the Earth Explorer Missions in the frame of ESA's Living Planet Program. We report simulations under a variety of atmospheric scenarios, demonstrating the capability of a space Raman lidar to provide global-scale water vapour and temperature measurements in the troposphere with an accuracy fulfilling most observational requirements for numerical weather prediction (NWP) and climate research.

4.8.4 (Raman) Aircraft Instrumentation

In a paper titled Onboard (Raman) Lidar Detects Turbulence, Volcanic Ash Near and Far Photonics Spectra[49] it is demonstrated how Raman Lidar can 'read the air', all on quantum mechanics Raman spectroscopy. This is something IR-thermoelectrics spectroscopy cannot do. This application is not allowed by GH theory. N_2 and O_2 are assumed not to emit or radiate. Here they are obeying the

physics, and contradicting GH theory. The measured modes are in the IR, just as with the RER above.

"Short- and midrange (Raman) lidar systems for planes can deliver strong data for automatic correction manoeuvres, while long-range systems that track potentially dangerous atmospheric conditions miles away are still being researched."

Figure 4. *Aircraft being equipped with forward-looking lidar are able to counterbalance turbulence and gust influence (lift change, wing loads, accelerations) by deflecting control surfaces. Courtesy of Airbus.*

Figure 33 Raman Lidar Laser future aircraft application [49].

"Other air data, such as density, temperature, pressure and humidity, can be derived from molecular scattering (direct detection) only. Promising approaches exploit ... scattering processes such as Raman scattering. There, the molecules are excited by the laser beam to rotate or vibrate.

The energy transfer to or from the molecules leads to a characteristic frequency shift of the backscattered light. ***Temperature measurements with 1K accuracy and humidity measurements with 1 percent accuracy*** *(under relatively high humidity conditions) are straightforward to achieve. But a major challenge remains: measuring the air pressure and air density at the required 0.3 percent accuracy level."*

4.8.5 Laser-based air data system for aircraft control using Raman

In support of the above, a paper called: Laser-based air data system for aircraft control using Raman and elastic backscatter for the measurement of temperature, density, pressure, moisture, and particle backscatter coefficient [50] was found; the following is taken from its abstract. This paper brings in the

role of Raman Spectroscopy in air pressure analysis – supporting the Nilolov and Zeller theory of planetary atmospheres.

"Flight safety in all weather conditions demands exact and reliable determination of flight-critical air parameters. Air speed, temperature, density, and pressure are essential for aircraft control. Conventional air data systems can be impacted by probe failure caused by mechanical damage from hail, volcanic ash, and icing. While optical air speed measurement methods have been discussed elsewhere, in this paper, a new concept for optically measuring the air temperature, density, pressure, moisture, and particle backscatter is presented, being independent on assumptions on the atmospheric state and eliminating the drawbacks of conventional aircraft probes by providing a different measurement principle. The concept is based on a laser emitting laser pulses into the atmosphere through a window and detecting the signals backscattered from a fixed region just outside the disturbed area of the fuselage flows. With four receiver channels, different spectral portions of the backscattered light are extracted. The measurement principle of air temperature and density is based on extracting two signals out of the rotational Raman (RR) backscatter signal of air molecules. For measuring the water vapor mixing ratio—and thus the density of the moist air—a water vapor Raman channel is included. The fourth channel serves to detect the elastic backscatter signal, which is essential for extending the measurements into clouds. This channel contributes to the detection of aerosols, which is interesting for developing a future volcanic ash warning system for aircraft. Detailed and realistic optimization and performance calculations have been performed based on the parameters of a first prototype of such a measurement system. The impact and correction of systematic error sources, such as solar background at daytime and elastic signal cross talk appearing in optically dense clouds, have been investigated. The results of the simulations show the high potential of the proposed system for reliable operation in different atmospheric conditions. Based on a laser emitting pulses at a wavelength of 532 nm with 200 mJ pulse energy, the expected measurement precisions (1−σ statistical uncertainty) are <0.6 K for temperature, <0.3% for density, and <0.4% for pressure for the detection of a single laser pulse at a flight altitude of 13,000 m at daytime. The errors will be smaller during

nighttime or at lower altitudes. Even in optically very dense clouds with backscatter ratios of 10,000 and RR filters suppressing the elastic backscatter by 6 orders of magnitude, total errors of <1.4 K, <0.4%, and <0.9%, are expected, respectively. The calculations show that aerospace accuracy standards will be met with even lower pulse energies of 75 mJ for pressure and 18 mJ for temperature measurements when the backscatter signals of 10 laser pulses are averaged. Using laser sources at 355 nm will lead to a further reduction of the necessary pulse energies by more than a factor of 3."

4.8.6 Raman LIDAR and the Atmosphere

Raman Lidar is used to measure the temperature and gaseous constituents of the atmosphere. Many papers are published on this area, the following is typical.

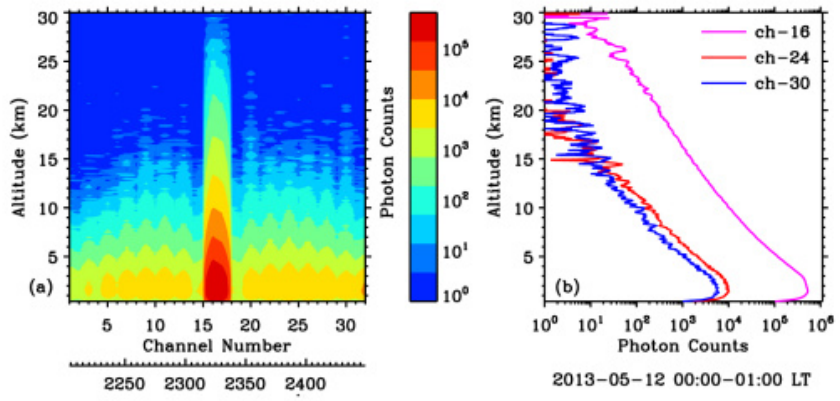

Fig. 3 (a) Altitude-dependent atmospheric N_2 Stokes vibrational-rotational Raman spectra derived from the spectrally resolved Raman lidar measurement at Wuhan during 0000-0100 LT on 12 May 2013. (b) Signal intensity profiles for the 16th (Q branch; magenta), 24th (S branch, J = 6; red) and 30th (S branch, J = 12; blue) channels, respectively.

Figure 34. Diagram showing N2 by Lidar, altitude and wavenumber, more evidence to N2 2349cm-1 vibration mode. [51]

In the diagram below N_2, O_2, and H_2O are shown with their Raman scatter wavelength – 580, 607, and 660nm from the incident laser 532nm align with their respective wavenumbers, 1553, 2330, and 3652 cm^{-1}.

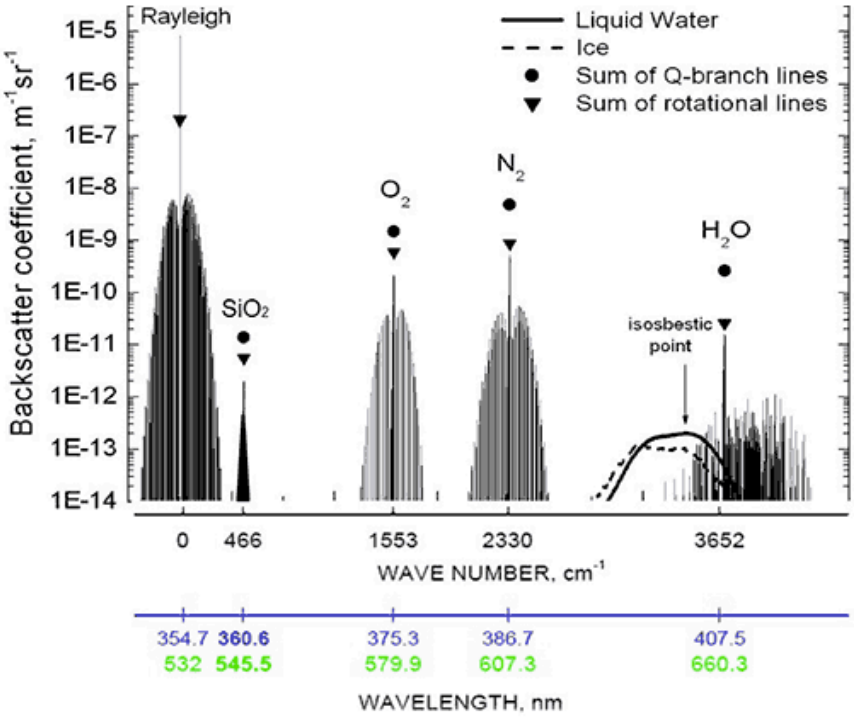

Figure 35. Showing N_2 O_2 H_2O with Raman Number 112]

4.8.6.1 Lidar can reveal the temperature of the atmosphere:

"The RL measures atmospheric temperature using the ratio of two signals from the lidar's rotational Raman (RR) channels. The RR channels sense Raman-shifted backscatter arising from rotational energy state transitions in atmospheric N_2 and O_2 molecules due to excitation at the laser wavelength of 354.7 nm (Di Girolamo et al. 2004, Behrendt et al. 2004, Radlach et al. 2008)." [53].

6.0 Example Plots

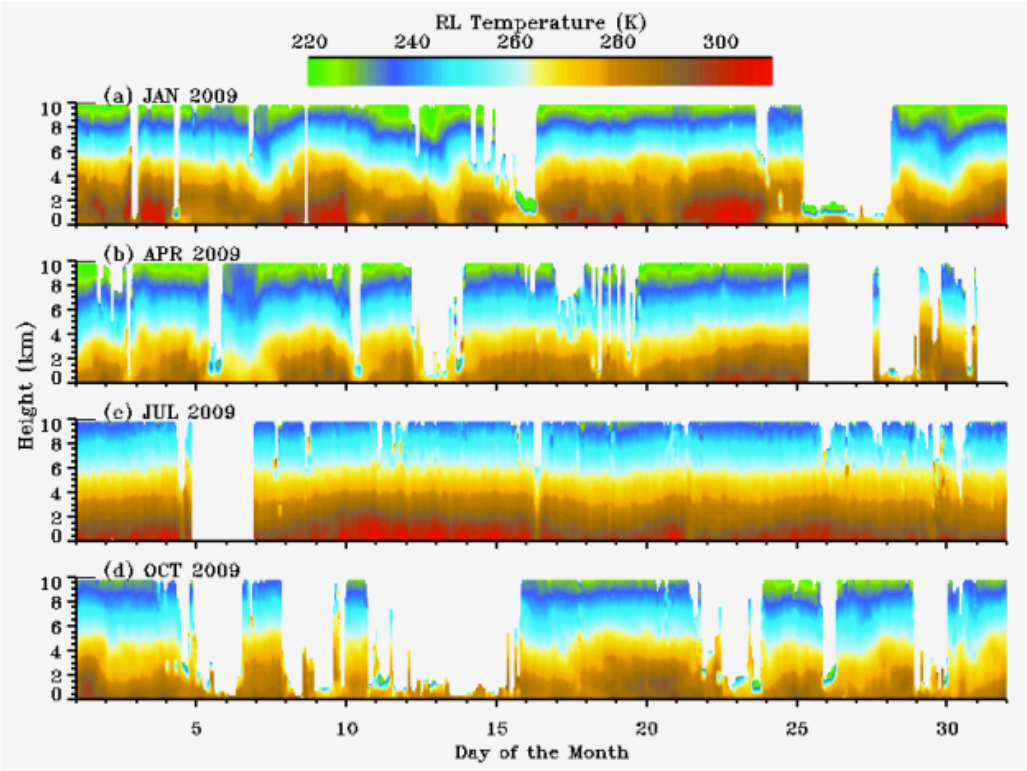

Figure 4. Sample output from the RLPROFTEMP VAP covering four selected months. Results are shown for (a) January 2009, (b) April 2009, (c) July 2009, and (d) October 2009.

Figure 36. Raman Atmosphere Profiles [53]

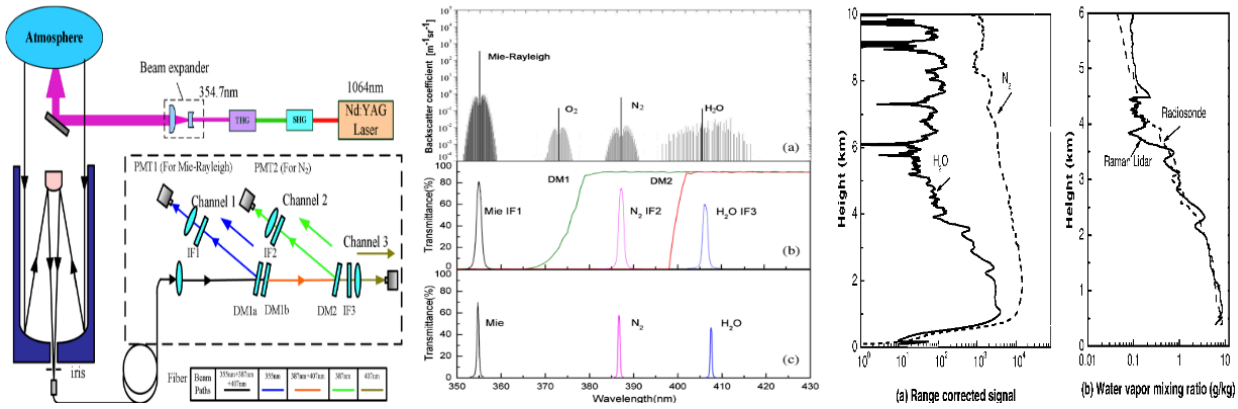

Figure 37. Raman Lidar [54]. Showing the ability of Raman Lidar to measure most atmospheric gases.

In another example, Raman spectrometers use methane and Nitrogen to measure temperature.

"*An airborne Lidar to measure methane, water vapor, and temperature on board NASA's flying laboratory, the DC-8, has been developed at Goddard Space Flight Center. Methane and water are measured using Raman (inelastic) scattering, while temperatures are determined from both Rayleigh (elastic) scattering and nitrogen Raman. Methane's long stratospheric lifetime (approximately a decade) makes it an ideal conserved tracer to track the motions of streamers or filaments of air as they peel off the polar vortex. Temperature measurements allow a calculation of the quasi-conserved quantity, potential temperature, which is useful in following the motions of large air parcels. The water measurement allows stratospheric water transport across the subtropical boundary to be studied."* [54] " Page 273"

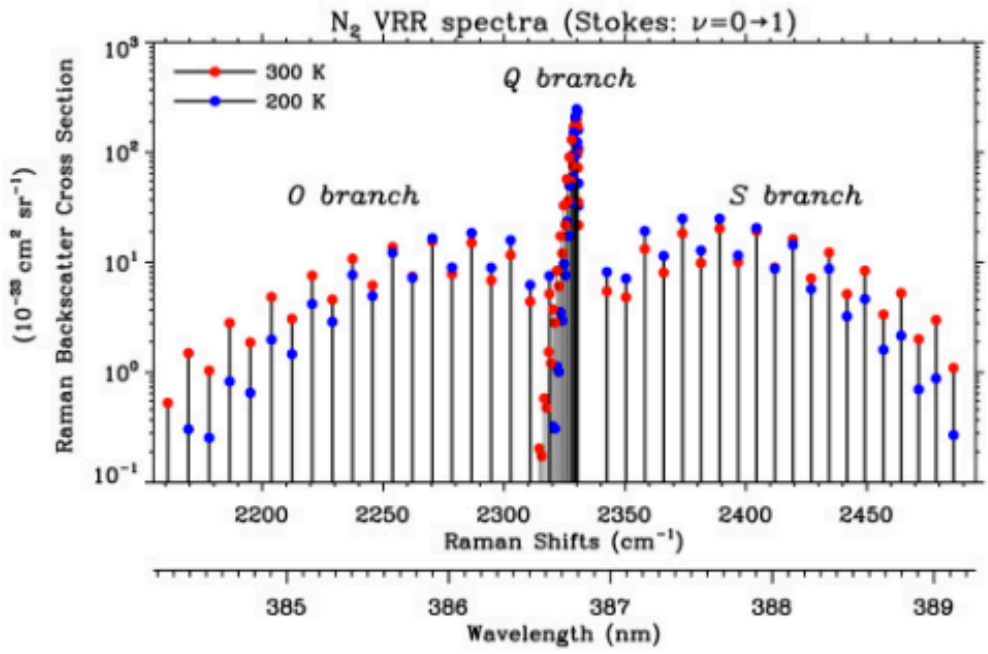

Fig. 1 The Stokes vibrational-rotational Raman (VRR) spectra of atmospheric N_2 obtained from a theoretical calculation for temperatures of 200 K (blue) and 300 K (red) respectively. The incident laser wavelength is 354.8 nm. Note that the S- and O-branch lines have nearly the same line spacing (~0.12 nm) from J = 0 (2) to 20.

Figure 38. Atmospheric N2 by Raman Lidar at laser stimulation 354.8nm. Notice the wavenumber of 2330cm-1 is shown and also temperature is deduced. [51]

Supporting papers to the above are as follows:

The impact of vibrational Raman scattering of air on DOAS measurements of atmospheric trace gases [55]

"Abstract. In remote sensing applications, such as differential optical absorption spectroscopy (DOAS), atmospheric scattering processes need to be considered. After inelastic scattering on N2 and O2 molecules, the scattered photons occur as additional intensity at a different wavelength, effectively leading to "filling-in" of both solar Fraunhofer lines and absorptions of atmospheric constituents, if the inelastic scattering happens after the absorption…"

Atmospheric temperature profiling in the presence of clouds with a pure rotational Raman lidar by use of an interference-filter-based polychromator[56]

"A lidar polychromator design for the measurement of atmospheric temperature profiles in the presence of clouds with the rotational Raman method is presented. The design utilizes multicavity interference filters mounted sequentially at small angles of incidence…"

Measurement of Atmospheric Temperature Profiles by Raman Backscatter [57]

"Abstract: A technique for measuring instantaneous atmospheric temperature profiles is given. Utilizing the portion of the laser backscatter arising from the Raman rotational spectrum of N2, profiles up to 2 km with 100 m depth resolution provide temperature to within a degree with signal-to-noise ratios of order unity. Examples are given."

4.8.7 Other Uses for Raman Spectroscopy

See Appendix 8.1 for other uses for Raman; including: measuring automobile emissions; RAman SCattering AnaLyzer (RASCAL), Geology CO_2 1388 cm^{-1}; CO_2's 1388cm^{-1} Excitation, and the 'Dicke effect' (see appendix).

4.9 'Radiating' N_2: N_2-CO_2 LASER – Discussions

The N_2-CO_2 laser 'pumping' process demonstrates N_2 – a non-GHG that is assumed not be able to absorb any (IR) radiation by any 'particle' whether photon or electron –is excited at its **2338** cm^{-1} spectra. This excitation is claimed to further excite the molecule CO_2's **2349** cm^{-1} mode. By 'excite', it presumably means energised and thus heated up. I have asked experts for clarity on this claim and they have concurred. This excitation is in total contradiction to GH theory where N_2 is assumed not to absorb any radiation. This application shows it is N_2 that directly affects, and excites the CO_2 molecule – though they do claim it is by collision and not radiation.

There are a number of questions that stem from this pumping process:

1. Does the same process from the Sun heat the air?
2. Does the same work for a bar heater?

The power output of a CO2 laser is measured in wattage and its efficiency (input verses out wattage) is said to be amount to around 20%. If we were able to configure the input wattage of this laser to the output equivalence of the Sun, would the laser still operate? And, if so would this not contradict GH theory? Yes, it would; and this should be an area of discussion.

4.9.1 Stimulated and Spontaneous Emission

'Stimulated' and 'Spontaneous' Emission are quantum mechanical features, and together point to the absorption and emission of photons of light. In the case of the CO_2 laser, it is the 'stimulated' and 'spontaneous' emission and absorption of IR photons between N_2 and CO_2 molecules. It, on its own, stands as a proof of emission and absorption of N_2 of light photons.

4.9.2 Does Discharge of Electrons Constitute Radiation?

The Laser demonstrates how different substances are excited when 'fired upon' (excited) by electrons through an electrical discharge in a cathode ray tube. The important question for this investigation is: does this 'firing upon' constitute as radiation – as a transfer of energy? This is an important question as N_2 is assumed – the topic of this paper – not to absorb radiation.

"Thermal radiation is generated when heat from the movement of charges in the material (electrons and protons in common forms of matter) is converted to electromagnetic radiation."[58]

From this definition; do the 'discharged electrons' used to excite the N_2 constitute 'charged particles'?

"In physics, a charged particle is a particle with an electric charge. It may be an ion, such as a molecule or atom with a surplus or deficit of electrons relative to protons. It can be the electrons and protons themselves, as well as other elementary particles, like positrons." [59]

It can be deduced cathode rays are a form of radiation; and the Frank-Hertz experiment supports this claim, not to mention knowledge surrounding beta (electron) radiation[60]. The 'fired electrons' are charged particles, and they , it can be inferred, radiate energy at N_2's **2338** cm^{-1} spectra.

4.9.3 Frank-Hertz Experiment

To support this claim non-IR spectra radiate, the **Frank-Hertz experiment** shows electrons – from a variable electrical discharge – affect a gas molecule to reveal its emission spectra mode – the spectra predicted by the quantum mechanical Schrödinger equation. It can be shown to work for all gases. Even without radiation – it is assumed to be by 'collision' – the Frank-Hertz experiment shows N_2 absorbs, and thus emits. From this it is plausible energy is transferred from its excited **2338 cm^{-1}** to CO_2's **2349 cm^{-1}** from emission from its mode.

4.9.4 Collisions Implausible: Convection Paradox

If excitation of other molecules close to N_2 were by collisions alone and not by radiation, it would imply energy transfer is done so by only conduction. Again, it can be shown this is unlikely as N_2 has a very low conduction coefficient – of $0.024k$ – so this form of transfer is unlikely too. This leaves only radiation as convection relies on convection and radiation. Radiation is the most plausible; and in this investigation a mechanism is revealed. N_2 can and does absorb IR radiation from any particle.

4.9.5 Implications for IR Spectroscopy

To conclude from the CO_2 Laser and show the implications of it on IR spectroscopy; the symmetric vibrational modes of N_2 and O_2, and CO_2's **1388** cm^{-1} – assumed '**non**-IR active' as they do not, emit or absorb IR radiation due to their lack of a dipole – has been refuted. The 'symmetric stretch' N_2 mode excites the CO_2, having been radiated. Not only does the N_2's symmetric mode vibrate from radiant excitation, heating and so forcing the CO_2 up an energy level, but CO_2's own symmetric vibration (at **1388** cm^{-1}) is affected – or necessarily implicated in the process by the equipartition principle in what can arguably only be by radiation (by photon collision). Atmospheric CO_2 has this same **1388** cm^{-1} symmetric mode, but there is no mention of this in atmospheric spectra, or its effect on climate forcing; it is assumed not to be part of the standard model, and this will need to change.

4.9.6 N_2 and Kirchhoff's Law

Kirchhoff's Law states 'good absorber, good emitter'. As it can be shown N_2 is absorbing charged electron particles from the electron discharge as if from radiation: from this it must also be assumed – in compliance with quantum mechanics, by definition – N_2 is also to be a 'good emitter'.

4.9.7 Metastable N_2 and the Greenhouse Atmosphere

I shall first define metastable and then discuss it in terms of N_2 and CO_2.

*"Metastable state**,** in physics and chemistry, particular excited state of an atom, nucleus, or other system that **has a longer lifetime than the ordinary excited states** and that generally has a shorter lifetime than the lowest, often stable, energy state, called the ground state. A metastable state may thus be considered a kind of temporary energy trap or a somewhat stable intermediate stage of a system the energy of which may be lost in discrete amounts.*
In quantum mechanical terms, transitions from metastable states are "forbidden" and are much less probable than the "allowed" transitions from other excited states." [61]

N_2 is said to be **Metastable** – long-lasting (absorption) – and this property is central to the CO_2 laser; the (greenhouse) gas CO_2 is not said to be metastable.

This metastable N_2 has ramifications on greenhouse theory, as N_2 is the Earth's atmospheres major constituent gas. This is not to say the atmosphere is a laser (though this is discussed by experts for other planets); it is only to say N_2 has this property when excited, and this is supported by experiment [62],[63] and may be assumed to be a property in the troposphere atmosphere also. Meschad – on the topic of planetary lasers and metastable N_2 – says:

'The occupation of the upper laser level is possible directly, but is much more favourable with the addition of nitrogen. Metastable N_2 levels not only can discharge but also can transfer the energy to the CO_2 molecules very profitably as well." (Pg. 274 [64])

4.9.8 Metastable N_2 from 'Collisions' and not Radiation Inconsistency

All explanations that metastable N_2 – in the context of the CO_2 laser – do not point to radiation but rather support the non-radiating N_2 hypothesis, all explained by collisions must be reviewed. It is claimed as follows:

"Electron collisions excite date nitrogen molecules to their vibrational level. Once in this level, the nitrogen molecules are metastable, they cannot really lose energy radiatively and can only return to the ground state as a result of collisions. Because into nitrogen is what is called a homo nuclear diatomic is it vibrates it has no dipole moment, and a direful moment is needed for spontaneous emission to occur. The population of N_2 molecules builds up and these molecules transport fare their excitation to CO_2 molecules, thereby populating the upper CO_2 laser level." (P.220)[65]

Here again we have problem, a paradox: does 'collision' – by electrons or photons, at this level – constitute radiation? I say it does (radiate), but if it does, this is a striking and damning revelation, totally contradicting GH theory and even radiation theory as we currently know it. Equally, if it doesn't, it stands is a contradiction to quantum mechanics: where all matter is said to radiate, including accelerated electrons.

The reason given for this metastable N_2 assumption is that it does not emit photons when excited; this, I believe this needs to be reviewed, and is, on its

own, a repeat of the mistakes made in GH theory where diatomics (N_2 and O_2) are assumed not to radiate.

4.9.9 Radiationless Transfer of Energy

In this book CO2 Lasers Effects and Applications [18] page 6, this transfer of energy is explained to be 'radiationless'. Figure 39 shows this mechanism and points to it being a property of N_2

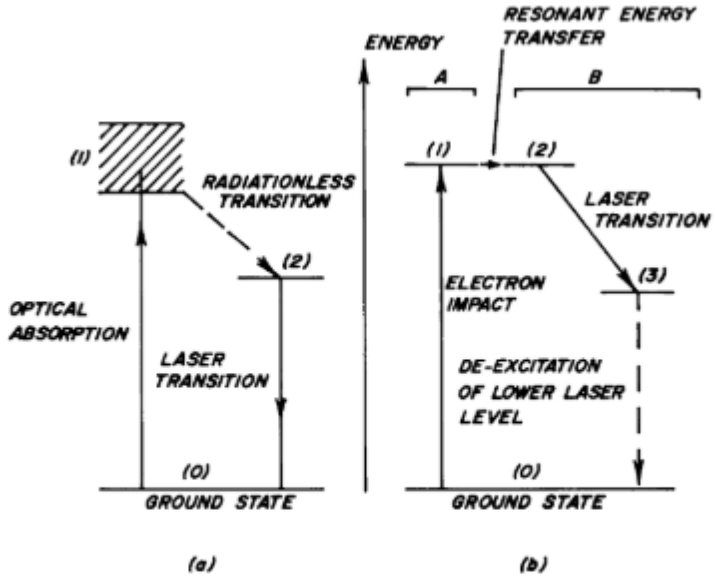

Fig. 1.3. Pumping mechanisms in two representative laser systems. (a) Solid state laser, e.g., ruby. (b) Gaseous laser, e.g., CO_2, N_2, or He. A could be N_2, while B would be CO_2.

Figure 39. Laser Pumping and Radiationless Transition [18].

I believe, based on the discoveries from this investigation, it is a 'throwback' to a lone reliance on 'IR' – thermo-electric – radiation theory and that N_2 does radiate and would radiate if under the same conditions in isolation. N_2 can be shown (as it has been attempted in this paper) to emit IR photons. If it is that N_2 does emit and absorb radiation the assumption N_2 is metastable because it does not emit suggests radiation theory is incomplete.

4.9.10 IR Photon Absorbing Atmospheric N_2: An Atmospheric Law of Physics

The experiment shows – consistent with quantum mechanics theory – electron excitation is equivalent to solar photon excitation (as discussed throughout this paper). As a consequence, concentrated IR photons can be assumed to heat the N_2 by the same physics as the CO_2 Laser; only there is no electrical discharge.

What is more, the experiment shows CO_2 is 'pumped' or stimulated by N_2 in this process: this behaviour constitutes a law of physics and so it must be for the atmosphere. Again, this process is not allowed in current GH theory.

4.10 Raman and IR Spectroscopy Complementary Instruments and Spectra

It is well understood by chemists Raman spectroscopy is a complement to 'IR' spectroscopy; it completes the IR picture. No one has brought them together with regards to the infrared atmosphere. This complementarity is revealed clearly below in Figure 40, Figure 41, and Figure 42, where some spectra modes are even identified by both Raman and thermoelectrics.

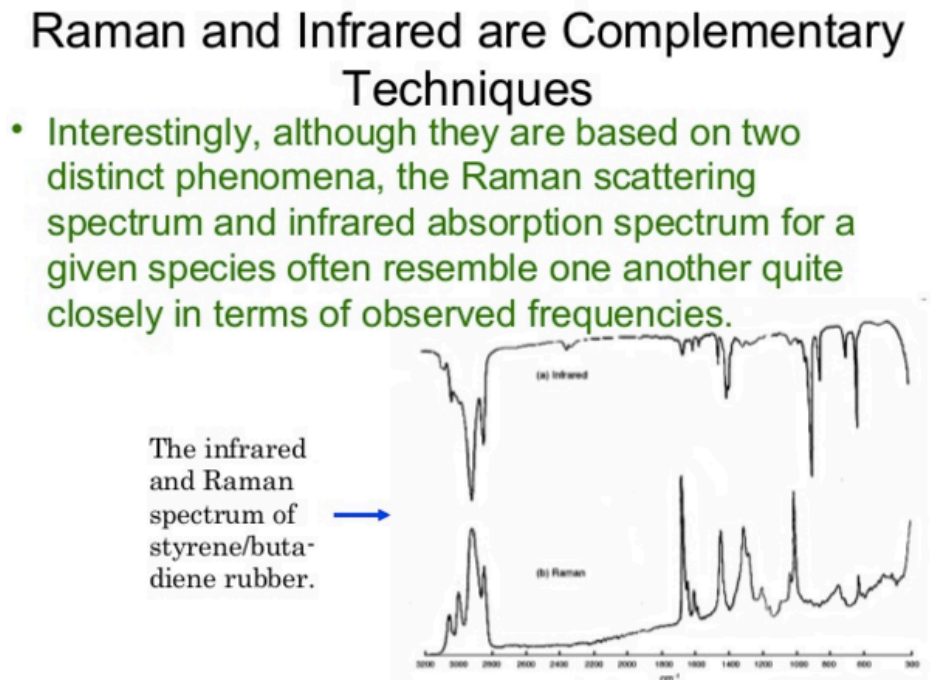

Figure 40. Complementary IR and Raman Spectroscopy. Infrared above; Raman below[66]

4.10.1 Other Molecules with Dual Raman thermoelectric.

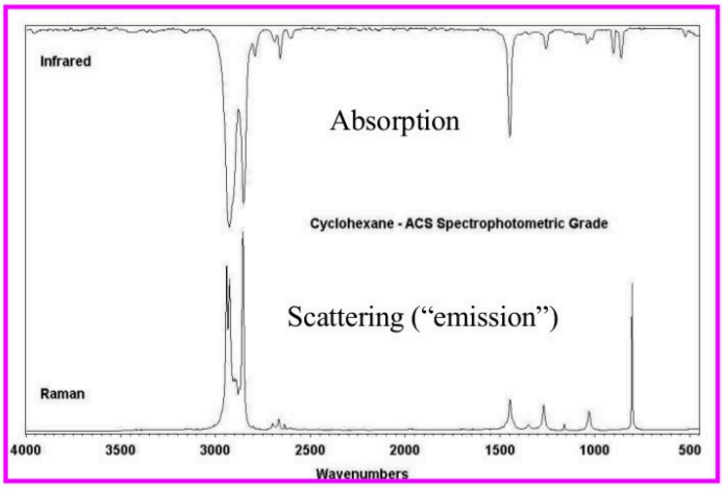

A molecule can be characterised (and identified) based on the position and intensity of the spectral peaks by either FT/IR or Raman spectroscopy

Figure 41. Demonstrating Dual Raman and IR Thermoelectric Modes of Cyclohexane. [67]

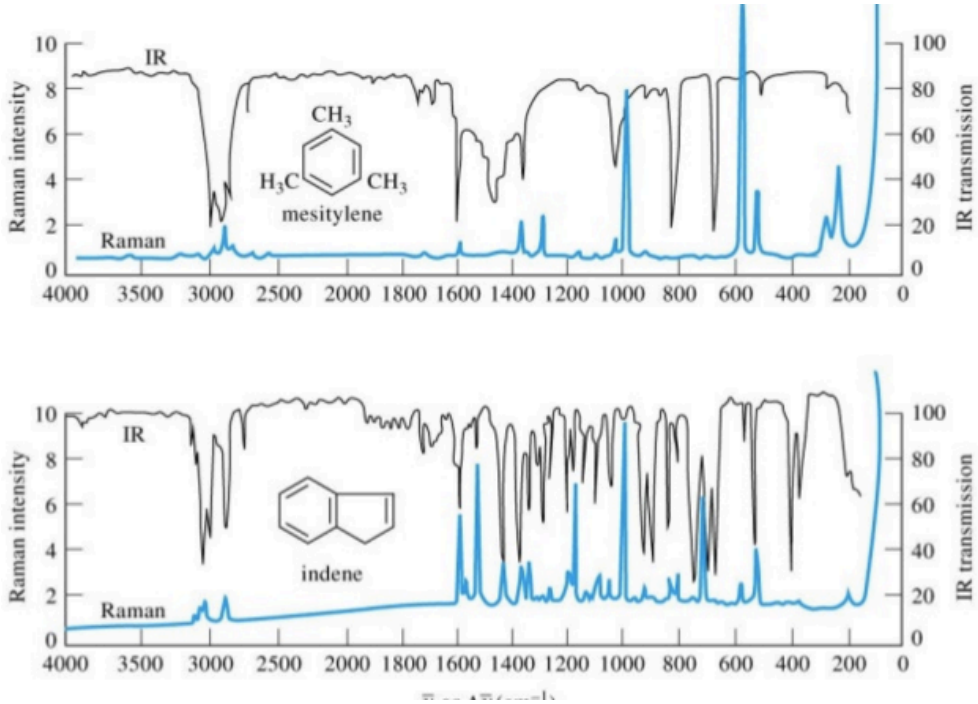

Figure 42 Demonstrating Dual Raman and IR Thermoelectric Modes of Mesitylene and Indene.

4.10.1.1 Ethanol

The following is an interesting (Raman image) reference: Ethanol has both and shared Raman and thermoelectric modes. Figure 43 clearly shows matching spectra measure measurement from both Raman and thermoelectric; and finally, CO_2 to an informed chemist is both Raman and IR-thermoelectric (Figure 44).

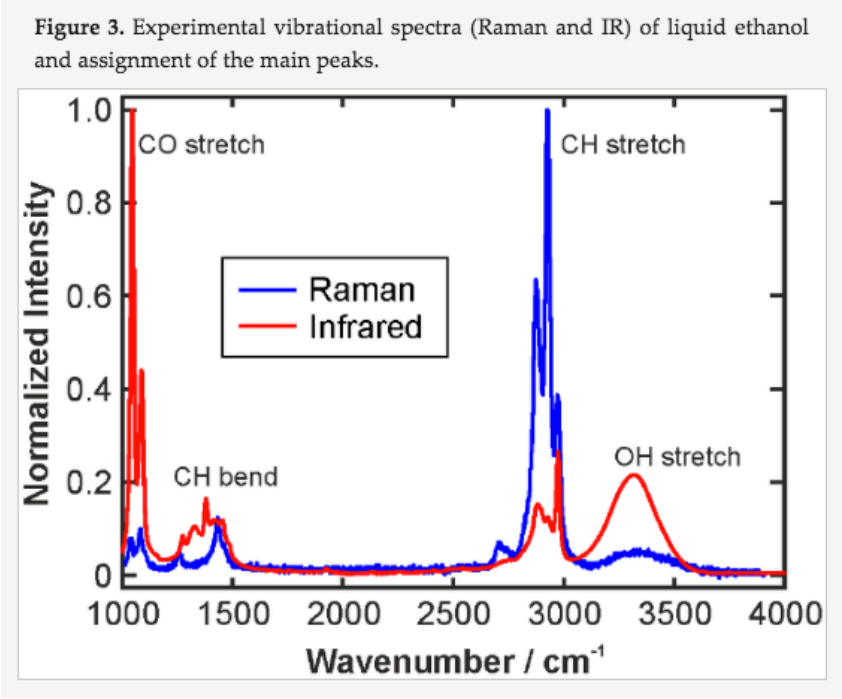

Figure 43. Ethanol Sharing Both Raman and Thermoelectric. [68]

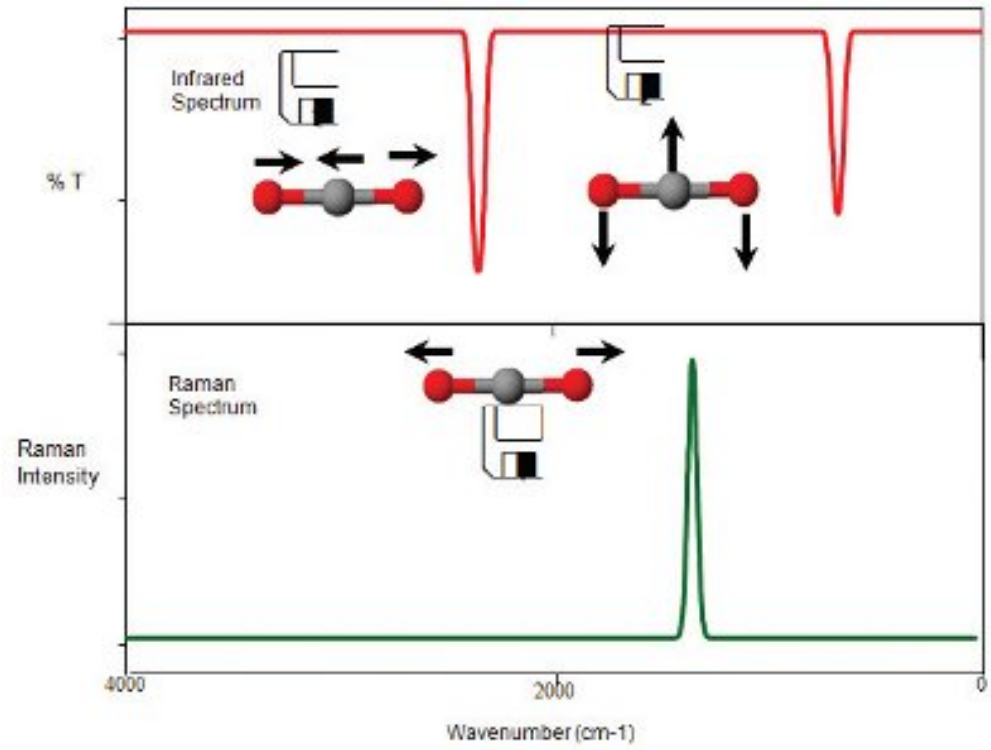

Figure 44. Schematic of CO2 Raman and IR Spectra. "In gas phase spectra of CO_2, two infrared modes are observed at 2350 and 667 cm^{-1} (red) and a single Raman band at ~1388 cm^{-1} (green). (The latter band is actually a doublet due to quantum mechanical resonance effects, which is beyond this discussion)." [69]

4.10.2 CO_2's 1338 cm^{-1} Raman Active mode showing on IR spectra.

In Figure 45 and Figure 46 [70], and Figure 47 [71] and it is clearly shown CO_2's 1338cm^{-1} Raman Active spectra mode on IR (thermoelectric) spectrograms. This strengthens the case this mode is equivalent.

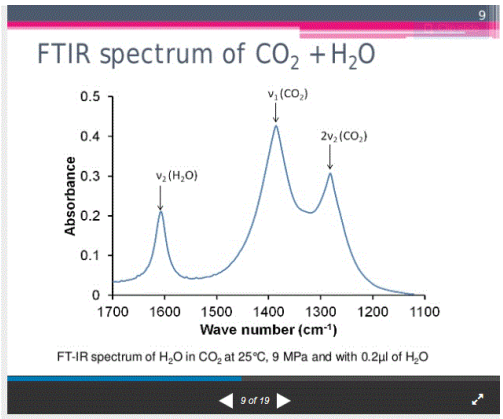

Figure 45. CO_2's 1338cm-1 Raman Mode showing on IR (thermoelectric)

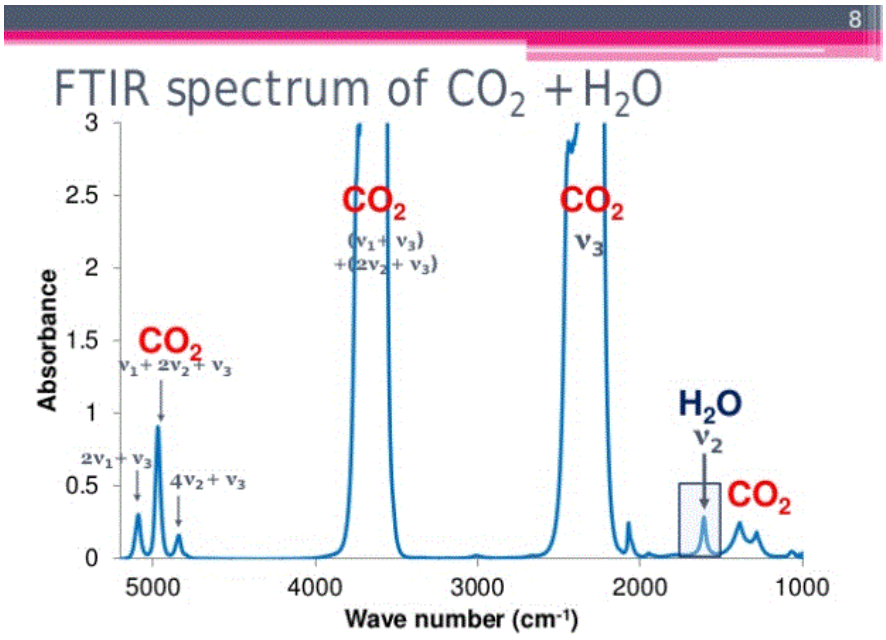

Figure 46 CO_2's 1338cm^{-1} Raman Mode showing on IR (thermoelectric).

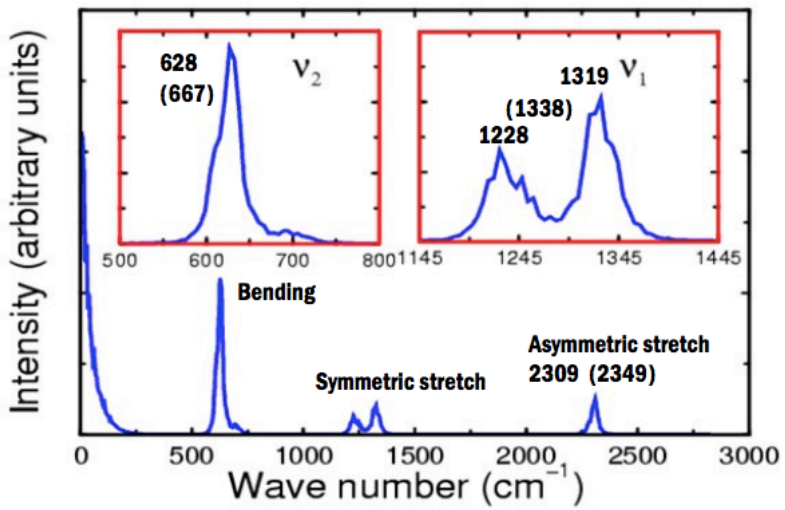

Figure 47. CO_2's 1338cm^{-1} Raman Mode showing on IR (thermoelectric).

4.10.3 N_2O's Shared IR and Raman Modes

Just as with H_2O N_2O, another strong so called GHG also shares modes with Raman, though the Raman is weak as shown in Table 3. [72]

Table 3. N2O IR Raman Equivalence.

$\bar{\upsilon}$ (cm^{-1})	Infra-red	Raman
589	Strong PQR contour	-
1285	Very strong PR contour	Very strong polarized
2224	Very strong PR contour	strong depolarized

4.11 H_2O: Dual Raman and IR Active

Water has a special property significant to vibrational mode theory, it is both Raman active and 'IR' active at: 1590 cm^{-1}, 3652cm^{-1}, and 3790cm^{-1} and this is revealed in the Raman Exhaust Report in Figure 11. The Raman observation of H_2O's 3652 cm^{-1} vibrational mode is significant as this mode is both TE- 'IR active' (as shown in Figure 48 below) and Raman-active; it is a 'dual' Raman-TE mode.

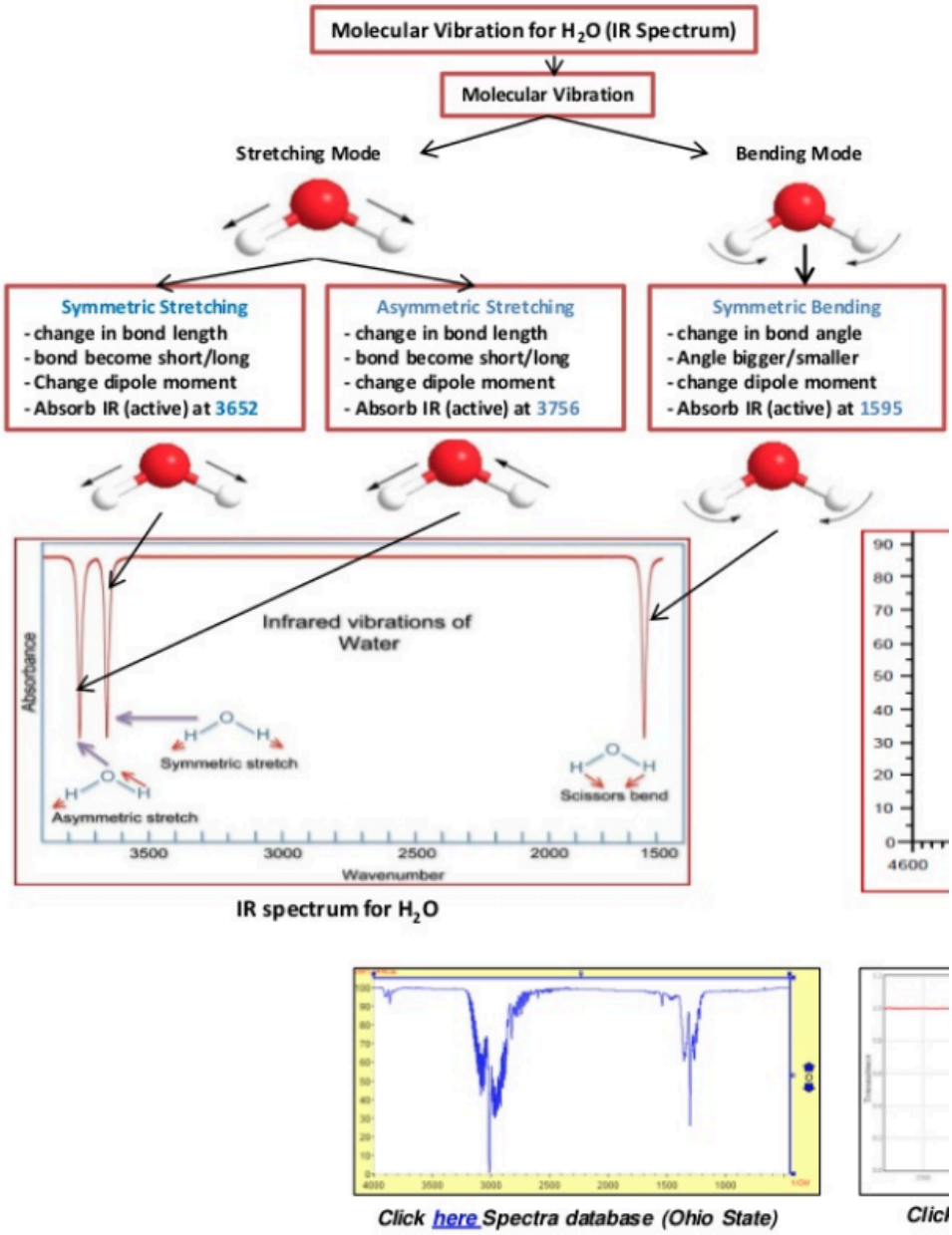

Figure 48. H_2O IR (thermoelectric) Vibration Modes and Respective Spectrum. Notice the 3652cm^{-1} is clearly shown to be IR. [73]

4.11.1 H_2O's 3652 cm^{-1} a Contravention of the Rule of Mutual Exclusion

This 'dual' mode of H_2O'sis an absolute demonstration, observation, and the practical application, via the Principle of Equipartition, that these modes are equivalent. This also shows the detectors are equivalent. What is separating our understanding of the modes will be addressed when we look at how the IR modes are derived. This discovery has ramifications on the outcome of this

investigation's conclusion, and radiation physics as a whole – water has a dual means of absorption and emission detection.

It appears the above H_2O 3652 cm^{-1} mode is a contravention of the rule of mutual exclusion, where "*no normal modes can be both Infrared and Raman active in a molecule that possesses a centre of symmetry*". This exception of H_2O is explained:

"The fact that H_2O does not obey the rule of mutual exclusion indicates that the H_2O molecule is not centrosymmetric (it is bent). As expected, the ν1 symmetric stretch is also strongly Raman active (Table 4).

Table 4. H_2O Raman IR Band Strength

Band H_2O	Infrared	Raman
ν1 - symmetric stretching (3652cm^{-1})	strong	strong
ν2 - asymmetric stretching (3755cm^{-1})	very strong	weak
ν3 - bending (1595cm^{-1})	very strong	weak

(Source, online lecture notes).

Does this mean H_2O offers the best example and application of the law of equipartition? An explanation is beyond the scope of this investigation.

4.11.2 Solar IR Insolation Radiation Heats Water

In the euphotic zone of water bodies: "*almost all of the (IR) radiation is absorbed converting electromagnetic energy into heat. Most of this absorption is carried out by water molecules with the first 50 metres".* Pg. 38 [74] From this it can be deduced the air ('the ocean of if) absorbs IR photons just as an ocean of water does. The question is why is this principle not so for the atmospheric gases? The answer is, as claimed here, the air does, absorb with its Raman and TE modes.

4.12 Ozone O_3 IR and – inferred by – Raman

Ozone is a greenhouse gas; it has IR spectra, and these spectra are observed at and around 1000cm^{-1} observed on the general atmosphere blackbody emission spectra similar to Figure 52. This position is – interestingly – at the same as CO_2's 960cm^{-1} output frequency of the CO_2 laser. If this is the case; is CO_2's 960cm^{-1} masked by the ozone spectra in the similar position? The CO_2 laser output frequency does not otherwise show in atmospheric spectrograms.

Ozone is also able to be detected by – at least by inference – Raman Spectroscopy.

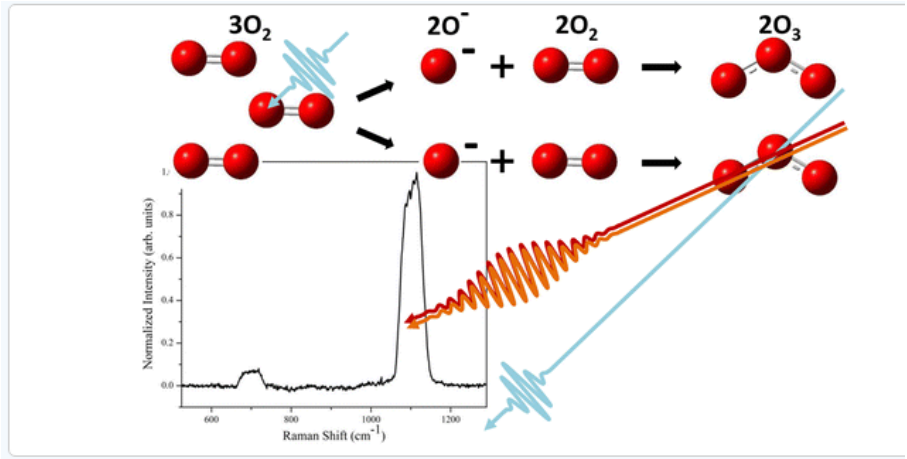

The filament-assisted impulsive Raman spectra of ozone, nitric oxide, and nitrogen dioxide are presented. The Raman response as a function of ozone concentration scales as N^2, where N is the number of oscillators in the interaction region. The system described has a detection limit of ~300 ppm for gas-phase ozone. Ozone produced via the strong field chemistry occurring within the filament pump was also detected. The measurements reveal spectral interference in the Raman features. Simulations show the spectral fringing results from interference of the Raman signal with pump-induced cross-phase modulation. The fringes are used to classify the symmetric mode of the low concentration filament-generated ozone.

Figure 49. O_3 Raman Spectrograph Showing its 1103cm^{-1} [75]

The following are a collection of findings defending this claim. Firstly, a paper was found with the title: *Monitoring O_3 with solar-blind Raman Lidars* [76] which speaks for itself, and then one by the title of: *Ozone and Water Vapor Measurements by Raman Lidar in the Planetary Boundary Layer[77].*

The following is said:

"To retrieve the ozone concentration profile, we take advantage of the simultaneous spontaneous Raman backscattering on the molecules of nitrogen (N_2)

and oxygen (O_2) that have different ozone absorption cross-sections. Thus with a modified DIAL technique, the ozone concentration can be measured without most of the interference from poorly known backscatter by particles. Water vapor mixing ratio profile can also be obtained with a set of three Raman backscattered signals, simultaneously detected, from the molecules of H_2O, N_2 and O_2. The main advantage of this Raman system is its essential independence to the wavelength dependent backscatter problems as induced by aerosols, and the fact that the N_2 and O_2 concentrations are well known as well as the ***Raman cross-sections of interest.*** *Although the Raman cross-sections are two or three orders of magnitude lower than the elastic backscattering cross-sections, they are compensated by the proportionally much higher concentrations of O_2, N_2 and H_2O compared to trace gases like O_3."*

Backing this up, a paper titled Tropospheric ozone profiles by DIAL at Maïdo Observatory (Reunion Island): system description, instrumental performance and result comparison with ozone external data set [78]

"Comparisons with 11 ground-based Network for Detection of Atmospheric Composition Change (NDACC) Fourier transform infrared (FTIR) spectrometer measurements acquired during the daytime in a ±24 h window around ***lidar shooting show good agreement*** *between data sets with a D of 11.8 % for the 8.5–16 km partial column (LIO3T higher than FTIR), and comparisons with 39 simultaneous Infrared Atmospheric Sounding Interferometer (IASI) observations over Reunion Island show good agreement between data sets with a D of 11.3 % for the 6–16 km partial column (LIO3T higher than IASI)."*

4.13 Augmenting the IR Spectroscopy and Raman Atmosphere

Based on findings made in my second paper: 'Greenhouse Gases and Radiation Theory a Misconception of Thermoelectric (TE) Transducers' [79] – where it was found the greenhouse gases are really only thermoelectric gases, detected only by thermoelectric transducers, the two methods of IR spectra detection were brought together – augmented; the IR-Raman modes with the IR/TE modes. Raman spectroscopy spectra, as identified and used in the Raman Exhaust Report, show the predicted N_2 and O_2 vibrational modes of these abundant

molecules. These 'Raman- active' modes along with the TE/IR modes of the EMS, can now be brought together – augmented – to complete the GHGs.

Figure 50 below is a schematic of the predicted and observed Raman vibrational modes in the Earth's atmosphere at different electromagnetic frequencies.

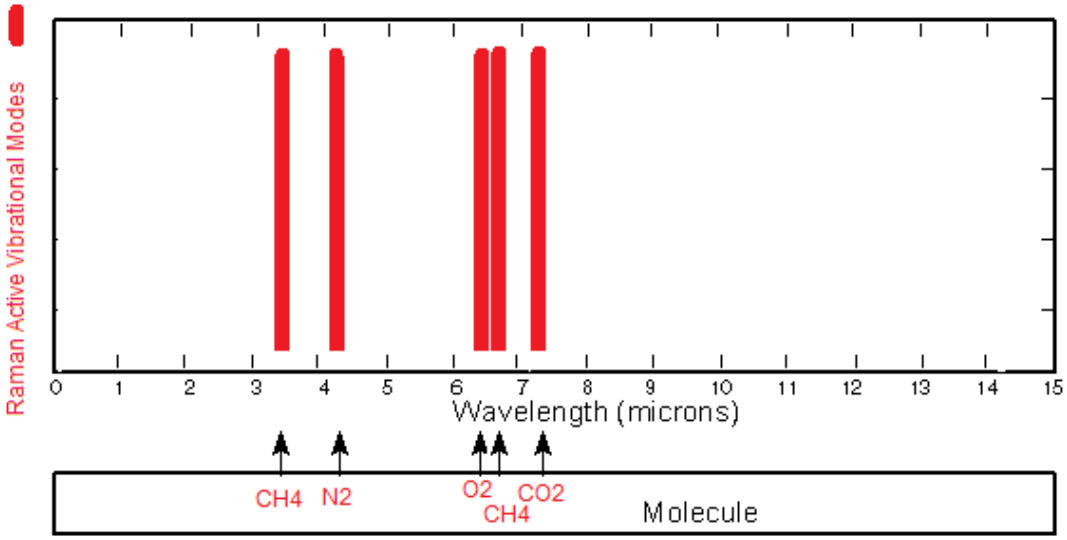

Figure 50. Raman Vibrational Modes of the Atmosphere. Predicted and Raman measured vibrational modes of (some) atmospheric gases CH4, CO2, N2 and O2.

4.13.1 The Augmented Raman active TE Greenhouse Atmosphere Spectrum

Combining TE and Raman- active Spectrographs (Figure 51 below) reveals all the predicted and observed vibrational modes of the atmosphere. The augmented atmospheric spectrum now accounts for the hidden 'dark' 98% non-GHGs.

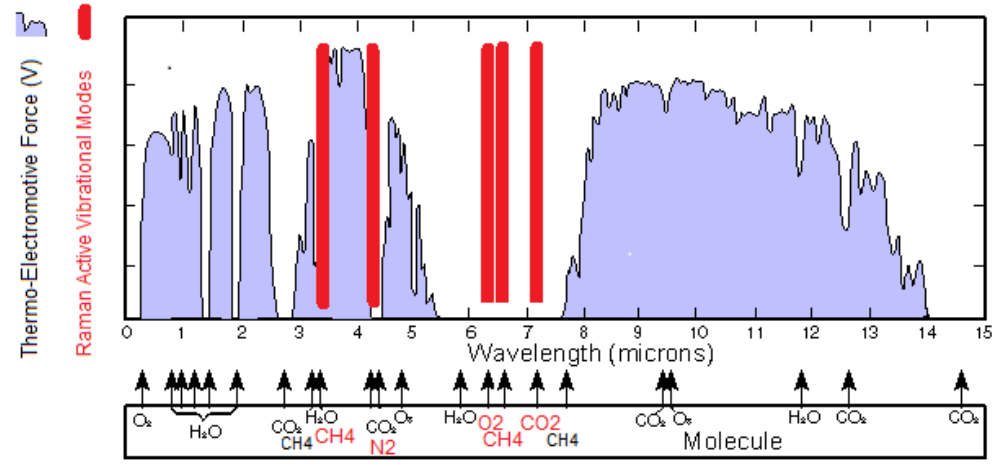

Figure 51. The Augmented Greenhouse Atmosphere. Combining Thermoelectric spectra with Raman spectra to reveal the complement of atmospheric vibrational modes and the greenhouse atmosphere of planet Earth.

The black line shows the thermoelectric response at different frequencies correctly revealing the 'IR-TE modes.

4.14 *Ad hoc* Inclusion of N_2, O_2, and CO_2 's Non-IR Raman Active Modes on Blackbody Emission Spectra [80]

As N_2 and O_2, (and CO_2's 2349cm^{-1} spectra) are not measured by IR-thermoelectric spectroscopy and thus do not show on the Earth's blackbody radiation curve (itself derived by pyranometers using thermoelectric thermopile detectors [81]), there has been an attempt to explain or reconcile their absence by including them anyway – purely as a response to my claims during early review. Their *ad hoc* outside position on the IR blackbody 'Planck curve' emission spectrum of the atmosphere (red line) is shown in Figure 52.

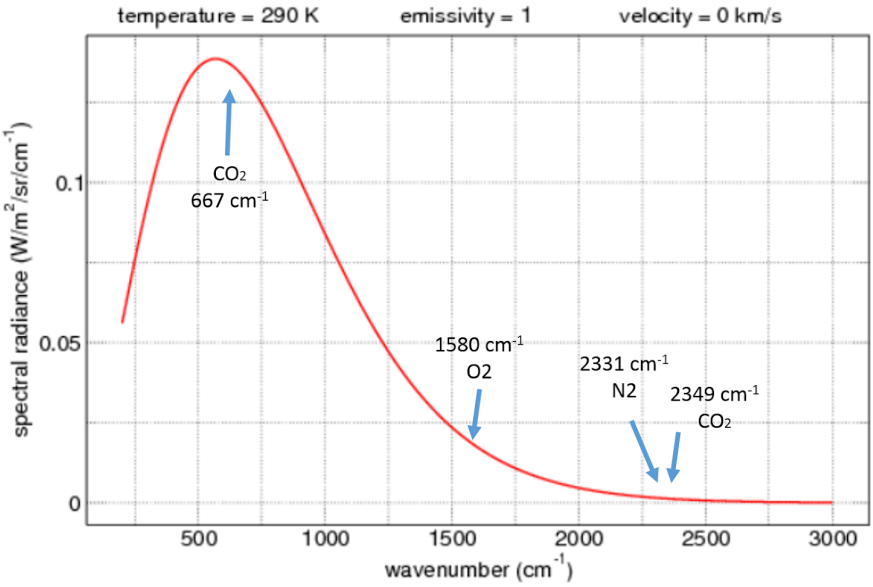

Figure 52. Blackbody Emission Spectrum with Non- GHG modes N_2 O_2 and CO_2. The solar blackbody emission spectra (red) is used to show the output of the non- GHG modes of N_2 O_2 and CO_2

These Non- GHG modes N_2, O_2, and CO_2 are shown, and their calculated irradiance presented in Table 5. It is from this analysis their effect (absorption/emission) is said to be very poor, even negligible.

Their respective position is said to cause their low radiance; justifying their respective weakness in absorption (Table 5). The *ad hoc* inclusion of the non-GHG modes is in part an acceptance of the existence of Raman spectroscopy (IR's complementary) and the quantum theory that predicts them.

Table 5. Non- GHG modes N_2 O_2 and CO2 Irradiance by Wavenumber (frequency).

	Vibrational Freq	Radiance $W/m^2/sr/cm^{-1}$
CO_2	Bend/ 667 cm^{-1}	0.134
CO_2	Asym Stretch/ 2349 cm^{-1}	0.001
O_2	1580 cm^{-1}	0.018
N_2	2330 cm^{-1}	0.001

What is really neglected their *ad hoc* claim is these modes are only detected by Raman spectrometers – the focus of this paper. When this fact is included it should help make the Planck blackbody curve redundant.

4.14.1 Addressing Raman Spectra between Solar and Earth 'Blackbody Curves

Continuing from the claims made with respect to Figure 52 and Table 5 above, Figure 53 shows all the (important) predicted IR spectra (red thermoelectric, purple both Raman-active and TE, and blue Raman-active only from Table 2) and the Sun's and Earth's blackbody radiation curves (*b* – *b*).

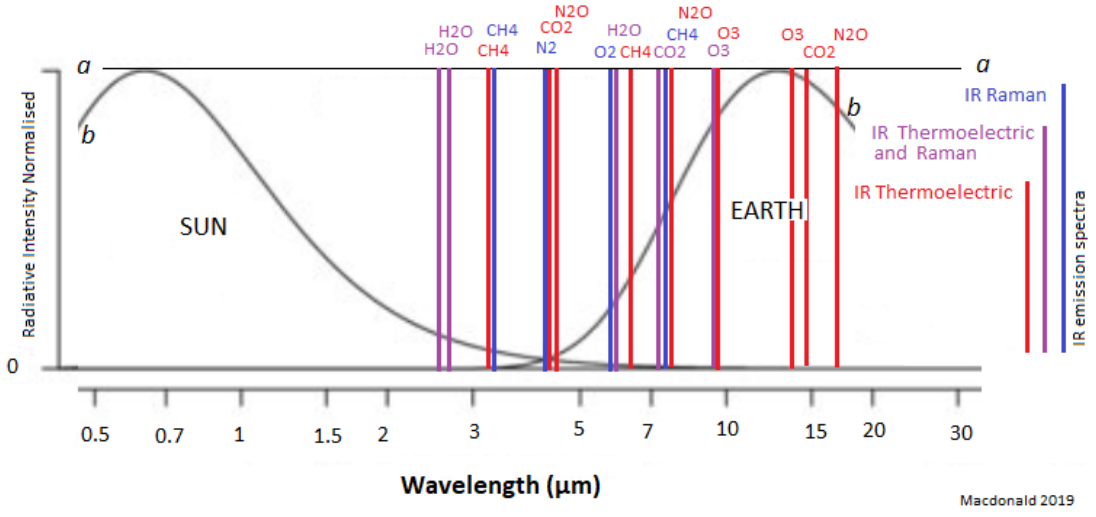

Figure 53. Quantum Predicted IR Spectra with Sun and 'Earth Blackbody' Curves. Spectrogram shows positions and type of the predicted IR emission spectra of gas molecules within the EMS

matching the normalised – thermoelectric derived 'Blackbody' curves (*b* – *b*) – Planck intensity curve' (*a* – *a*).

Based on findings made in my second paper: 'Greenhouse Gases and Radiation Theory a Misconception of Thermoelectric Transducers' [79] – where it was found the blackbody curves are really only thermoelectric curves, produced by thermoelectric transducers [81] – it was concluded blackbody diagrams only show the thermoelectric properties of the atmosphere. They are assumed to be envelope curves: any energy values outside them are unattainable – as claimed in Figure 52. However, from Raman spectroscopy – the findings of this paper – the observations and quantitative properties (temperature etc.) taken from the Raman spectra lines (both purple and blue spectra lines) this claim is refuted. As a result of the augmentation of Raman-active modes with thermoelectric modes are can exist outside the blackbody domains. This is in total contradiction to current GH theory.

As the Raman-active spectra behave as IR radiators in accordance with quantum mechanics; they all have the potential to output – in terms of intensity – at the (*a* – *a*) 'Wein law' Line. This claim challenges Radiation theory as we know it. In conclusion; the so-termed blackbody radiation curves are a misconception of thermoelectrics and are refuted with Laser Raman Spectroscopy.

4.15 The Implications of Raman Spectroscopy on Current GH Theory

The current model assumes and is dependent upon the premise the non-GHGs do not absorb or emit any IR radiation[82], at any temperature; if they did, standard GH model would collapse. As it stands, if the simple question is asked; 'does that air gain heat from the sun?' The obvious and intuitive answer is – yes – it is heated (directly) by the sunlight. But, this intuitive answer is not the answer by and understanding of GH theory. The GHGs are assumed by GH theory (Figure 54) to be the only gases to absorb 'outgoing long-wave' IR radiation which have in turn been re-radiated ('back' radiation) from the Earth's surface heat – after it has been absorbed by the Sun – by 'insolation'.

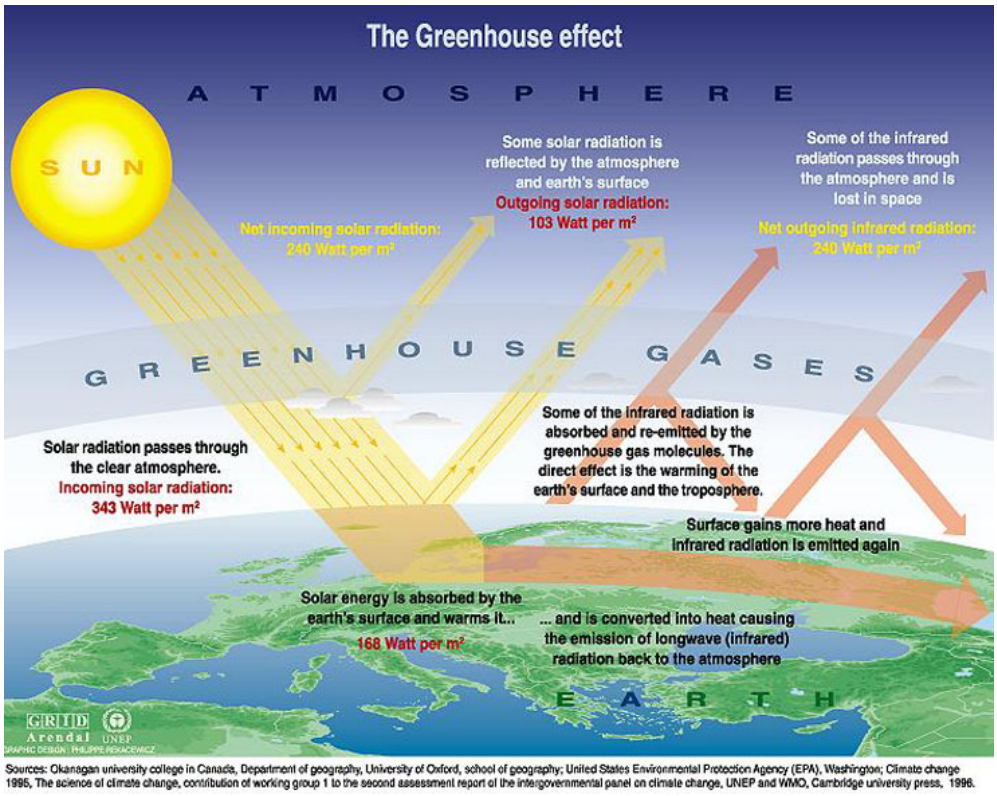

Figure 54. 'Natural Greenhouse effect[83]. The standard GH model where the atmosphere does not absorb any solar radiation and it is the 'special' GHGs that absorb and emit 'longwave (infrared) back to the atmosphere after been heated from the Earth's surface. This claim is totally challenged in this paper: all the atmosphere absorbs, directly from the sun, and from the surface.

IR-heat radiation is not directly absorbed by the Sun in the atmosphere itself[5][6]. This paper has overturned this assumption: The Sun's radiance does not pass 'through the clear atmosphere' as assumed in the schematic above; it interacts on the way and energises all the molecules.

4.15.1 Fog Dispersal and Evidence of Direct Solar IR Radiation

Returning to the misuse of explanations of radiation I stated in my introduction, the claim the Sun - by radiation - first heats the Earth and this warm Earth then warms the air via the GH gases is also claimed to explain fog dissipation. I am always looking for instances where the Sun clearly heats the air. It was when I was in the mountains recently and I saw the fog disappear as the day warmed up, I thought about my Raman work. Does direct IR radiation explain it? I think so. But to best demonstrate the air first being heated there needs to be no land under but water or snow.

I searched and found two Youtube time-lapse clips that show fog 'burn-off' shown in Figure 55.

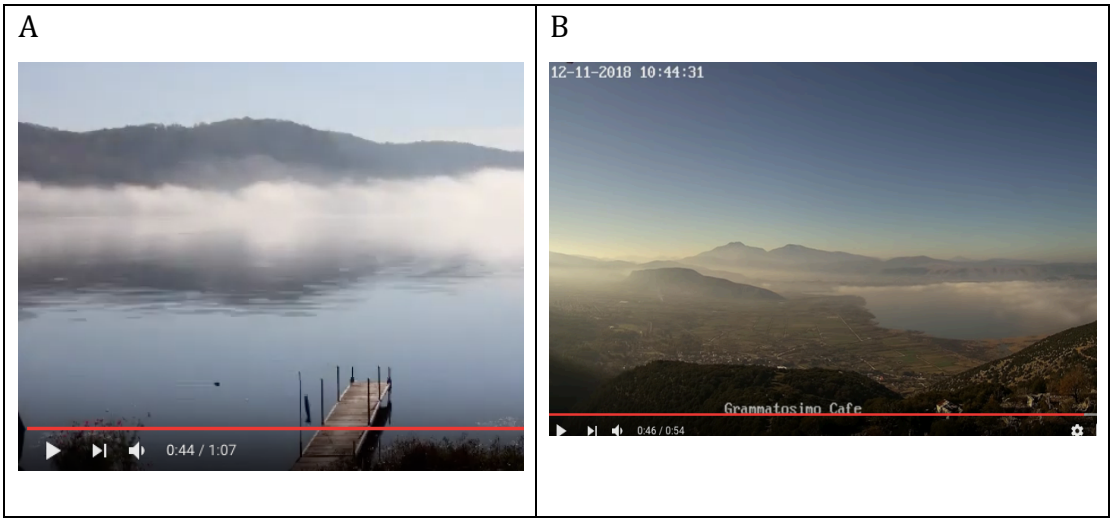

Figure 55. Fog Dispersion Over Lakes from Solar Radiation. Time-lapse videos of fog dispersing over lakes. 'A' [84] notice there is no wind (a calm lake) and it must be assumed the lake water temperature cannot be affecting the air temperature above, so the fog must be dispersing from solar radiation. 'B' [85] again the lake is calm and no sign of wind.

Meteorological fog theory says to disperse fog the land is heated by the sun, and then the Earth warmed air warms the air around the fog and the fog thus dissipates - just the same as GH theory basically.

In the clips we see the fog disperse with the coming of the morning sun over lakes. There is little to no wind and I assume the lake temperature is constant and is not affected by the Sun during the time filmed and does not affect the air temperature above the water.

I think what we are seeing here is the air being directly warmed by IR radiation at its quantum IR absorption emission spectra. The air temperature rises directly by the sun, pressure changes, the water evaporates - and then blue skies.

With a Raman IR lidar spectrometer, we could measure the temperature of the air by all its molecules - CO2 included - and I am sure the temperature would be rising as the sun intensity increases.

4.15.2 Towards a Complete Theory of the Atmosphere

While the addition of these IR 'Raman-active' spectra augment override and correct the deviation made by John Tyndall (and others) in what was up until

then Joseph Fourier's general 'greenhouse' atmosphere[86], there is more to understanding the atmosphere – and thus climate – than the consequences of this revelation alone.

The findings of this paper, ending the spell of the special GHGs as a sole climate forcing mechanism, clears the way for recent work produced by Peter Zeller and Ned Nikolov, and Henrik Svensmark et al. Together the three works complement each other towards a new theory of the atmosphere. Zeller and Nikolov[87] have shown the Earth's average temperature – and that of all planets in general – is a function of the air pressure; and Svensmark et al. – in his 2017/18 work [88][89]– has finally offered – ending some 300 years of mystery – a solar modulated galactic cosmic ray mechanism explaining climate change on all time scales. CO_2 flux on all scales, as by Henry's – temperature gas – Law, is a by-product of temperature, and not at all temperature and thus climate causal. In recognition of the first person to posit a 'greenhouse' atmosphere – before the advent of both thermoelectrics and quantum mechanics – the augmented atmosphere maybe known as the Fourier Atmosphere: where all gases are 'greenhouse gases', as first conjectured.

4.16 Strengths and Limitations

The following has been derived from, and is in anticipation of, 'reviewers' questions and criticisms. The following are instances atmospheric N_2 absorbs IR photons.

4.16.1 N_2 Absorbing in the 'Hot' Thermosphere and the Aurora

N_2 and O_2 are excited by charged particles in the thermosphere and temperatures for these molecules reach up to 2000^0C; it is **Raman spectrometry** instruments that are used to measure this temperature – in the lower thermosphere [90]. This is added proof that N_2 and O_2 are directly affected by IR photon radiation: if they absorb, they emit also. It can also be shown charged particles heat the N_2 atmosphere during an aurora: further evidence of absorption.

4.16.2 IR Absorption and Thunder Creation: Lightning Heating the Air

From lightening radiation, the air is heated to 5 to 7 times the temperature of the sun. This radiation is consistent with N_2 absorption of IR photons and may stand as a 'natural' demonstration or experiment of the hypothesised claim of this examination.

4.16.3 Non-Radiant and Non-Conductive N_2 and O_2 Heat Capacity Paradox

The discrepancy between the GHGs and the non-GHGs presents another paradox associated IR radiation theory, and it is to do with the gases respective specific heat capacities (SHC). All the atmospheric gases have specific heat capacities (as shown in Table 6, column two) which implies they transfer energy by at least one type of the three general transfers of heat; radiation, conduction or convection. The paradox sits with how the non-GHGs N_2 and O_2, as assumed by GH theory, are also – like all other atmospheric gases – very poor conductors of heat (column 3) with values of near 0. This, without radiation, leaves only convection, but this is improbable due to the former types being poor or exempt (as addressed below in 4.8.5). The question is: how can these Non-GHG gases, specifically N_2 and O_2, have specific heat capacities if they cannot transfer heat energy without radiation as assumed or conduction as known?

Table 6. Comparing Gas Specific Heat Capacity with Thermal Conductivity and Radiation Properties. Source: 'engineeringtoolbox.com.

Atmospheric Gas	Specific Heat Capacity -C_p- kJ(kgK)	Thermal Conductivity -k- w/(mK)	Assumed to Absorb IR Radiation? Yes/No
Ar	0.520	0.016	No
N_2	1.04	0.024	No
O_2	0.919	0.024	No
CO_2	0.844	0.0146	Yes
CH_4	2.22	0.003	Yes

He	5.19	0.142	No
Air	1.01	0.0262	Only the GHGs

The only way to reconcile this paradox is to assume radiation absorption does take place with the non-GHGs – as demonstrated throughout this investigation, and presumably does so at their respective Raman modes.

4.16.4 Standard (bottle) Greenhouse Experiments, and SHC Measurement

One of the most popular demonstrations of the greenhouse gasses is the 'greenhouse bottle experiment'[91] where CO_2 in one bottle and air in another is radiated by thermal radiation and temperature through time recorded (Figure 56). The CO_2 bottle temperature rises highest as shown below. However, with knowledge of specific heat theory and the specific heat capacities of the respective gases – notwithstanding the difference between constant volume (as assumed in the demonstrations) and constant pressure; I claim is this not an experiment demonstrating the specific heat capacity of air and CO_2, where CO_2 has a low heat capacity relative to air – as described in the next subsection.

Figure 56. Greenhouse Gas Bottle Demonstration [92]. Bottles with CO2 and air are radiated and temperature measured – CO2 in blue. Is this not an experiment to measure the heat capacities of the respective gases?

Below is an image taken from a specific heat capacity demonstration; if two more boxes were added showing the effect of air (Cp 1.01) and CO_2 (0.8), it would be understandable the CO_2 would have a higher temperature, concurring with GH demonstrations.

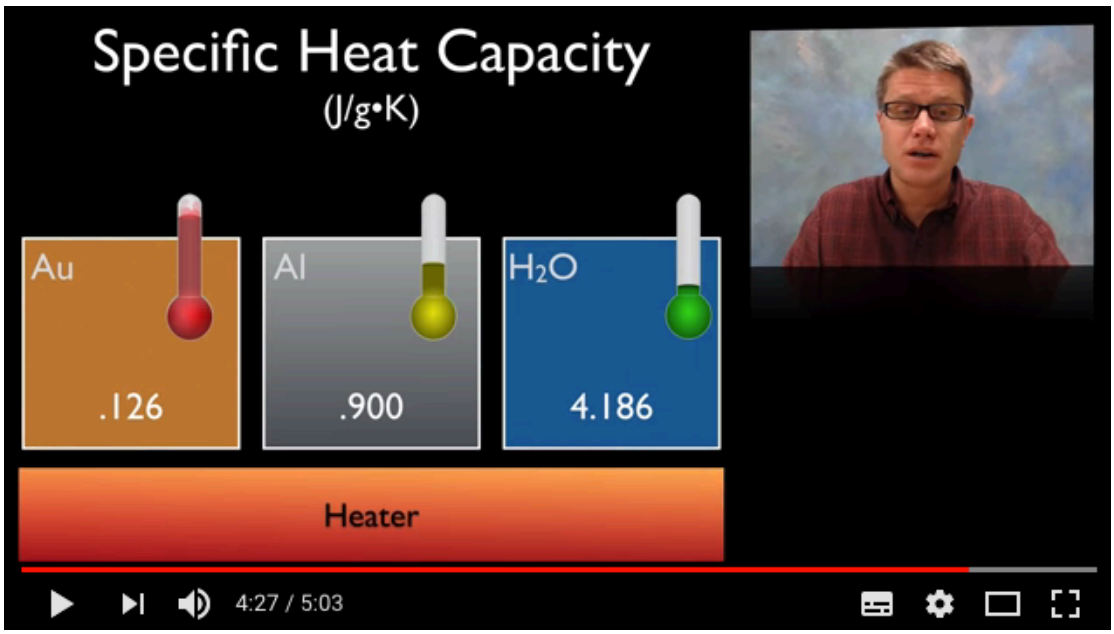

Figure 57. Specific Heat Capacity. The lower the heat capacity, the higher the temperature from single heat source.

4.16.5 Real Measurement of Gas Heat Capacity: Equivalent to GH Demonstrations

The method or the standard experimental procedure to measure gaseous heat capacities points to an 'electric heater' element – used to heat the gas - Figure 58. The apparatus and method is inseparable from the above GH demonstrations – they are equivalent[93]. The electric heater implies radiation as conduction is so low. And as a result of this radiation absorption, there will be convection. The closest solid to share the conduction properties of air – with a conduction value of 0.017 – is Aerogel – and is used on spacecraft for these properties. It is said to be 'extraordinary' with respect to this property.

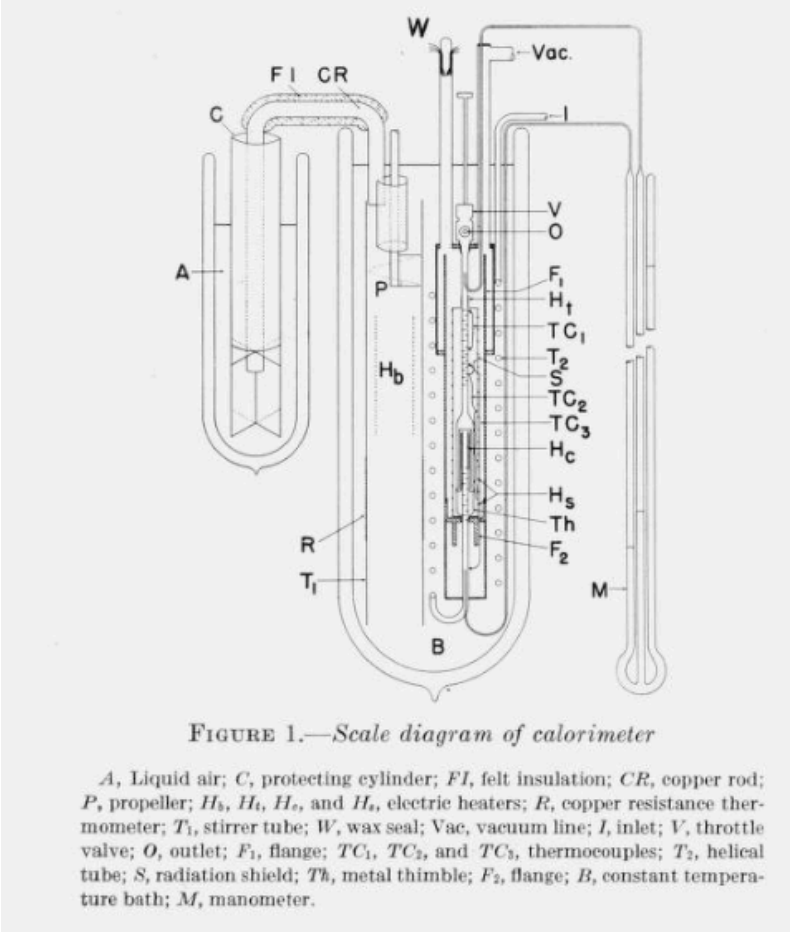

FIGURE 1.—*Scale diagram of calorimeter*

A, Liquid air; *C*, protecting cylinder; *FI*, felt insulation; *CR*, copper rod; *P*, propeller; H_b, H_t, H_c, and H_s, electric heaters; *R*, copper resistance thermometer; T_1, stirrer tube; *W*, wax seal; Vac, vacuum line; *I*, inlet; *V*, throttle valve; *O*, outlet; F_1, flange; TC_1, TC_2, and TC_3, thermocouples; T_2, helical tube; *S*, radiation shield; *Th*, metal thimble; F_2, flange; *B*, constant temperature bath; *M*, manometer.

Figure 58. O_2 Heat Capacity Measurement by Radiation. [93]

4.16.5.1 Measurement of GHGs Specific Heat proves non-GHGs absorb IR

As it is assumed the GHGs absorb IR heat radiation in Specific Heat measurement – at their respective TE/IR and Raman modes as presented in this investigation – it is equally plausible the non-GHGs, on the same principles, are absorbing IR heat radiation at their respective Raman modes, proportional to the resulting and measured specific heat capacities. Support for this claim is found with CO_2 and CH_4; both are poor thermal conductors (as with 'air') and both are IR (thermoelectric) emitters. From this investigation, and the equipartition principle, all their modes (TE and Raman) are equivalent; and so, this must be so for the non-GHGs N_2 and O_2 also.

4.16.6 Vibrational Behaviour and Specific Heat Capacity

It is interesting to read when investigating the fundamental knowledge behind Specific Heat of matter: it is defined 'by the vibrational behaviour of molecules' –

as described earlier in this investigation – including the 'degrees of freedom' that determines the specific heat capacity of a substance. This adds further weight to including the Raman modes to radiation theory. Molecules such as N_2 and O_2 vibrate, they have degrees of freedom, and they have specific heats – so they must radiate IR also, at their Raman modes.

4.16.7 IR Absorption and the Incandescent Light Bulb

Further 4.16.3, while looking for supporting evidence of IR absorbing N_2 and O_2 and noticing the hot air is moving around the outside of the bulb when on. I wondered; what if the bulb were filled with air or N_2, what would result? Pressure increases? It turns out light bulbs are filled with gas – mostly Argon (Ar) and small percentage of N_2[94]. Neither of these gases are IR (thermoelectric), and they are also said to warm inside the bulb by conduction. However, given the pressure inside the bulb is 70% of an atmosphere (to deal with the pressure problem of operation temperature) and Ar and N_2 are both very poor thermal conductors (argon even less that N_2 at 0.016 W/m K [95] and Table 6), it is plausible the gases heat mostly – if not all – by radiation, as I have claimed and demonstrated in this paper. See 4.17.2 for a proposed experiment to test of IR absorption of N_2 and O_2.

4.16.7.1 Non-TE/IR Non-Raman Argon

In this discussion of IR absorbing gases, Ar presents itself as an odd one out. It is neither a GHG (it is not thermoelectric), nor a Raman-active gas. This is said to be due to it vibrational behaviour as an atom alone. However, Ar has a specific heat capacity of 0.520 (kJ/kg K) compared to air of 1.01, and does, (be it low) conduct heat. The dismissing of it radiating IR may be due to the said detectors being unable to detect its behaviour, just as thermoelectric-IR cannot detect Raman modes. Again, if it does not radiate IR, this is in contradiction to quantum physics.

4.17 What is Next?

There are unanswered questions from this work that need to be addressed:

4.17.1 Why is it N_2 and O_2 do not show up in – what I have termed thermoelectric – IR Spectroscopy?

I believe (and have presented in my second paper [79]) the answer to this problem is to do with the mode type of the spectra in question (shown in column 4 Table 1). I claim the so-called IR-active modes are thermoelectric modes and these modes transmit IR radiation received by thermoelectric transducers.

4.17.2 A Proposed N_2 and O_2 Absorption Experiment

To test and prove N_2 and O_2 directly absorb IR photons in isolation from an IR heat source; an experiment utilizing a Raman spectrometer could be conducted measuring changes in temperature of molecule surrounding the radiating heat source. This will clear any conjectures heat transfer is from 'forced convection' alone. It is expected the molecules respond to the radiation raising in temperature proportional to the energy transmitted from the radiating energy source in accordance with the Stefan-Boltzmann law.

5 Conclusions

It was found there has been systematic error in measuring the IR properties of the atmospheric gases. N_2 and O_2, and all of the atmospheric gases, consistent to quantum mechanic's Schrödinger equation, have predicted spectra bands or modes – at 2338 cm^{-1} and 1556 cm^{-1} respectively – in the IR range of the EMS and these predicted spectra are observed by IR spectroscopies complement – and when on its own, GHG deriving – instrument, Raman spectrometers.

Consistent with standard radiation theory, by Raman Spectroscopy the temperature of the atom or molecule was measured at these predicted spectra, and I uncovered an equation to explain this:

$$T = p / (k \cdot N_{total}) \quad (1)$$

Where T is the temperature of the atmosphere or gas; p the pressure, k the Boltzmann constant, and N_{total} to total species of gases (identified by the Raman Spectrometer).

Raman instruments measurements concur with standard physical principles – including the Boltzmann constant – to the extent they can measure temperature

and gas concentration to an equal of the greater degree of precision than its similar thermoelectric counterpart.

It was found modern Raman spectroscopy technology can measure the concentrations of the all the gases constituents of the atmosphere, equivalent to, and may stand as a substitute to, the current Keeling curve 'IR' spectrographic method. It is for this reason it is one of the instruments of choice on solar system space probes.

Further to this, it was shown, by practical application, the N_2 molecule absorbs IR photons in the quantum theory and operation of the (solar) N_2-CO_2 laser. The operation of this laser is dependent upon of N_2's quantum predicted 2338 cm^{-1} absorption mode. When the N_2 is radiated by electron discharge, or photons, it was also found to be long lasting 'metastable' absorption – essential in the laser process – and this heat-energy gained (pumped) is transferred directly to CO_2's close mode at 2349 cm^{-1}. From this understanding of the IR absorption-emission properties of N_2, at its one absorption mode, it can be inferred N_2 absorbs in the atmosphere infrared photons **by law**, by the identical process as demonstrated as in its role in the N_2-CO_2 Laser. In this process, solar insolation – of IR photons – accounts for changing air temperature. By the photon absorption process of N_2, it can be said, it is the N_2 that affects the CO_2. This finding is totally inconsistent with current greenhouse theory; however, it has the quantum physics and the quantum application – not to mention the real constituent volume of the gas – directly supporting this claim. This may well explain how air instantly rises in temperature – in the process of thunder production – to some '3 times the temperature of the surface of the sun', and how N_2 molecule reaches the temperature of 2700 degrees Kelvin in the thermosphere. It can be concluded the atmosphere absorbs IR radiation from the sun by (solar) insolation directly and warms the air just as it does the H_2O of the oceans and the like are, rather than indirectly, as it is currently assumed. It can also be concluded from this work it is not the gases that are special but rather it is the instruments that measure them. In support of this it was found all three of H_2O's IR radiating modes – the modes pointing to them being GHGs, particularly the 3652 cm^{-1}

mode – are both or dual Raman and IR active. CO_2's only Raman active mode at 1388 cm^{-1} must be temperature equivalent – by the equipartition principle – to it's complementary 'IR active' modes – measured at 2349 cm^{-1} and 667 cm^{-1} (section 4.5.1). This says the detectors are equivalent: both can and should measure the temperature of these molecules. Modern Raman spectroscopy is so accurate – it does not suffer the emissivity problem – it should make 19th Century IR spectroscopy redundant. This finding has implications also on the IR (alone) derived 'blackbody spectrum' – where it was found the quantum predicted spectra of gas molecules are absorbing outside the domain of the Sun's and Earth's blackbody curves. It was concluded here this curve needs updating and may even be redundant with Raman Laser technology.

In respect to heat capacities, it was discussed Raman spectra properties also correspond to the nominal heat capacities of the said gases where with IR theory alone they are both non-absorbent and non-thermal conductive.

With this inclusion of the quantum mechanics to atmospheric models – and the direct mechanics behind Raman spectroscopy – it was revealed the current understanding of the 'greenhouse' atmosphere is fallacious, and built on out-dated methods and equipment. Raman spectroscopy makes IR spectroscopy redundant. Quantum mechanics holds, not GH theory; all matter does radiate. It should finally be concluded all gases are GHGs; just as first posited by Joseph Fourier (and maybe others) ca. 1828. The non-GHGs should be known as the Raman gases; and together they all should constitute as the GHGs. There are no special gases. With this new understanding, all gases comply with the 0th and 1st Laws of Thermodynamics – transferring energy towards equilibrium where previous to this N_2 and O_2 were exempt. Any extrapolation based on IR spectroscopy technology alone – without reference to Raman spectroscopy – interpreting these as the only special 'IR absorbent' GHGs should be seen as inadmissible – not only in climate and atmospheric theory, but also any radiation theory. Climate models will need to be updated to take account of the – currently well understood method by all chemists – Raman spectroscopy.

6 Acknowledgements

Aside from the support from family and colleagues and friends, due to the nature of the investigation I do not have anyone to acknowledge directly for this work; I have been totally unsupported. I do however thank the many prepublication reviewers, the sceptics of my theory, some from the sceptic side of the climate debate. They have helped my process no end.

7 References

1. Carbon Dioxide Absorbs and Re-emits Infrared Radiation | UCAR Center for Science Education [Internet]. [cited 10 Feb 2019]. Available: https://scied.ucar.edu/carbon-dioxide-absorbs-and-re-emits-infrared-radiation

2. Greenhouse Gases. Greenhouse Gases [Internet]. Available: http://butane.chem.uiuc.edu/pshapley/Environmental/L13/2.html

3. Bozeman Science. The Greenhouse Effect [Internet]. Available: https://www.youtube.com/watch?v=3ojaDMadZXU

4. Why are some gases greenhouse gases? Lecture 14 Slide 5 [Internet]. 2013. Available: http://www.atmos.washington.edu/~davidc/ATMS211/Lecture14-handout-PDF.pdf

5. Heat Transfer in the Atmosphere | Physical Geography [Internet]. [cited 23 Feb 2018]. Available: https://courses.lumenlearning.com/geophysical/chapter/heat-transfer-in-the-atmosphere/

6. UQx Denial101x Making Sense of Climate Science Denial. UQx DENIAL101x 3.3.5.1 From the experts: Greenhouse effect [Internet]. Available: https://www.youtube.com/watch?v=H4YSwajvFAY

7. Definition of Raman spectroscopy. In: Photonics.com [Internet]. [cited 18 Sep 2018]. Available: https://www.photonics.com/EDU/Raman_spectroscopy/d6589

8. Leonard DA. Field Tests of a Laser Raman Measurement System for Aircraft Engine Exhaust Emissions [Internet]. AVCO EVERETT RESEARCH LAB INC EVERETT MA, AVCO EVERETT RESEARCH LAB INC EVERETT MA; 1974 Oct. Available: http://www.dtic.mil/docs/citations/ADA003648

9. Leonard D. DEVELOPMENT OF A LASER RAMAN AIRCRAFT TURBINE ENGINE EXHAUST EMISSIONS MEASUREMENT SYSTEM [Internet]. AVCO EVERETT RESEARCH LABORATORY a division of AVCO CORPORATION Everett, Massachusetts; 1972 May. Report No.: F33615-71-C–1875. Available: http://www.dtic.mil/dtic/tr/fulltext/u2/a003648.pdf

10. Tuschel D. Raman Thermometry [Internet]. [cited 23 Sep 2018]. Available: http://www.spectroscopyonline.com/raman-thermometry

11. Kim D, Kang H, Ryu JY, Jun SC, Yun ST, Choi SC, et al. Development of Raman lidar for remote sensing of CO2 leakage at an artificial carbon capture and storage site. Remote Sens. 2018;10: 1439. doi:10.3390/rs10091439

12. Duley W. CO2 Lasers Effects and Applications. Elsevier; 2012.

13. Gordillo-V-Uuml FJ, zquez, Kunc JA. High-Accuracy Expressions for Rotational-Vibrational Energies of O, N, NO, and CO Molecules. J Thermophys Heat Transf. 1998;12: 52–56. doi:10.2514/2.6301

14. Vibrational spectroscopy [Internet]. 2013. Available: https://www.youtube.com/watch?v=rdj992LnWDo&feature=youtube_gdata_player

15. Normal modes [Internet]. 2013. Available: https://www.youtube.com/watch?v=TTkZpDDOOOw&feature=youtube_gdata_player

16. Number of vibrational modes for a molecule. In: chemwiki.ucdavis.edu [Internet]. [cited 12 Feb 2015]. Available: http://chemwiki.ucdavis.edu/Physical_Chemistry/Spectroscopy/Vibrational_Spectroscopy/Vibrational_Modes/Number_of_vibrational_modes_for_a_molecule

17. Sharma SK, Misra AK, Singh UN. Remote Raman Spectroscopy of Minerals at Elevated Temperature Relevant to Venus Exploration. Noumea, New Caledonia; 2008. Available: http://ntrs.nasa.gov/search.jsp?R=20080046999

18. Aroca R, Rodriguez-Llorente S. Surface-enhanced vibrational spectroscopy. J Mol Struct. 1997;408–409: 17–22. doi:10.1016/S0022-2860(96)09489-6

19. Leonard DA. Field Tests of a Laser Raman Measurement System for Aircraft Engine Exhaust Emissions [Internet]. AVCO EVERETT RESEARCH LAB INC EVERETT MA, AVCO EVERETT RESEARCH LAB INC EVERETT MA; 1974 Oct. Available: http://www.dtic.mil/docs/citations/ADA003648

20. Milonni PW, Eberly JH. Laser Physics. John Wiley & Sons; 2010.

21. Laser History - Near Infrared Lasers on Mars and Venus [Internet]. [cited 25 Jan 2018]. Available: http://laserstars.org/history/mars.html

22. Letokhov V, Johansson S. Astrophysical Lasers. Oxford, New York: Oxford University Press; 2008.

23. Deyoung RJH. A blackbody-pumped CO2-N2 transfer laser [Internet]. 1984 Aug. Available: https://ntrs.nasa.gov/search.jsp?R=19840023547

24. Climate Science Investigations South Florida - Energy: The Driver of Climate [Internet]. [cited 30 Sep 2017]. Available: http://www.ces.fau.edu/nasa/module-2/correlation-between-temperature-and-radiation.php

25. Spectroscopy & Materials Analysis. Raman Basics [Internet]. Available: https://www.youtube.com/watch?v=Gok7jRuer1k&index=35&list=PLUlOlLDYaBHX1EmAZVRkpOidQHTKAp34i&t=0s

26. CHEM Study C of C. Molecular Spectroscopy [Internet]. 1962. Available: http://archive.org/details/molecular_spectroscopy

27. The Equipartition Principle. In: Chemistry LibreTexts [Internet]. 24 Jul 2016 [cited 1 Apr 2018]. Available: https://chem.libretexts.org/Textbook_Maps/Physical_and_Theoretical_Chemistry_Textbook_Maps/Map%3A_Physical_Chemistry_(McQuarrie_and_Simon)/18%3A_Partition_Functions_and_Ideal_Gases/The_Equipartition_Principle

28. Robinson A. The Scientists: An Epic of Discovery. Thames & Hudson; 2012.

29. Quantitative Laser Raman Spectroscopy of Gases | White Papers | Photonics.com [Internet]. [cited 18 Sep 2018]. Available: https://www.photonics.com/WhitePaper.aspx?WPID=1620

30. Petrov DV, Matrosov II, Zaripov AR. Determination of atmospheric carbon dioxide concentration using Raman spectroscopy. J Mol Spectrosc. 2018;348: 137–141. doi:10.1016/j.jms.2018.01.001

31. Angel SM, Gomer NR, Sharma SK, McKay C. Remote Raman spectroscopy for planetary exploration: a review. Appl Spectrosc. 2012;66: 137–150. doi:10.1366/11-06535

32. Shiv Sharma, Paul Lucey, Upedra Singh, and Nurul Abedin. Exploring Atmosphere & Surface Mineralogy of Venus with a Combined Remote Raman Spectroscopy & Elastic Lidar [Internet]. 2015 Apr 9; National Institute for Aerospace Hampton, Virginia. Available: http://www.lpi.usra.edu/vexag/meetings/archive/vexag_12/presentations/OM3_Sharma_etal.pdf

33. Onboard Lidar Detects Turbulence, Volcanic Ash Near and Far | Features | Feb 2018 | Photonics Spectra [Internet]. [cited 25 Jan 2019]. Available: https://www.photonics.com/Articles/Onboard_Lidar_Detects_Turbulence_Volcanic_Ash/a62913

34. Liu F, Yi F. Lidar-measured atmospheric N_2 vibrational-rotational Raman spectra and consequent temperature retrieval. Opt Express. 2014;22: 27833. doi:10.1364/OE.22.027833

35. Raman Lidar: Theoretical Background | University of Hertfordshire [Internet]. [cited 9 Aug 2016]. Available: http://www.herts.ac.uk/research/centres-and-groups/cair/atmospheric-remote-sensing-laboratory/instruments/raman-lidar-theoretical-background

36. Newsom, Sivaraman, MaFarlane. Raman Lidar Profiles–Temperature (RLPROFTEMP) Value-Added Product [Internet]. 2012 Oct. Available: https://www.arm.gov/publications/tech_reports/doe-sc-arm-tr-120.pdf

37. Yufeng W, Fei G, Chengxuan Z, Qing Y, Dengxin H. Observations of atmospheric water vapor, aerosol, and cloud with a Raman lidar. Opt Eng. 2014;53: 114105–114105. doi:10.1117/1.OE.53.11.114105

38. Thermal Radiation - an overview | ScienceDirect Topics [Internet]. [cited 12 Feb 2019]. Available: https://www.sciencedirect.com/topics/pharmacology-toxicology-and-pharmaceutical-science/thermal-radiation

39. Charged particle [Internet]. Wikipedia. 2017. Available: https://en.wikipedia.org/w/index.php?title=Charged_particle&oldid=802130885

40. What is the difference between cathode rays and beta particles? - Quora [Internet]. [cited 12 Feb 2019]. Available: https://www.quora.com/What-is-the-difference-between-cathode-rays-and-beta-particles

41. metastable state | chemistry and physics. In: Encyclopedia Britannica [Internet]. [cited 24 Jul 2017]. Available: https://www.britannica.com/science/metastable-state

42. Guerra V, Sá PA, Loureiro J. Role played by the N 2 (A 3 Σ u +) metastable in stationary N 2 and N 2 -O 2 discharges. J Phys Appl Phys. 2001;34: 1745. doi:10.1088/0022-3727/34/12/301

43. Kaslow DE, Zorn JC. Time-of-Flight Measurements of Metastable State Lifetimes. Rev Sci Instrum. 1973;44: 1209–1212. doi:10.1063/1.1686355

44. Meschede D. Optics, Light and Lasers: The Practical Approach to Modern Aspects of Photonics and Laser Physics. John Wiley & Sons; 2008.

45. Davis CC. Lasers and Electro-optics: Fundamentals and Engineering. Cambridge University Press; 1996.

46. V. Krishnakumar. Raman Spectroscopy [Internet]. 03:38:05 UTC. Available: http://www.slideshare.net/krishslide/raman-spectroscopy-39462565

47. Raman spectroscpy presentation by zakia afzal [Internet]. 07:10:28 UTC. Available: http://www.slideshare.net/ZakiaAfzal/raman-spectroscpy-presentation-by-zakia-afzal

48. Kiefer J. Recent Advances in the Characterization of Gaseous and Liquid Fuels by Vibrational Spectroscopy. Energies. 2015;8: 3165–3197. doi:10.3390/en8043165

49. 01 PM, Comments 2011 inShare0 Email Print. Understanding Infrared and Raman Spectra of Pharmaceutical Polymorphs | American Pharmaceutical Review - The Review of American Pharmaceutical Business & Technology [Internet]. [cited 24 Feb 2015]. Available: http://www.americanpharmaceuticalreview.com/Featured-Articles/37183-Understanding-Infrared-and-Raman-Spectra-of-Pharmaceutical-Polymorphs/

50. UK Carbon Capture and Storage Research Centre. Determination of water solubility limits in CO2 mixtures to deliver w… [Internet]. Science presented at; 06:58:06 UTC. Available: https://www.slideshare.net/UKCCSRC/determination-of-water-solubility-limits-in-co2-mixtures-to-deliver-water-specification-levels-for-co2-transportation-project-update-dr-stephanie-foltran-at-ukccsrc-biannual-meeting-cambridge-april-2014

51. Ab initio and Classical Molecular Dynamics Simulations of Supercritical Carbon Dioxide Moumita Saharay and S. Balasubramanian Jawaharlal Nehru Center for. - ppt download [Internet]. [cited 13 Nov 2018]. Available: https://slideplayer.com/slide/4796706/

52. IfAS : India’s No - 1 Life Science & Chemical Science (NET , GATE , M.Sc. , SET) Institute [Internet]. [cited 13 Nov 2018]. Available: http://ifasonline.com/chemicalScience_topic56c.jsp

53. Lawrence kok. IB Chemistry on Infrared Spectroscopy [Internet]. Education presented at; 02:05:16 UTC. Available: https://www.slideshare.net/wkkok1957/ib-chemistry-on-infrared-spectroscopy-53759660

54. Bigg GR. The Oceans and Climate. Cambridge University Press; 2003.

55. McCole Dlugosz ET, Fisher R, Filin A, Romanov DA, Odhner JH, Levis RJ. Filament-Assisted Impulsive Raman Spectroscopy of Ozone and Nitrogen Oxides. J Phys Chem A. 2015;119: 9272–9280. doi:10.1021/acs.jpca.5b06319

56. Tomasi F de, Perrone MR, Protopapa ML. Monitoring O_3 with solar-blind Raman lidars. Appl Opt. 2001;40: 1314–1320. doi:10.1364/AO.40.001314

57. Lazzarotto B, Frioud M, Larchevêque G, Mitev V, Quaglia P, Simeonov V, et al. Ozone and water-vapor measurements by Raman lidar in the planetary boundary layer: error sources and field measurements. Appl Opt. 2001;40: 2985–2997. doi:10.1364/AO.40.002985

58. Duflot V, Baray J-L, Payen G, Marquestaut N, Posny F, Metzger J-M, et al. Tropospheric ozone profiles by DIAL at Maïdo Observatory (Reunion Island): system description, instrumental performance and result comparison with ozone external data set. Atmospheric Meas Tech. 2017;10: 3359–3373. doi:https://doi.org/10.5194/amt-10-3359-2017

59. Macdonald BD. The Greenhouse Gases and Infrared Radiation Misconceived by Thermoelectric Transducers. 2018; Available: http://vixra.org/abs/1811.0499

60. Dear Judge Alsup: The Quantum Interlude [Internet]. [cited 13 May 2018]. Available: http://rabett.blogspot.com/2018/03/dear-judge-alsop-quantum-interlude.html

61. What is a solar pyranometer? In: Solar Power World [Internet]. 20 Mar 2015 [cited 31 May 2018]. Available: https://www.solarpowerworldonline.com/2015/03/what-is-a-solar-pyranometer/

62. Characteristics of Greenhouse Gases (GHGs) [Internet]. [cited 3 May 2018]. Available: http://www.environbusiness.com/cchangemain/cofghg

63. Greenhouse Effect [Internet]. [cited 25 Jun 2018]. Available: http://www.dnrec.delaware.gov/ClimateChange/Pages/Greenhouse%20Effect.aspx

64. Wogan D. Why we know about the greenhouse gas effect. In: Scientific American Blog Network [Internet]. [cited 10 Feb 2019]. Available: https://blogs.scientificamerican.com/plugged-in/why-we-know-about-the-greenhouse-gas-effect/

65. New Insights on the Physical Nature of the Atmospheric Greenhouse Effect Deduced from an Empirical Planetary Temperature Model | OMICS International [Internet]. [cited 10 Feb 2019]. Available: https://www.omicsonline.org/open-access/new-insights-on-the-physical-nature-of-the-atmospheric-greenhouse-effect-deduced-from-an-empirical-planetary-temperature-model.php?aid=88574

66. Svensmark H, Enghoff MB, Shaviv NJ, Svensmark J. Increased ionization supports growth of aerosols into cloud condensation nuclei. Nat Commun. 2017;8: 2199. doi:10.1038/s41467-017-02082-2

67. Tomicic M, Bødker Enghoff M, Svensmark H. Experimental study of H2SO4 aerosol nucleation at high ionization levels. Atmospheric Chem Phys. 2018;18: 5921–5930. doi:10.5194/acp-18-5921-2018

68. Weitkamp C. Lidar: Range-Resolved Optical Remote Sensing of the Atmosphere. Springer Science & Business; 2006.

69. lab-greenhousegas.pdf [Internet]. Available: https://www.acs.org/content/dam/AACT/middle-school/gases/Temperature/lab-greenhousegas.pdf

70. SpanglerScienceTV. The Greenhouse Effect - Cool Science Experiment [Internet]. Available: https://www.youtube.com/watch?v=vFajQNg9yUY

71. Wacker PF, Cheney RK, Scott RB. Heat capacities of gaseous oxygen, isobutane, and 1-butene from -30 degrees to +90 degreesC [Internet]. National Bureau of Standards; 1947. Available: http://archive.org/details/jresv38n6p651

72. MacIsaac D, Kanner G, Anderson G. Basic physics of the incandescent lamp (lightbulb). Phys Teach. 1999;37: 520–525. doi:10.1119/1.880392

73. Thermal Conductivity of common Materials and Gases [Internet]. [cited 1 May 2017]. Available: http://www.engineeringtoolbox.com/thermal-conductivity-d_429.html

74. Kuznetsov DS, Morozov VB, Olenin AN, Tunkin VG. High resolution study of 1388 cm−1 CO2 vibration by time-domain CARS: spectral exchange and Dicke effect. Chem Phys. 2000;257: 117–122. doi:10.1016/S0301-0104(00)00125-7

75. Dicke effect [Internet]. Wikipedia, the free encyclopedia. 2014. Available: https://en.wikipedia.org/w/index.php?title=Dicke_effect&oldid=633168376

76. Thomas ME. Optical Propagation in Linear Media: Atmospheric Gases and Particles, Solid-State Components, and Water. Oxford University Press; 2006.

77. Gravenstein JS, Jaffe MB, Gravenstein N, Paulus DA. Capnography. Cambridge University Press; 2011.

78. Garg R, Gupta RC. Analysis of Oxygen, Anaesthesia Agent and Flows in Anaesthesia Machine. Indian J Anaesth. 2013;57: 481–488. doi:10.4103/0019-5049.120144

79. Morizet Y, Brooker RA, Iacono-Marziano G, Kjarsgaard BA. Quantification of dissolved CO2 in silicate glasses using micro-Raman spectroscopy. Am Mineral. 2013;98: 1788–1802. doi:10.2138/am.2013.4516

80. Final Report | Remote Sensing of Automobile Emissions Using Raman LIDAR| Research Project Database | Grantee Research Project | ORD | US EPA [Internet]. [cited 6 Aug 2017]. Available: https://cfpub.epa.gov/ncer_abstracts/index.cfm/fuseaction/display.highlight/abstract/1704/report/F

81. Thomas P, Hummel RL, Smith JW. Rotational Raman Spectroscopy for the Remote Sensing of Carbon Dioxide. J Air Pollut Control Assoc. 1979;29: 390–391. doi:10.1080/00022470.1979.10470810

82. Klingenberg H. Automobile Exhaust Emission Testing: Measurement of Regulated and Unregulated Exhaust Gas Components, Exhaust Emission Tests. Springer Science & Business Media; 2012.

83. Schwiesow RL, Derr VE. A Raman scattering method for precise measurement of atmospheric oxygen balance. J Geophys Res. 1970;75: 1629–1632. doi:10.1029/JC075i009p01629

84. Analysis of influence of atmosphere extinction to Raman lidar monitoring CO2 concentration profile. In: ResearchGate [Internet]. [cited 24 Jul 2017]. Available: https://www.researchgate.net/publication/231038895_Analysis_of_influence_of_atmosphere_extinction_to_Raman_lidar_monitoring_CO2_concentration_profile

85. NDACC lidar working group - Raman water vapour [Internet]. [cited 9 Mar 2018]. Available: http://ndacc-lidar.org/index.php?id=45/Raman+water+vapour.htm

86. LIDAR FOR ATMOSPHERIC TRACE GAS DETECTION| IEEE | Geoscience & Remote Sensing Society. In: GRSS | IEEE | Geoscience & Remote Sensing Society [Internet]. [cited 9 Mar 2018]. Available: http://www.grss-ieee.org/lidar-for-atmospheric-trace-gas-detection/

87. Fouche DG, Chang RK. Relative Raman Cross Section for N2, O2, CO, CO2, SO2, and H2S. Appl Phys Lett. 1971;18: 579–580. doi:10.1063/1.1653548

88. Visual guide to Raman spectroscopy | Nanophoton - YouTube [Internet]. [cited 9 Aug 2016]. Available: https://www.youtube.com/watch?v=TyKmhI_kFgY

89. Lecture-8-Raman.pdf [Internet]. Available: https://www.princeton.edu/cefrc/Files/2011%20Lecture%20Notes/Alden/Lecture-8-Raman.pdf

90. Ehlerding A, Johansson I, Wallin S, Östmark H. Resonance-Enhanced Raman Spectroscopy on Explosives Vapor at Standoff Distances. Int J Spectrosc. 2012;2012: e158715. doi:10.1155/2012/158715

91. Using Kaiser's RamanRxn1™ Microprobe for Headspace Gas Analysis [Internet]. 26 Aug 2014. Available: http://www.azom.com/article.aspx?ArticleID=11271

92. Hanf S, Keiner R, Yan D, Popp J, Frosch T. Fiber-enhanced Raman multigas spectroscopy: a versatile tool for environmental gas sensing and breath analysis. Anal Chem. 2014;86: 5278–5285. doi:10.1021/ac404162w

93. Haken H, Wolf HC. Molecular Physics and Elements of Quantum Chemistry: Introduction to Experiments and Theory. Springer Science & Business Media; 2004.

94. Lobanov SS, Chen P-N, Chen X-J, Zha C-S, Litasov KD, Mao H-K, et al. Carbon precipitation from heavy hydrocarbon fluid in deep planetary interiors. Nat Commun. 2013;4. doi:10.1038/ncomms3446

95. Ferini G, Baratta GA, Palumbo ME. A Raman study of ion irradiated icy mixtures. Astron Astrophys. 2004;414: 757–766. doi:10.1051/0004-6361:20031641

96. AZO Materials. Using Raman Spectroscopy to Assist in the REACH Registration of Gases [Internet]. Available: http://www.azom.com/article.aspx?ArticleID=12431

97. Kolesov B. Raman investigation of H2O molecule and hydroxyl groups in the channels of hemimorphite. Am Mineral. 2006;91: 1355–1362. doi:10.2138/am.2006.2179

98. Characterizing Carbon Nanomaterials. In: Laboratory Equipment [Internet]. [cited 29 Mar 2016]. Available: http://www.laboratoryequipment.com/articles/2011/06/characterizing-carbon-nanomaterials

99. Sanson A, Napolitani E, Impellizzeri G, Giarola M, De Salvador D, Privitera V, et al. Investigation of germanium implanted with aluminum by multi-laser micro-Raman spectroscopy. Thin Solid Films. 2013;541: 76–78. doi:10.1016/j.tsf.2012.11.133

100. Using Raman and IR Spectrosocpy to Monitor Soil Gases and the Sequestration of CO2. In: http://www.azom.com/article.aspx?ArticleID=12432 [Internet]. Available: http://www.azom.com/article.aspx?ArticleID=12432

101. Figure 4: Raman and thermal imaging of a covered epitaxial graphene device. [Internet]. [cited 22 Jun 2017]. Available: https://www.nature.com/articles/srep26457/figures/4

8 Appendix

8.1 Other Uses for Raman

8.1.1 CO2's 1388cm-1 Excitation: The Dicke effect

Investigating whether CO_2's 1388cm^{-1} is excited in any way by radiation – it should not as this mode, like N_2 and O_2's is 'Raman active' and not 'IR active' and thus, by current assumptions, should not transmit photon energy – it was found this mode is affected 'where the spectral exchange and Dicke effect play a noticeable role' [96]. The Dicke effect: 'refers to the Doppler broadening of a spectral line due to collisions the emitting species (atom or molecule) experiences with other particles' (photons) ;…the atom changes velocity and direction many times during the emission and absorption of the photon[97].

This is clear evidence this mode is active and they do radiate.

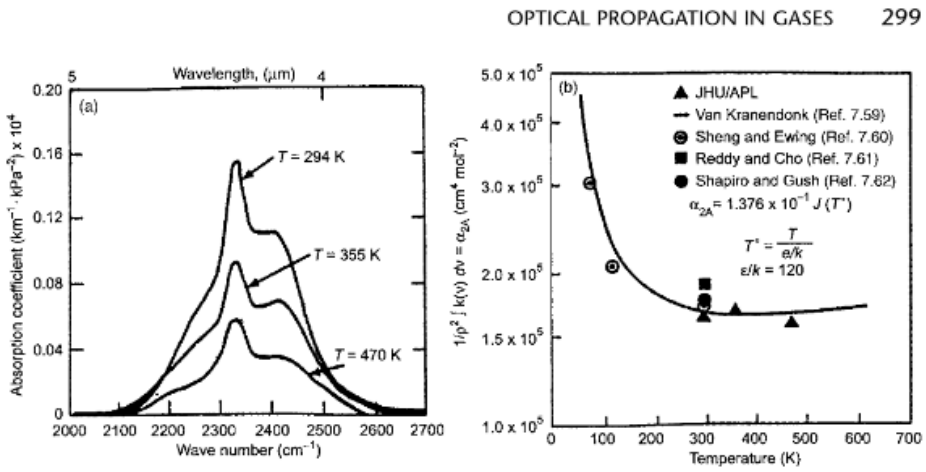

Fig. 7.21 Collision-induced absorption in the fundamental vibration band of N_2. (a) Band shape at various temperatures and (b) integrated intensity versus temperature (Thomas, Ref. 7.50).

[98]

8.1.2 Medical – anesthetic RASCAL – Capnography Application

"In 1988 a Raman scattering instrument was introduced for clinical use. The RAman SCattering AnaLyzer (RASCAL)…for O_2, CO_2, N_2, N_2O; both identify and quantify these gases." "This device is no longer marketed"[99].

These Raman devices have since advanced and are used.

'These analysers have fast response times. They can analyze multiple anesthetic agents with good accuracy (greater than infrared spectroscopy, approaching mass spectrometry)' [100].

8.1.3 Geology CO_2 1388 cm^{-1}

In the following study: "Quantification of dissolved CO_2 in silicate glasses using micro-Raman spectroscopy" CO_2 is identified at its IR 1388 (or near about) cm^{-1} mode.

'we propose the calibration accuracy is better than ±0.4 wt% CO2 for our data set'[101]

8.1.4 Automobile Emission Testing.

Raman is an accepted instrument in measuring automobile emissions; it is so by exploiting the 'radiative' behaviour of the non- GHGs. This is a contradiction.

The from the USA EPA: *"Raman LIDAR is self-calibrating to atmospheric oxygen and nitrogen, eliminating requirements for periodic calibration with test gases."[102]*

"The results indicate an excellent ability to identify and quantify the test species. By analyzing the sensitivity of these Phase I laboratory experiments, we estimate that the Compact UV Raman LIDAR system will be capable of achieving better than 120 parts per million (PPM) sensitivity for NO, 40 ppm for N_2 and CO, and 10 ppm for NO_2 and hydrocarbons."

Truth be known, Raman can equally detect and quantify CO_2 (by its Raman 1388 cm^{-1} mode) as revealed in the following study. However, before we go there, in the study 'Rotational Raman Spectroscopy for the Remote Sensing of Carbon Dioxide' [103] they concluded: "No Raman peaks were observed, so that the usefulness of rotational Raman for the remote sensing of CO_2 was not demonstrated."

This maybe so for 'remote' solutions; however, it does not match the many results from other studies.

In the book 'Automotive Exhaust Emission Testing..' they acknowledged the (potential) use of Raman "Both methods (IR and Raman) are complementary" [104] pg. 128; however, it did not go onto show the use of Raman.

8.1.5 Atmospheric measurement using Raman Spectroscopy

A Raman scattering method for precise measurement of atmospheric oxygen balance

Abstract

Quantitative measurements of Raman scattering intensities from N_2, O_2, and CO_2 under ambient atmospheric conditions are given. The atmosphere was illuminated with 20,489 cm^{-1} Ar^+ laser radiation. These scattering intensities are sufficiently strong to ***allow measurement of O_2/N_2 and CO_2/N_2 concentration ratios in the atmosphere to*** *a precision of 0.3 and 0.006 ppm total atmosphere, respectively, by means of scattered photon counting over a 174-hour integration period.* ***The Raman technique represents an improvement in precision over existing techniques by almost two orders of magnitude****, and a substantial but less easily determined improvement in accuracy by using the transition probabilities of a monomolecular reference gas as a standard, rather than the properties of a mixed gas standard as is done in current measurements. [105]*

Analysis of influence of atmosphere extinction to Raman Lidar monitoring CO_2 concentration profile∗

"Lidar (Light detection and ranging) system monitoring of the atmosphere is a novel and powerful technique tool. The Raman lidar is well established today as a leading research tool in the study of numerous important areas in the atmospheric sciences. ***In this paper, the principle of Raman lidar technique measurement CO_2 concentration profile is presented…****" [106]*

NDACC are using Raman Lidar to measure H_2O, with N_2 as "*a reference molecule having a well-known mixing ratio throughout the altitude range considered*" [107]

This process is also discussed by the IEEE under: LIDAR FOR ATMOSPHERIC TRACE GAS DETECTION [108], and in a paper "Relative Raman Cross Section for

N_2, O_2, CO, CO_2, SO_2, and H_2S"[109]: where an (inferred) argon ion laser (5145Å) is used to identify the gases.

8.2 Understanding Raman Backscatter and the Low Wavenumbers

It has been quoted to me that these lower Lidar wavenumbers – at 580nm and 607nm respectively – are inconsistence with my theory and show N_2 and O_2 in the atmosphere do not vibrate – emit and absorb – in the IR range of the EMS as these modes or bands are in the visible range of the EMS; I have researched these lower modes and found they indeed reveal the IR modes – they need correction. The reason the Lidar wavenumbers are quoted low is because they are quoted in relation or reference to the laser frequency of the Lidar laser. They work on the 'Raman backscatter'. When adjusted for, the differences are corrected (up) and correspond the predicted wavenumbers. This is demonstrated in the youtube presentation below[110] where in the last moments it is said: ". By using wavenumber, we see the excitation of water, independent of the excitation wavelength".

A	B
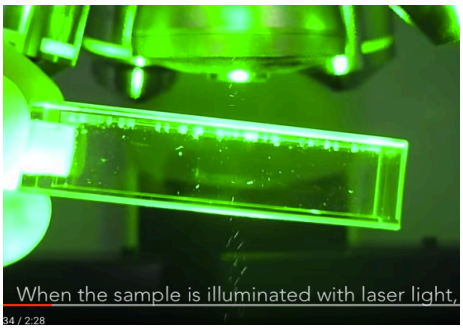	

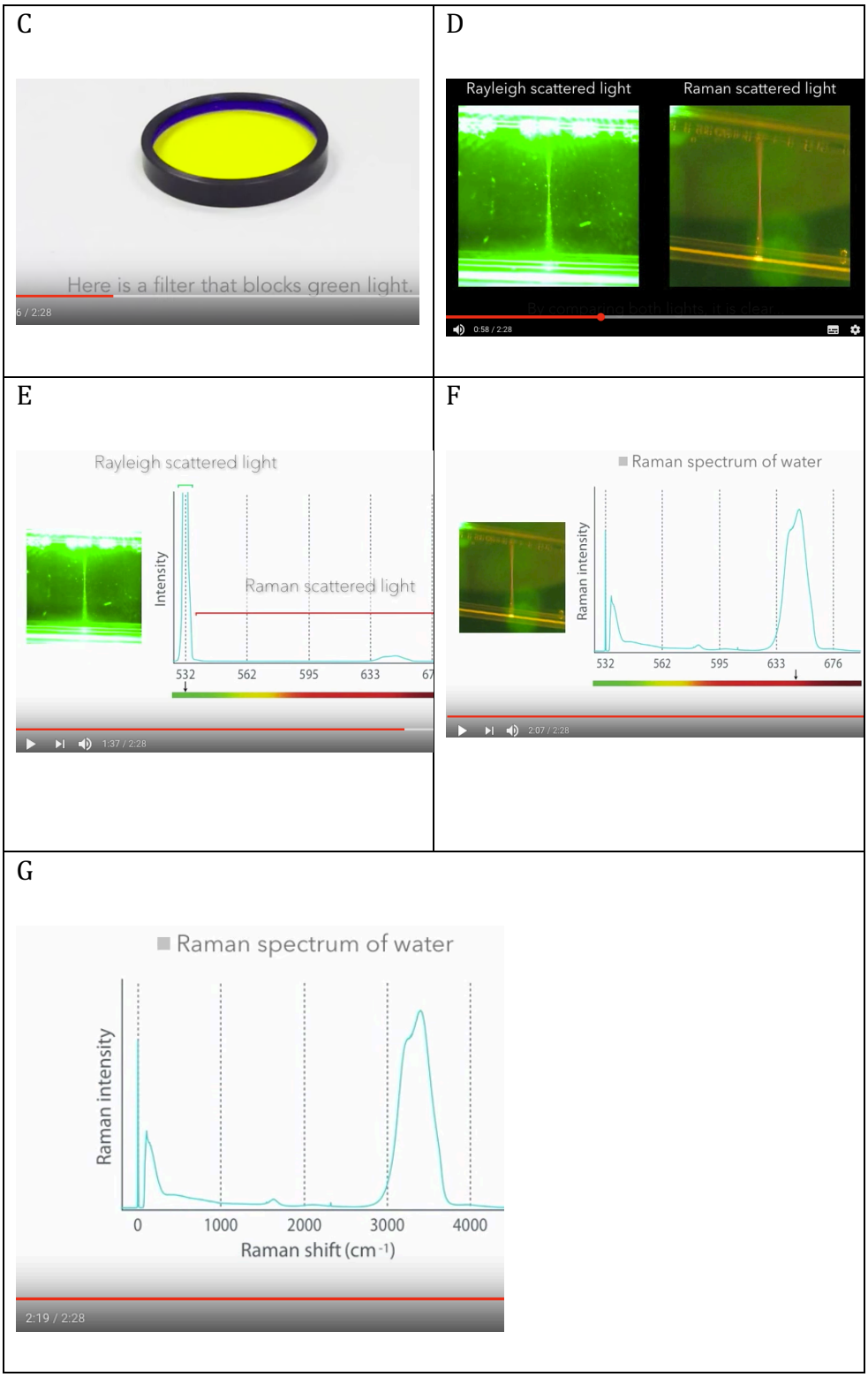

Figure 59. Raman Lidar wavenumber discrepancy Explained. Screen shots of a Youtube presentation [110]showing how green 532nm laser light is shone (A) onto water in the case Raleigh light is revealed (B and E), but when filtered Raman red 660nm light is revealed (D and F). When this adjusted for wavenumber (cm-1) H2O's vibration band 3652cm-1 is revealed.

8.2.1 Raman Laser to Wavenumber Correction Calculation

A demonstration and method of the calculation needed to correct from the low wavelength produced by Raman Lidar and Laser to the real wavenumber vibrational bands (in this case, O_2) was found. This is evidence the often quoted low wavenumbers must be corrected or understood to be relative to the incident Raman laser frequency and not the real vibration mode.

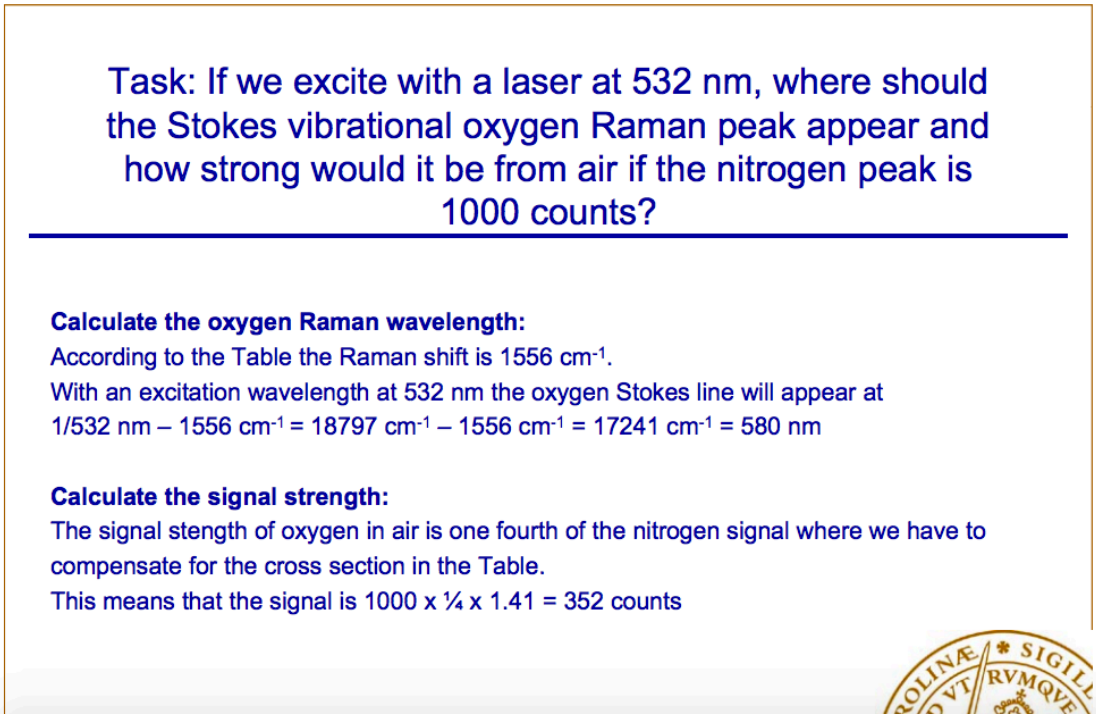

Figure 60. Scattering to Wavenumber calculation for Nitrogen. Nitrogen's 1556 cm-1 predicted and observed (with Raman spectroscopy) vibration mode is corrected for the 532nm laser. [111]

8.3 Raman spectra for Non-GHGs and GHGs

8.3.1 O_2 and N_2

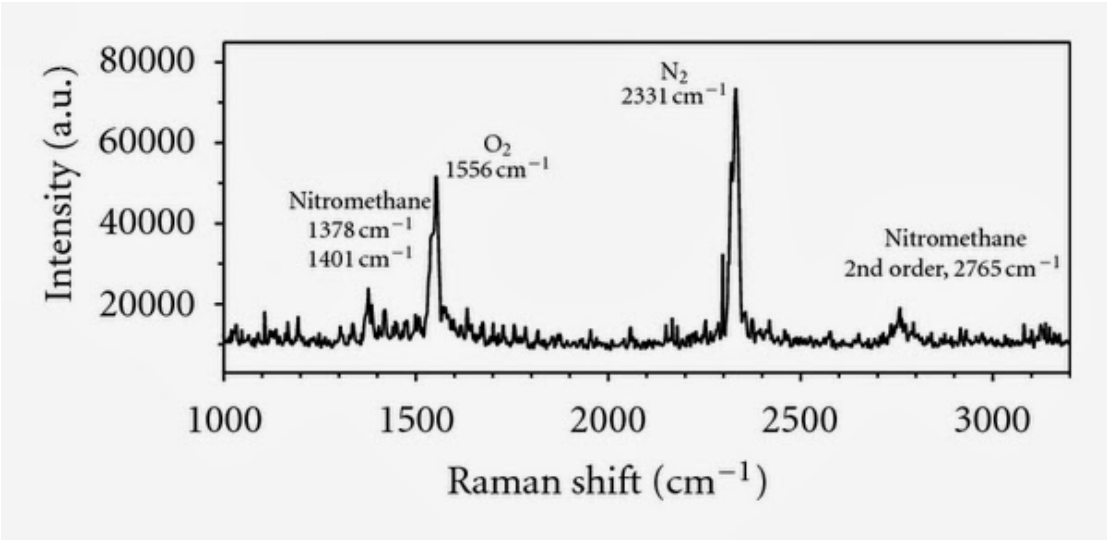

Figure 61. [112]

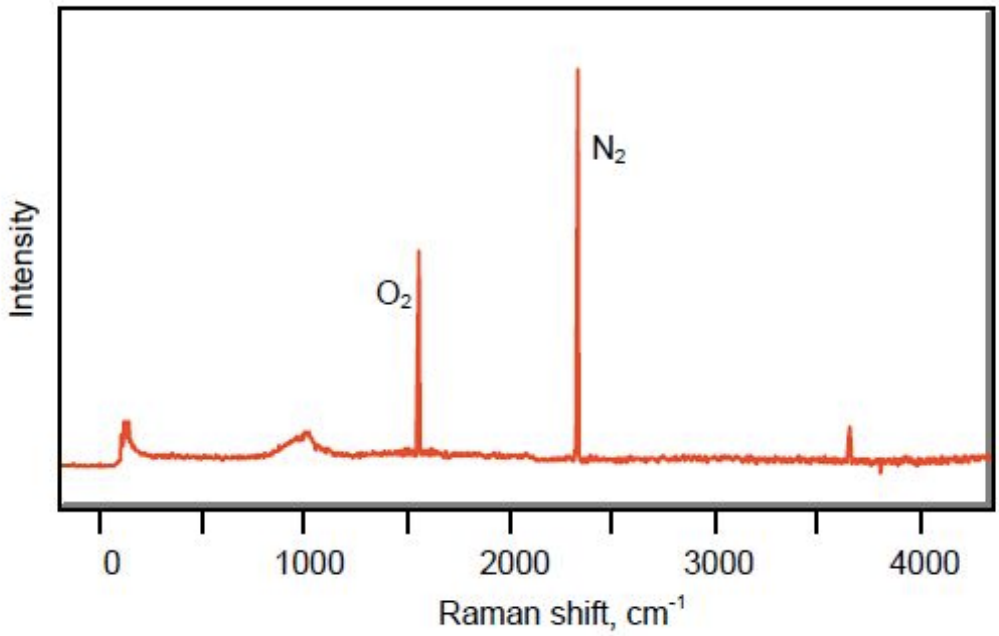

Figure 62. Raman spectrum of air, with the oxygen and nitrogen bands marked. [113]

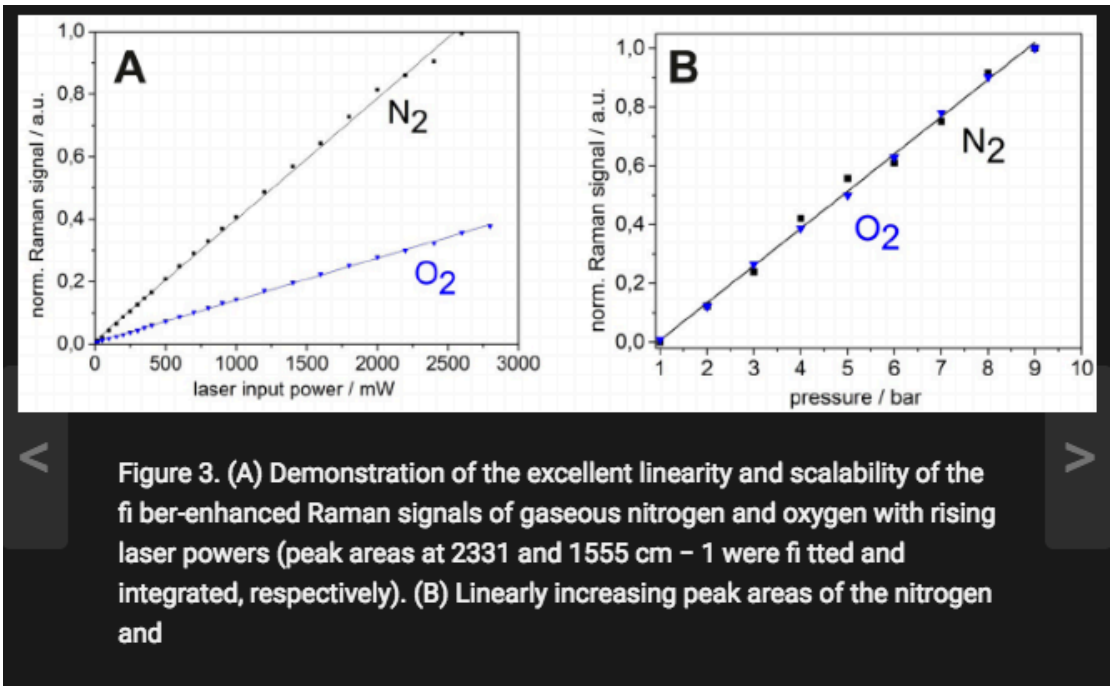

Figure 63. The above three images above: [114]

8.3.2 O_2 Spectra

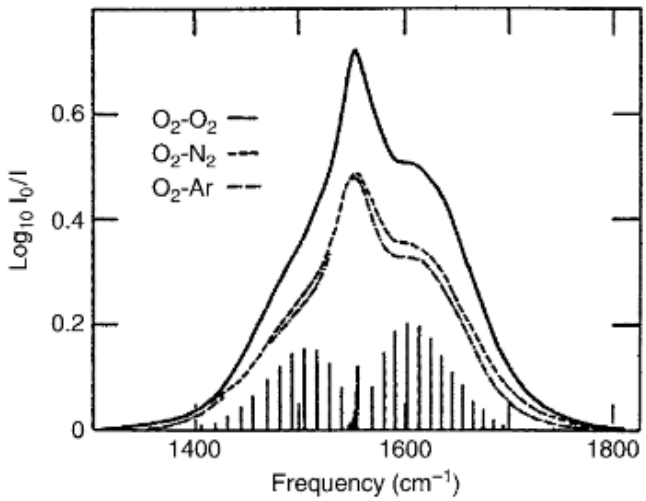

Fig. 7.22 The fundamental absorption band of oxygen for a path length of 40 meters. The densities are: pure oxygen 9.59 Amagats; oxygen–nitrogen mixture, $\rho_{O_2} = 1.09$ Amagats, $\rho_{N_2} = 56$ Amagats; oxygen–argon mixture, $\rho_{O_2} = 1.12$ Amagats, $\rho_{Ar} = 57.9$ Amagats (Shapiro and Gush, Ref. 7.62, with permission). (Note: 1 Amagat is the STP ratio of pressure in atm to temperature in K.)

Figure 64. [98]

8.3.3 N2 2338 cm-1

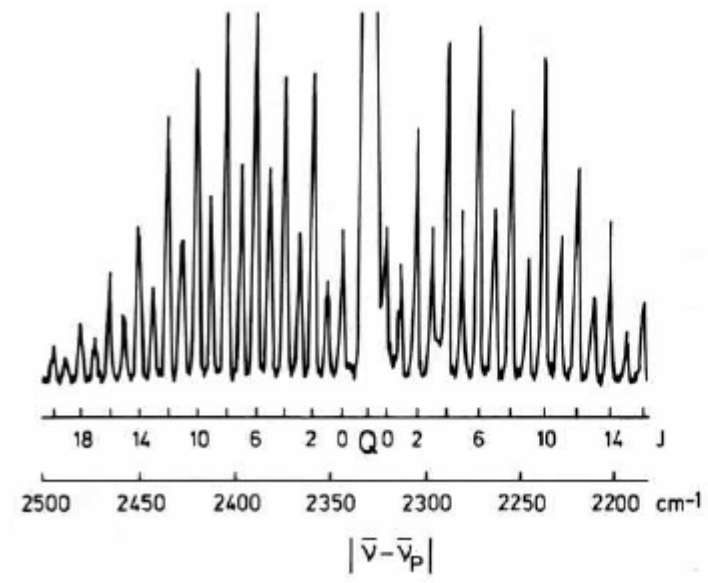

Fig. 12.11. The rotational-vibrational Raman spectrum of the nitrogen molecule, $^{14}N_2$. In the centre, at the position of the vibrational wavenumber $\bar{\nu}_e$ = 2330 cm^{-1}, the Q branch ($\Delta J = 0$) appears as a broad line. In $^{14}N_2$, with $I = 1$, an alternating intensity of the rotational lines with a ratio 1:2 is observed. After Hellwege

Figure 65. Raman peaks of N2 at the predicted 2330cm-1 – page 209 [115]

8.3.4 O_2 1556

Figure 63 and 64 show Raman spectrograph peaks of N_2 at O_2 at the predicted 1556cm-1 and 2330cm-1 (pages 205 and 209 respectively) both within the infrared range of the electromagnetic spectrum.

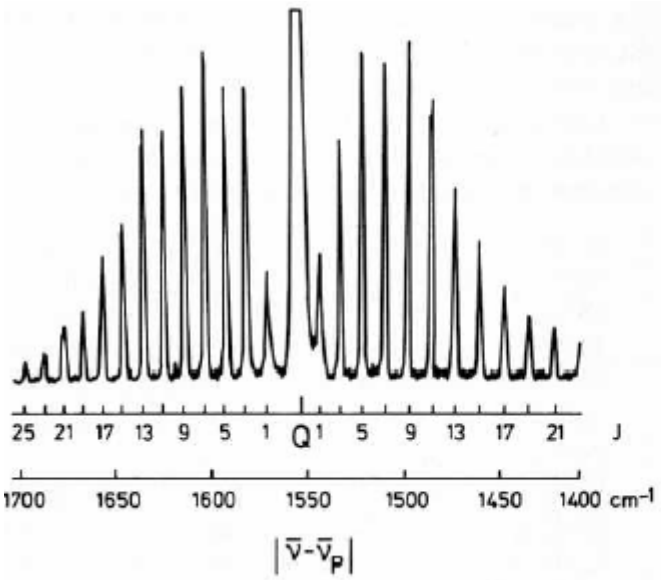

Fig. 12.7. A section of the rotational-vibrational Raman spectrum of oxygen, $^{16}O_2$. This is a vibrational line (Stokes line) with its accompanying rotational lines. In the centre, at the energy of the vibrational wavenumber $\bar{\nu}_e = 1556\ cm^{-1}$, we see the Q branch ($\Delta J = 0$) as a broad line. For $^{16}O_2$ ($I = 0$), the lines with even J are missing; cf. Sect. 12.4. After Hellwege

Figure 66. Raman peak of O_2 at the predicted 1556cm-1 [115] – page 205.

8.3.5 CH_4

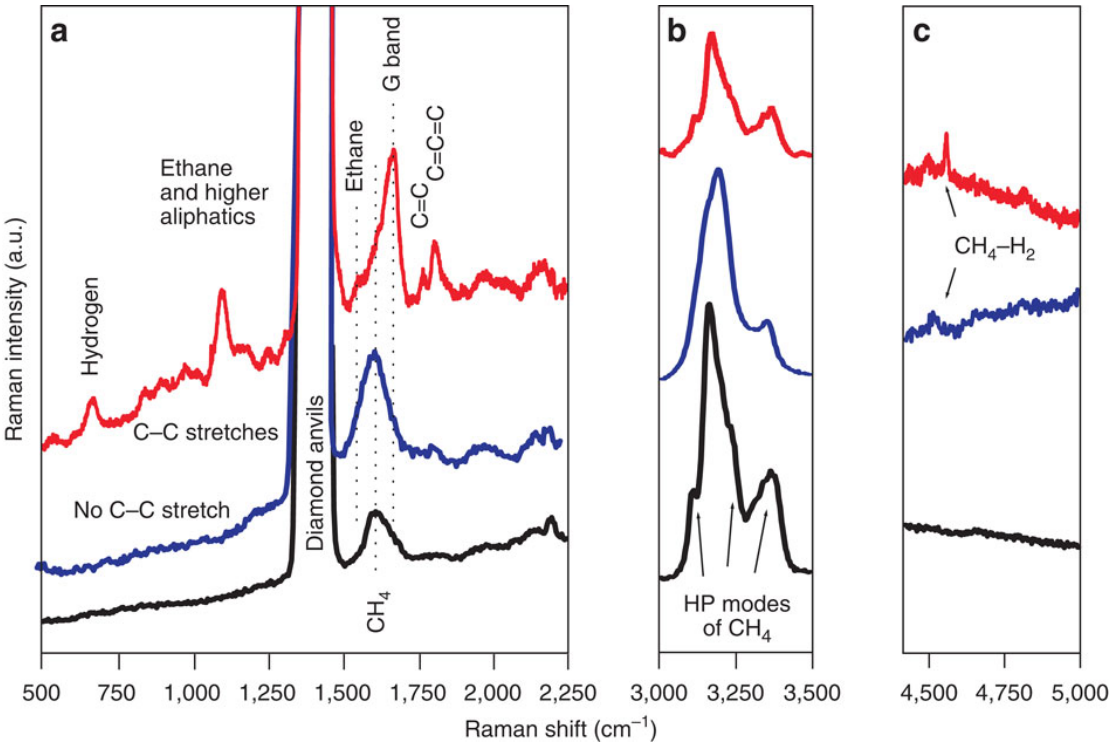

Figure 67. Synthesis in LH DAC at 48 GPa. Black line shows CH4 Raman spectrum before heating. Blue line shows Raman spectrum collected at 1,445 K with evident CH4 dissociation. Red line shows Raman spectrum of reaction products collected after heating to 2,000 K. The labels near the curves suggest the assignment of the Raman bands. HP modes of CH4 refer to vibrations caused by partial orientational ordering of methane HP phase. Panels a–c show different parts of the spectral range.[116]

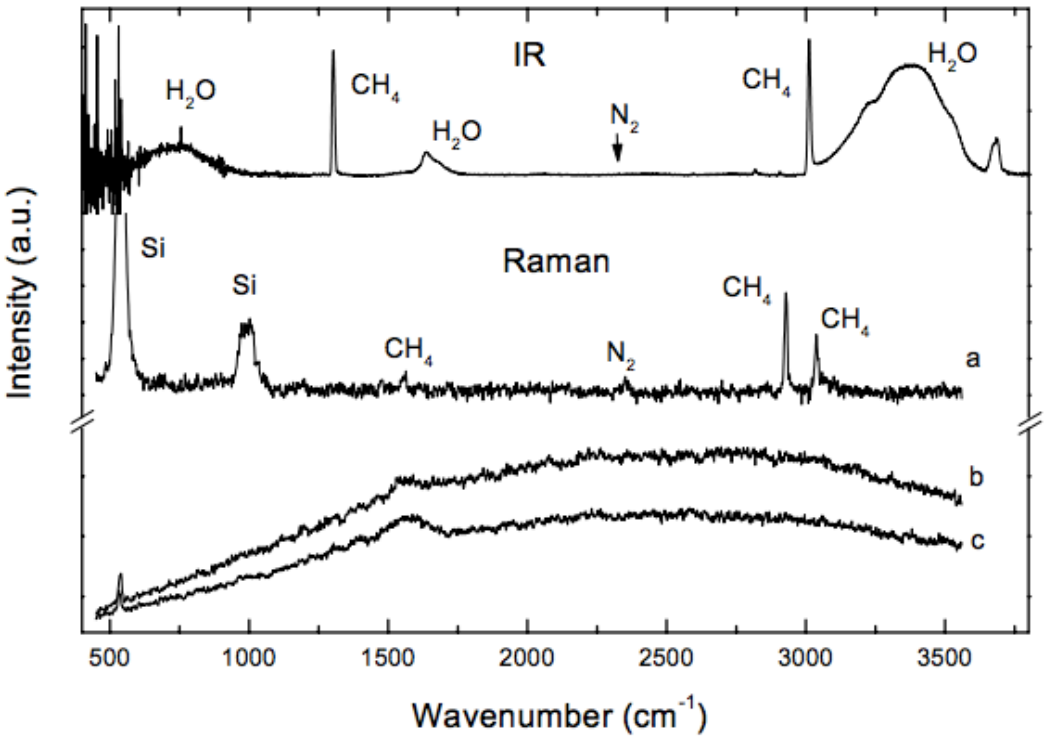

Figure 68. IR (top curve) and Raman spectra of the mixture H2O:CH4:N2 before (curve a) and after (curves b and c, corresponding to doses of 378 eV/16 amu and 825 eV/16 amu respectively) irradiation with He+ (30 keV) ions at low temperature (12 K). In spectra b and c the ice features are undetectable because of the intense fluorescence background. The arrow in the IR spectrum indicates the position of the N≡N symmetric stretching mode, which cannot be observed. Fig. 3 [117].

8.3.6 H_2

Hydrogen gas is assumed a non-GHG as it has similar properties to the other non-GHGs; however, it is predicted at 4342cm^{-1} (table 2) and observed by Raman spectrometers as below Figure 69.

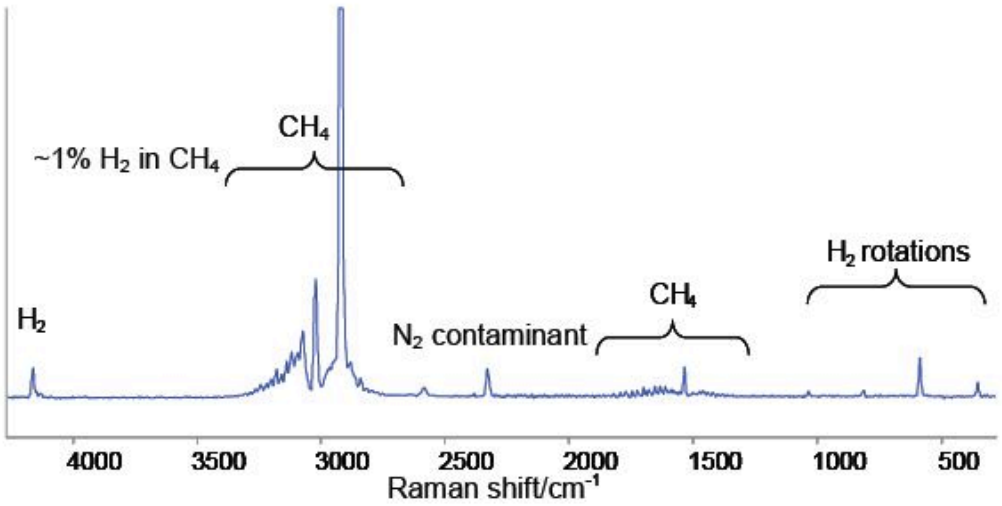

Figure 2. *Raman spectrum of 1% H_2 in CH_4. The sharp bands below 1040cm^{-1} are the pure rotational transitions of the H_2 molecule.*

Figure 69. CH_4, H_2, with N_2 Raman Spectra. [118]

8.3.7 H_20 Raman

Earth atmospheric temperatures are too warm for H_20's Raman signatures too show. The predicted vibrational modes are shown below.

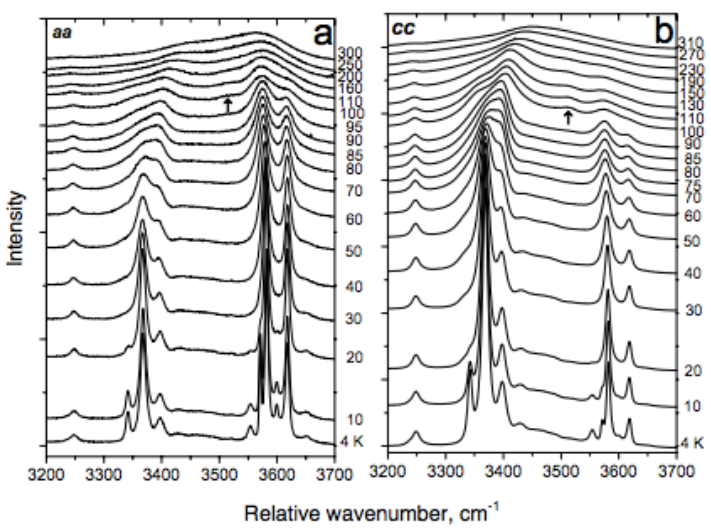

FIGURE 5. Temperature evolution of the polarized spectra showing the O-H and H_2O stretching modes in hemimorphite; (a) *aa*-spectra and (b) *cc*-spectra. The appearance of the new band at around 3500 cm^{-1} at $T \geq 100$ K is shown by the arrow.

Figure 70. [119]

8.3.8 H_2O TE IR

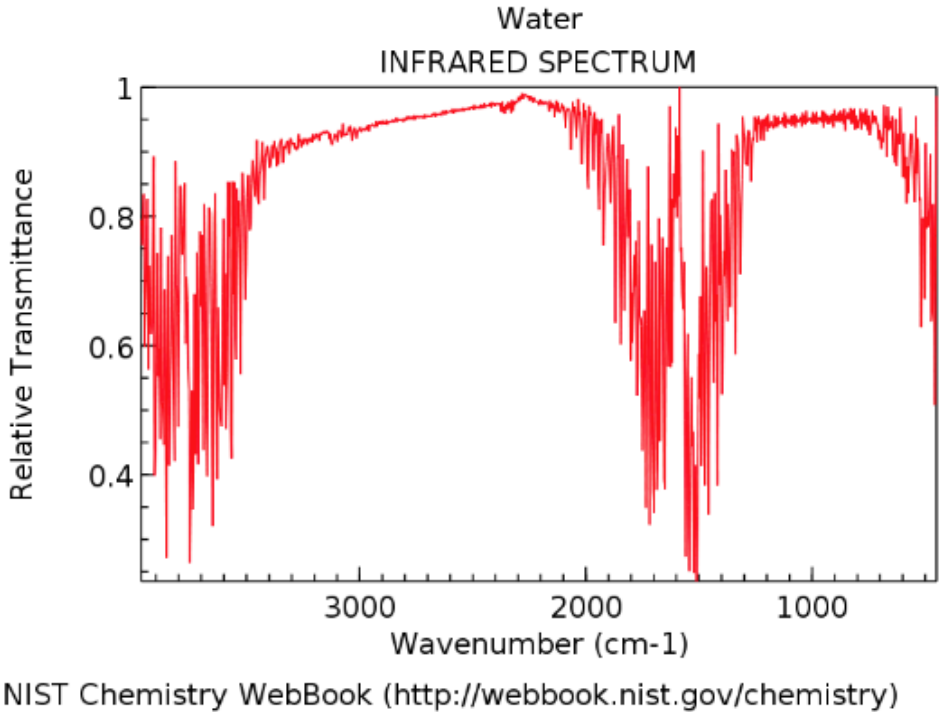

Figure 71. H2O IR Spectra Showing 3652cm Band.

8.3.9 Ge Germanium

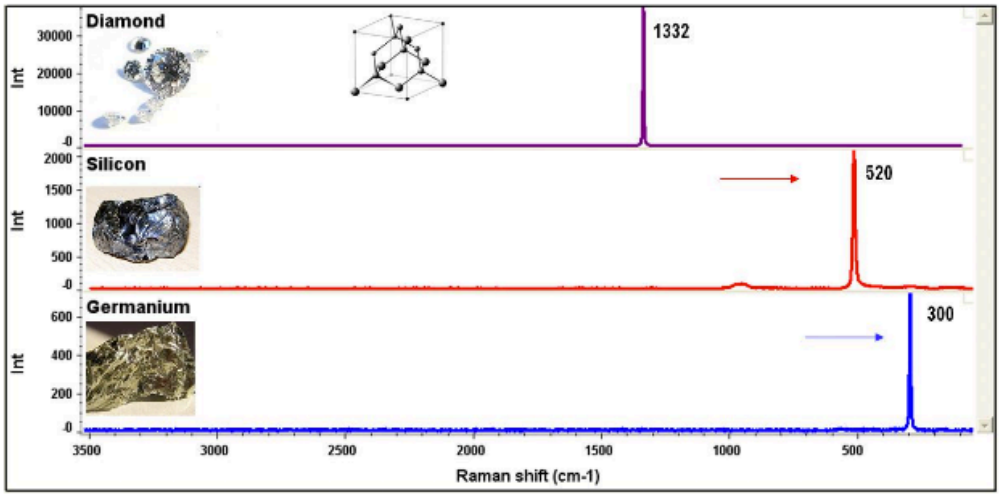

Figure 1: Raman spectra of diamond, crystalline silicon, and crystalline germanium

Figure 1: Raman spectra of diamond, crystalline silicon, and crystalline germanium.

Figure 72. [120],[121]

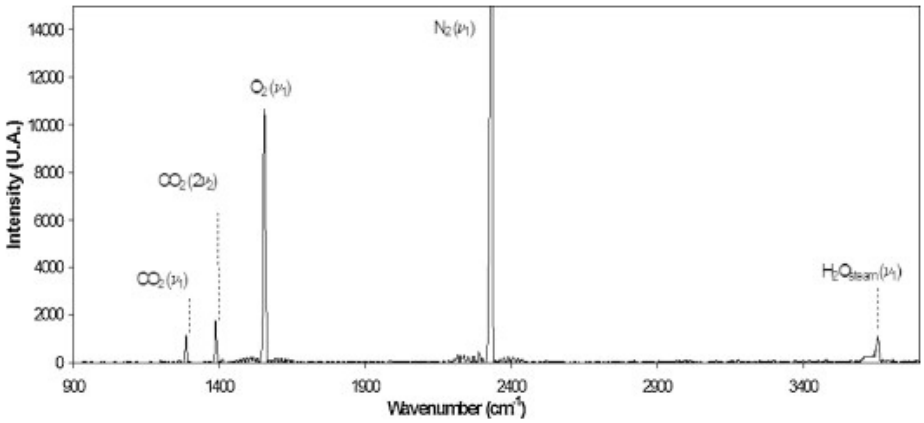

Figure 2. *A typical Raman spectrum measured at the site in this study. Key peaks: H_2O vapor (3657cm^{-1}), N_2 (2331cm^{-1}), O_2 (1555cm^{-1}), and CO_2 (Fermi dyad at 1388 and 1285cm^{-1}).*

Figure 73. Raman Spectra of N2, O2, CO2 and H20 together. [37]